



**NTNU – Trondheim**  
Norwegian University of  
Science and Technology

# Jobberget tunnel - Analysis of stability and support design for tunneling in soil

**Margrete Øie Langåker**

Geotechnology

Submission date: June 2014

Supervisor: Bjørn Nilsen, IGB

Co-supervisor: Bent Aagaard, Sweco Norge AS

Norwegian University of Science and Technology  
Department of Geology and Mineral Resources Engineering





## MASTEROPPGAVEN

**Kandidatens navn:** Margrete Øie Langåker

**Oppgavens tittel:** Joberget tunnel – Analysis of stability and support design for tunnelling in soil

**English title:**

**Utfyllende tekst:**

1.

This master assignment is a follow-up of project work conducted by the candidate during the autumn semester 2013 with main focus on collecting and systemizing geotechnical data for the 70-80 m long soil section of the planned Joberget tunnel, and on literature studies of the pipe umbrella method. In this master project a detailed analysis of the geotechnical aspects of the planned excavation based on the pipe umbrella method is to be carried out. The need for supplementary investigation is to be evaluated and carried out as part of the assignment if required and feasible. For analysis of stability and support design, numerical modelling based on Phase or a similar numerical tool should be included. Among important aspects of this study are particularly emphasized:

- Definition and evaluation of relevant input parameters for stability analysis, including assessment of uncertainties in these parameters.
- Numerical analysis of stresses, deformations and effects of alternative support designs, including parameter studies.
- Evaluation of relevancy of other methods for stability analysis, i.e. empirical and limit equilibrium analysis.
- Further evaluation of spiling as an alternative to the pipe umbrella method.

The master thesis is organized in co-operation with Sweco Norge AS, with Bent Aagaard as contact person and external co-supervisor.

**Studieretning:** Ingeniør- og miljøgeologi

**Hovedprofil:** Ingeniørgeologi og bergmekanikk

**Tidsrom:** 14.01.-10.06.2014

---

*Bjørn Nilsen, Professor/hovedveileder*

SKJEMAET TAS INN SOM SIDE 1 I MASTEROPPGAVEN  
NTNU, 24 januar 2014



## Acknowledgement

This master thesis is written as a part of the Master's Degree Programme, Geotechnology at the Department of Geology and Mineral Resources Engineering at the Norwegian University of Science and Technology (NTNU). The master thesis is performed in cooperation with Sweco Norge AS. Professor Bjørn Nilsen at NTNU has been my main supervisor. Senior Engineering Geologist Bent Aagaard has been my external co-supervisor and contact person at Sweco Trondheim.

I would first of all like to thank my supervisor, Professor Bjørn Nilsen for his good guidance. Thank you for always having time for discussions and for sharing your knowledge and giving good advices. You have inspired me to learn more. Secondly, I would like to thank Bent Aagaard together with the other Engineering Geologists at Sweco Trondheim for good advices and for providing useful information and materials to my research. A special thanks goes to engineering geologist Kine Wenberg Jacobsen (Sweco) and Ph.D. candidate Gareth Lord (NTNU) for their help to review this thesis.

I would also like to thank laboratory technician, Inge Hoff (NTNU) for all his help during triaxial testing. Thank you for sharing knowledge about triaxial testing, providing valuable feedback and for showing interest in my thesis. I am also grateful to Nghia Trinh (NTNU/SINTEF) for giving me advices regarding numerical modelling with Phase<sup>2</sup>. Thanks for always answering my questions.

To my friends and family, thank you for supporting me throughout these years, you are amazing! Last but not least, thanks to my classmates for all the fun times and for the good atmosphere at "Lesesalen". These five years would not have been the same without you!

Trondheim, 13.06.2014



Margrete Øie Langåker

*The picture on the front page shows Joberget with Granvinsvanet in the front during a site visit in September 2013.*



## Abstract

The Norwegian Public Roads Administration (NPRA) is planning a construction of a new road tunnel, Joberget tunnel in the Granvin Municipality of western Norway. Approximately 80 m from the southwestern entrance of the tunnel will be excavated, partly in soil and partly in rock. Soil tunneling will be performed in this section instead of excavation of large open cuts, to avoid difficult work conditions, landslide hazards and severe landscape interventions. Sweco Norge AS in cooperation with the Austrian company iC Consulenter from Austria are contracted to consult the soil tunneling section of Joberget tunnel.

This thesis is a continuation of a project assignment carried out in 2013 and analyses stability and support design of Joberget soil tunnel, based on empirical and numerical methods.

Empirical studies of Joberget soil tunnel include a study of experiences with soil tunneling and a rock mass classification based on the Q- and RMR-system. The importance of additional support in soil tunneling is due to instability of tunnel face, unsupported span and water leakage is revealed in this study. The pipe umbrella primary support method, providing reinforcement of tunnel heading, is found favorable when tunneling in similar ground condition as is present at Joberget.

The numerical analysis is performed with a two-dimensional finite element method in Phase<sup>2</sup>. Evaluation of the total displacement is used to investigate the stability of the proposed design of Joberget soil tunnel, in both cross section and longitudinal section. The pipe umbrella support method is simulated by an improved material layer which shows the supporting effect of the pipe umbrella. Additionally, numerical analyses reveal that subdivision of face, short round lengths and installation of permanent support immediately after excavation are favourable during soil tunneling.

The greatest limitation in numerical modelling is the reliability of the input parameters. Hence, a parameter study on moraine properties and field stresses is carried out. Young's Modulus,  $E$  is found to be the most sensitive parameter. To supplement the estimation of  $E$ , triaxial testing on the moraine material is performed. The reducing effect of water onto material strength is demonstrated by the triaxial test and the numerical analysis.

With a well prepared drainage plan, careful excavations and additional support measures such as the pipe umbrella method, soil tunneling in Joberget is considered to be feasible. However, the stability analyses include several simplifications and uncertainties. A detailed follow-up and monitoring during tunneling is therefore important to verify the model and to find the required support.





## Sammendrag

I forbindelse med oppgradering av riksveg 13 i Granvin kommune, planlegger Statens Vegvesen Region vest en tunnel langs Granvinsvatnet, Jobergtunnelen. Tunnelen på ca. 2 km vil hovedsakelig drives i fjell, men ca. 80 m fra søndre påhugg vil delvis drives i løsmasser. Tunneldriving i løsmasser er vurdert som et bedre alternativ enn store graveskråninger for å unngå vanskelige arbeidsforhold, rasfare og store inngrep i landskapet. Konsulentfirmaene, Sweco Norge AS og iC Consulente fra Østerrike er engasjert i forbindelse med prosjektering av Joberget løsmassetunnel.

Denne masteroppgaven er en oppfølging av prosjektoppgaven som ble utført i 2013 hvor en analyse av de ingeniørgeologiske forholdene for Joberget løsmassetunnel ble gjennomført. Masteroppgaven analyser stabilitet og planlagte sikringstiltak for løsmassetunnelen basert på empiriske og numeriske metoder.

Empiriske studier av Joberget løsmassetunnel inkluderer en studie av erfaringer med tunneldriving i løsmasser og bergmasse klassifisering med bruk av Q- og RMR-systemet. Ved tunneldriving i løsmasser er det ofte nødvendig med tung bergsikring for å sikre god stabilitet og unngå vannlekkasjer. Rørskjerm forsterker tunnelprofilen under driving og er ofte valgt som primær stabilitetssikring for løsmassetunneler i lignende grunnforhold som morenematerialet i Joberget.

Numeriske analyser er utført med Phase<sup>2</sup> basert på to-dimensjonal endelig elementmetode. Tolkning av total deformasjon i både tverrsnitt og lengdesnitt, blir brukt for å undersøke stabiliteten til den foreslåtte utforming av Joberget løsmassetunnel. Den planlagte rørskjermen er inkludert som et forbedret materiale i modellen som viser at rørskjermen gir effektiv sikringsstabilitet. De numeriske analysene viser også at oppdeling av stuff, korte tunnallengder og installasjon av permanent sikring umiddelbart etter utgraving er gunstig ved tunneldriving i løsmasser.

Den største begrensningen i numerisk modellering ligger i pålitelighet av inngangsparametere. Parameterstudie av morenematerialet og spenningsforholdet er derfor gjennomført. Youngs modul, E som beskriver materialets elastiske egenskaper er funnet til å være den mest følsomme parameteren. Treaksialtesting av morenemateriale fra Joberget er utført for å supplere estimering av E. Vannets sin reduserende virkning på materialets styrke er vurdert både ved hjelp av triaksialtesten og den numeriske analysen.

Med grunnlag i en godt forberedt dreneringsplan, forsiktig tunneldriving og arbeidssikring med rørskjerm, er løsmassetunnelen i Joberget vurdert som gjennomførbar. Stabilitetsanalysen er basert på forenklinger og forutsetninger som vil gi en viss usikkerhet til modellen. En detaljert oppfølging og overvåking under tunneldriving er derfor viktig for å verifisere modellen og for å vurdere de nødvendige sikringstiltak.



## Contents

Assignment.....	I
Acknowledgement.....	III
Abstract .....	V
Sammendrag.....	VII
1 Introduction.....	1
1.1 Background.....	1
1.2 Aim .....	2
1.3 Limitations.....	3
2 Background information and investigations .....	5
2.1 Conclusions from project assignment.....	5
3 Site condition .....	7
3.1 Bedrock geology.....	7
3.2 Quaternary geology .....	7
3.3 Topography.....	9
3.4 Hydrology.....	10
4 Joberget soil tunneling section.....	11
4.1 Excavation and support .....	11
4.1.1 Pipe umbrella method.....	12
4.1.2 Tunnel face support.....	14
4.1.3 Primary and inner lining.....	15
4.1.4 Drainage .....	15
4.1.5 Monitoring.....	15
4.1.6 Spiling .....	15
5 Laboratory work.....	17
5.1 Material classification.....	17
5.2 Laboratory results from Shear Box testing, Density and Sieve analysis.....	19
5.2.1 Shear Box testing .....	19
5.2.2 Density analysis.....	21
5.2.3 Sieve analysis .....	21
5.3 Triaxial testing.....	22
5.3.1 Theory .....	22

5.3.2	Working method.....	25
5.3.3	Results .....	28
5.4	Discussion.....	35
5.4.1	Soil Characteristics.....	35
5.4.2	Elasticity.....	35
5.4.3	Strength .....	35
5.4.4	Water content .....	36
5.4.5	Sources of error .....	37
6	Stability analysis in soil tunneling .....	39
6.1	Support analysis for tunneling in weak rock masses .....	40
6.1.1	Critical strain .....	40
6.1.2	Tunnel deformation and rock-support interactions .....	40
7	Empirical analysis.....	43
7.1	Experiences with soil tunneling.....	43
7.1.1	Spiling versus Pipe Umbrella.....	44
7.1.2	The significance of water .....	45
7.2	Rock mass classification.....	45
7.2.1	The Q-system .....	46
7.2.2	The RMR-system .....	49
7.3	Evaluation of Joberget soil tunnel based on empirical analysis .....	49
8	Numerical analysis.....	51
8.1	Finite Element Method (FEM) .....	51
8.2	Two-dimensional numerical analysis of the pipe umbrella method.....	51
8.2.1	Equivalent internal pressure .....	52
8.2.2	Improved material layer .....	52
8.3	2D- versus 3D-numerical analysis.....	53
9	Basics and procedure of the numerical modelling .....	55
9.1	Software.....	55
9.1.1	Phase <sup>2</sup> .....	55
9.1.2	RocLab .....	55
9.2	Model set up .....	55
9.2.1	Cross section .....	56
9.2.2	Longitudinal section.....	57

9.2.3	Mesh and external boundary .....	58
9.3	Field stress .....	58
9.4	Material properties.....	59
9.4.1	Plastic material .....	59
9.4.2	Rock mass properties .....	60
9.4.3	Soil properties .....	69
9.5	Support.....	70
9.5.1	Pipe umbrella.....	70
9.5.2	Permanent support.....	73
9.6	Ground water .....	75
9.7	Stability analyses performed in Phase <sup>2</sup> .....	76
9.7.1	Support analysis .....	76
9.7.2	Ground water analysis .....	76
9.7.3	Stress analysis .....	77
9.7.4	Parameter study of the moraine material.....	77
10	Results of the numerical analysis .....	79
10.1	Support analysis.....	79
10.1.1	Cross section .....	79
10.1.2	Longitudinal section.....	82
10.2	Stress analysis.....	85
10.3	Ground water analysis .....	86
10.4	Parameter study of the moraine material .....	88
11	Discussion .....	91
11.1	Stability and support design of Joberget soil tunnel.....	91
11.1.1	Cross section .....	91
11.1.2	Longitudinal section.....	92
11.2	The uncertainties of input parameters .....	92
11.2.1	Field stress.....	92
11.2.2	Soil properties .....	93
11.2.3	Improved material layer .....	93
11.3	Ground water influence on tunnel excavation.....	94
12	Conclusion and recommendation .....	95
12.1	Further investigations and follow-up.....	96

13	References .....	97
Appendices .....		A
A1	Longitudinal section of Joberget soil tunneling section .....	A
A2	Calculations of the Mohr Coulomb circles .....	C
A3	Plan view of investigations carried out at Joberget .....	D
A4	Calculations of $S_0$ and $M_d$ for material classification .....	E
A5	Calculations from sieve and density analysis .....	F
A5	The Q-system .....	G
A6	The RMR-system .....	I
A7	Analysis of Rock Strength using RocLab .....	K

# 1 Introduction

## 1.1 Background

The Norwegian Public Roads Administration (NPRA) and Voss Municipality are currently in cooperation to construct a new road system in a project called Vossapakko. The aim of this project is to upgrade the existing main road, E16 through the city of Voss in the western part of Norway. An extended part of Vossapakko is the planning for construction of Joberget tunnel.

Joberget tunnel will be located on the E13 highway in Granvin Municipality, west of Voss in Hordaland County. The tunnel will run in parallel to the lake Granvinsvatnet through the mountain of Joberget, with a length of approximately 2000 m. The northwestern entrance will be located approximately 35 metres above sea level (m.a.s.l.) at Øvre Vassenden, and the southeastern entrance will be located at approximately 30 m.a.s.l. near Holven. The construction of Joberget tunnel is planned to avoid the landslide exposed area along the lake as illustrated in Figure 1. A substantial rock-fall in 2007 and several smaller rock-falls have been registered along the lake Granvinsvatnet (NPRA, 2013a).

The tunnel will mainly be excavated through rock, but approximately 80 m of what will constitute the southwestern entrance of the tunnel will be excavated in moraine material. Soil tunneling is preferred in this section instead of large open cuts with backfilling, to avoid difficult work condition and landscape intervention. Sweco Norge AS in cooperation with iC Consulenten are contracted to consult the soil tunneling section. The section consists partly of soil and partly of bedrock and the chosen tunneling method is pipe umbrella (Sweco and iC-Consulenten, 2013).

Soil tunneling is challenging due to the soil being a weak, water bearing and unstable excavation material. Hence, additional support methods such as the pipe umbrella method are necessary to increase stability during construction and prevent severe construction induced deformations. The pipe umbrella method is a primary support method commonly performed in international soil tunneling. The method is carried out with overlapping long and stiff perforated pipes installed in the periphery of the tunnel, from tunnel face. Grout is applied into the perforated pipes and an “umbrella” of pipes and grout is created to increase stability (Volkman and Schubert, 2008).

If the soil material turns out to be strong and stable during excavation, spiling is suggested as an alternative for the soil tunneling section at Joberget. The method is similar to the pipe umbrella method, but instead of installing pipes, bolts are used to stabilize the tunnel during excavations. However, Spiling bolts are shorter, less stiff and have a lower flexural strength in comparison to umbrella pipes (Sweco and iC-Consulenten, 2013).

Stability analysis of the tunnel and surroundings, in both construction and permanent phase, is beneficial in soil tunneling to prevent collapses due to excessive deformations or failure of supporting structures (Nordal, 2013). Empirical methods such as experiences from similar

projects and rock mass classification systems together with numerical methods are carried out to analyse the stability during soil tunneling at Joberget.



**Figure 1: Air photo showing the location of Joberget tunnel. The rockfall hazard area in red and Joberget tunnel alignment in orange are illustrated based on information from NPRA (2013a). The figure is modified after the Norwegian website, norgebilder.no (2013).**

## 1.2 Aim

The master thesis is a continuation of a previous project assignment conducted in the autumn of 2013, by the author as a part of the Master's Degree Programme, Geotechnology at the Department of Geology and Mineral Resources Engineering at the NTNU, Trondheim. Engineering geological aspects of soil tunneling at Joberget based on the pipe umbrella method was evaluated in the project assignment. A more detailed analysis on the geotechnical aspects are carried out in this master thesis. The main aim of the thesis is to analyse stability and support design of Joberget soil tunnel.

Numerical modelling based on Phase<sup>2</sup> is performed to analyse and evaluate the stability and the proposed support of Joberget soil tunnel. A parameter study is carried out to investigate the uncertainties of input parameters to numerical modelling. Laboratory work with triaxial test is carried out to supplement the estimation of the deformation modulus input value. The relevancy of other stability methods, such as empirical analysis is also evaluated.



Additionally, the master thesis is written to assist Sweco Trondheim AS in their work on the soil tunneling section at Joberget.

### **1.3 Limitations**

The master thesis is limited to the soil tunneling section of Joberget tunnel located at the southeastern entrance near Holven. Structural details like for example the portal is not included in the thesis. Also, the cut and cover section seen in Appendix A1 is not included in this study.

In early project phase, pipe umbrella method was chosen as primary support method for the soil tunneling section at Joberget. Therefore, the thesis mainly discusses pipe umbrella method and only briefly describes other soil tunneling methods. Also, the numerical modelling is limited to the proposed support design with the pipe umbrella method.

The effect of time and frost are often important when stability and support of a tunnel are evaluated, but will not be discussed in this thesis.



## 2 Background information and investigations

Available literature and other relevant information about soil tunneling at Joberget:

- Relevant information about Joberget tunnel such as reports, maps, pictures and data from Sweco Trondheim and the NPRA.
- Project assignment about engineering geological aspects of soil tunneling at Joberget conducted by the author in autumn 2013.

### 2.1 Conclusions from project assignment

A literature study and site investigation project, *Joberget tunnel – Engineering geological aspects of soil tunneling based on pipe umbrella method* was carried out by Langåker (2013) at the Department of Geology and Mineral Resources Engineering, NTNU and was performed in cooperation with Sweco Norge AS. Shear Box testing, Sieve and Density analysis were carried out at the geological engineering and rock mechanical laboratory at NTNU/SINTEF during November 2013.

The project concluded that soil tunneling can be compared to tunneling in weakness zones with unstable and difficult excavation materials, requiring detailed investigations, good planning, careful tunneling and continuous monitoring.

Geotechnical category 3 for the soil tunneling section at Joberget was chosen by the NPRA. This is defined as “Very large and unusual structures, structures involving abnormal risks, or unusual or exceptionally difficult ground or loading conditions and structures in highly seismic areas” (Nilsen and Palmstrøm, 2000). Hence, additional investigations and supervision during construction are found necessary for Joberget soil tunnel due to the little overburden and the weak ground material.

Observations during site visit at Joberget in September 2013 confirmed the geological condition of an over-consolidated sub-glacial moraine material evaluated by Sweco and the NPRA (2013a). The excavated test pits in the area showed stable vertical slopes of soil material with a well packing degree and amount of fines increasing with depth, typical for sub-glacial moraines. Results from laboratory work also confirmed the evaluation of an over-consolidated sub-glacial moraine at Joberget (See chapter 5.2). Laboratory testing together with information gained at site visit were important when classifying material strength properties.

Providing if the moraine material is as strong as the field and laboratory observations indicated, with no weak and erodible pockets being found during excavation, the more time- and cost-consuming spiling could be chosen as primary support method. However, the pipe umbrella was considered to be a more favourable support method due to the opportunity of applying grout in both pipes and the surrounding (see chapter 7.1.1).



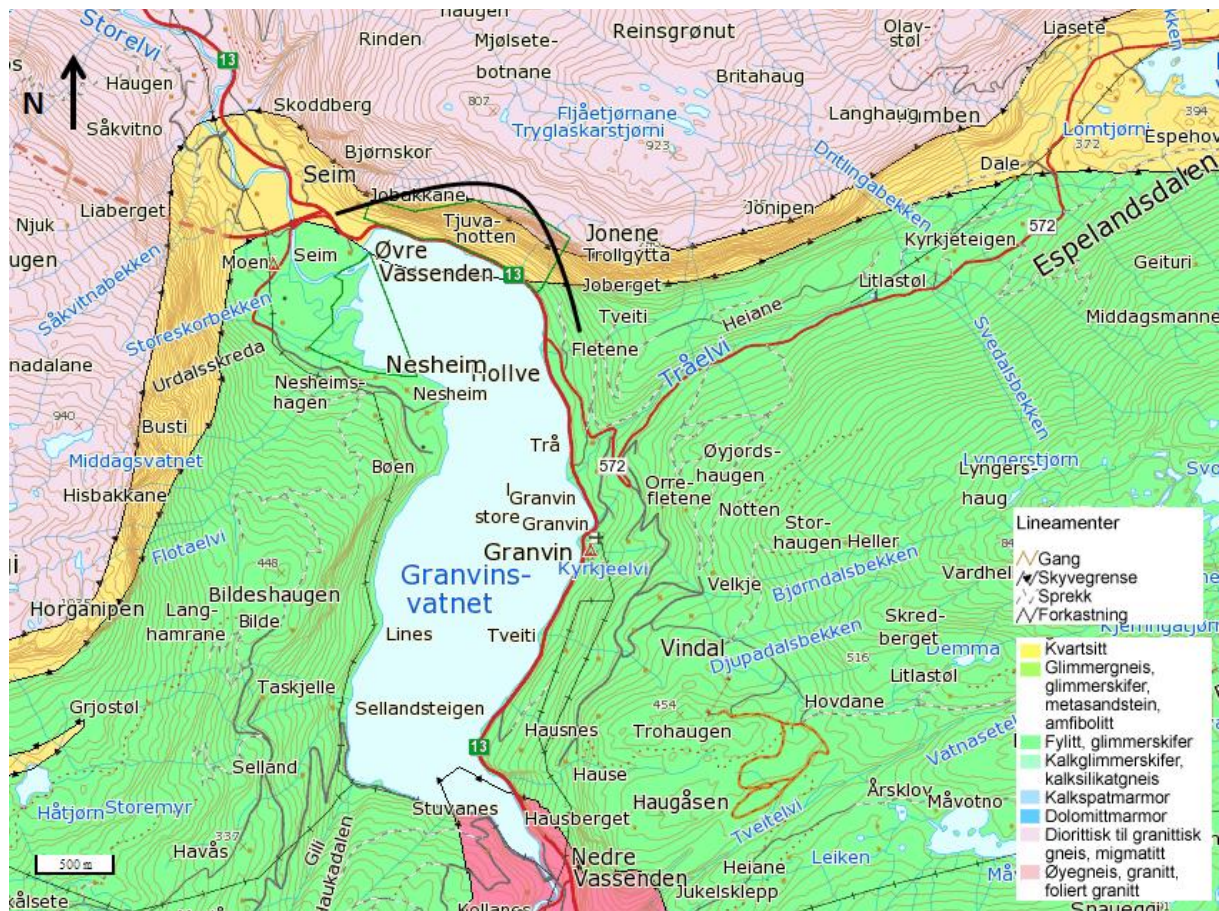
### 3 Site condition

#### 3.1 Bedrock geology

Two different nappes, Stavsnut nappe and Slettafjell nappe are located in the area around Joberget. These are formed during a great tectonic event in the Proterozoic Era. The nappes are separated from underlying bedrock by thrust faults and some of the underlying bedrock was metamorphosed during the Cambro-Silurian time (NPRA, 2013a).

The geological map provided by the Norwegian Geological Survey (NGU) seen in Figure 2, shows the geology in the area consisting of gneiss, quartzite, phyllite and foliated granite, metamorphosed during Proterozoic Era.

Four joint sets and weakness zones of more than 2.5 m have been observed at Joberget and are suggested to be related to thrusting (NPRA, 2013a).



**Figure 2:** A section of a 1:250 000 geological map showing the geological distribution around the lake Granvinsvatnet. Joberget tunnel alignment is illustrated in black. The figure is modified after Solli and Nordgulen (2007).

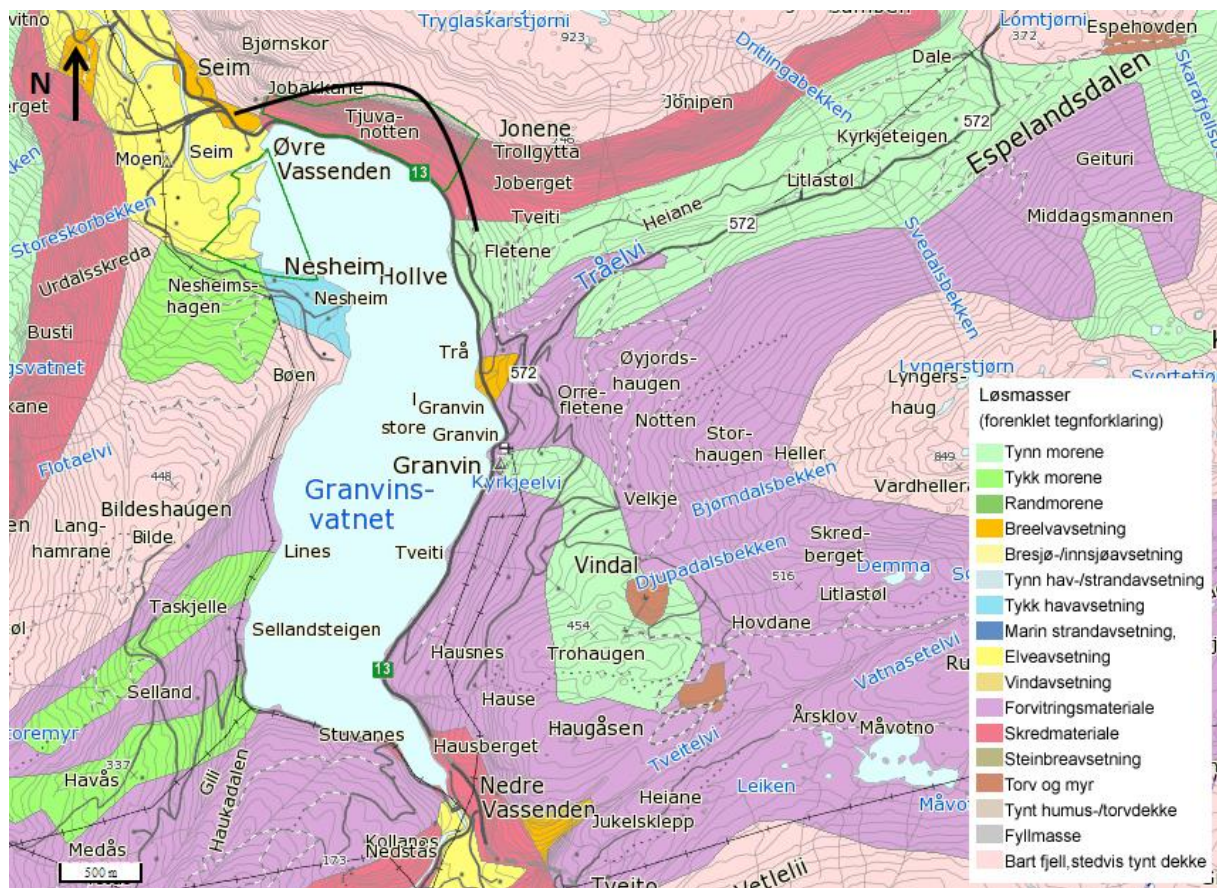
#### 3.2 Quaternary geology

Deglaciation of ice sheets that were covering western Norway during the last Ice Age, including the area of Joberget, occurred around 10 000 years ago. During this episode, the glaciers cleaned the bedrock of overlying soil and picked up fragments from the bedrock

below. Soil, rocks and boulders were transported within or beneath the glacier and most commonly deposited underneath or at the margin of the glacier as moraines.

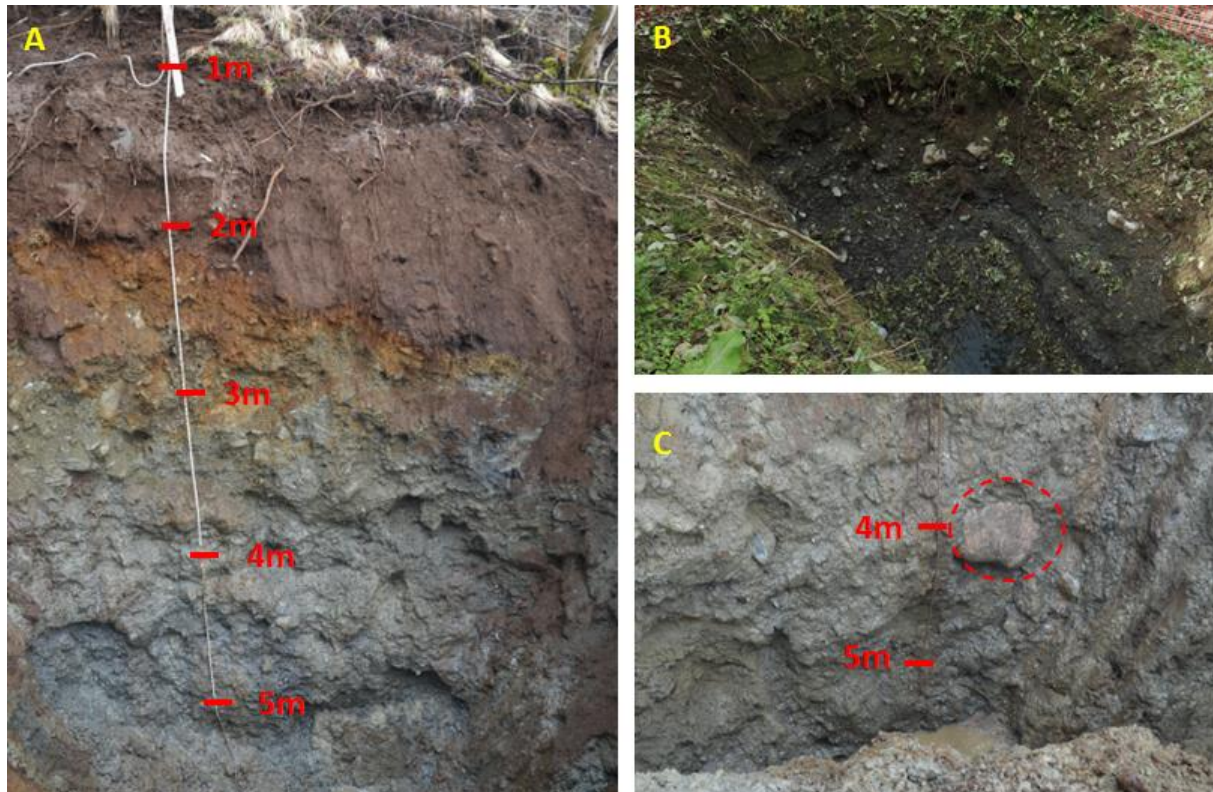
There is a great variation in the characteristics of the material deposited by glaciers. This is due to the different soils and composition of bedrock being eroded and transported and the varying distance and speed of transportation. Generally, the glacial deposits are heterogeneous in nature, are highly unsorted and contains of a range of grain sizes from silt to boulders. Material deposited at the ice margin is called marginal moraines, whereas material deposited beneath the glacier is called sub-glacial moraines or lodgement till. A sub-glacial moraine is over-consolidated due to the heavy load of the glacier and often consists of a great amount fines due to little melt water washing (Thoresen, 2009).

In Granvin valley, south of Joberget is the Hollve deposit which is located in a steep slope underneath the almost vertical south facing rock wall of Joberget. North of the Hollve deposit lies the outlet of the hanging U-valley called Espeland valley. The traveling direction of the glacier in Espeland valley was to the west. The Hollve deposit was most likely sheltered from this process which might be the reason for the preserved moraine material at Hollve (Sweco, 2013a). The soil deposits map provided by Thoresen et al. (1995), seen in Figure 3 show a thin moraine layer at Hollve.



**Figure 3: Map showing the soil deposits around the lake Granvinsvatnet. Joberget tunnel alignment is illustrated in black. The figure is modified after Thoresen et al. (1995).**

In relation to the soil tunneling section at Joberget, four test pits were excavated and several total drillings were carried out by the NPRA. The test pits were approximately 5-6 m deep, consisting of heterogeneous material. Picture A and B in Figure 4 show the heterogeneous material in test pit 2. Boulders of up to 40-50 cm were found and can be seen in picture C in Figure 4. The amount of fines found in the test pits was increasing with depth. Drillings and seismic measurements performed in 2009 and presented by the NPRA (2013a), show a varying depth of 8 – 22 m of soil.



**Figure 4:** Picture A and B show test pit 2 immediately after excavation and some months after excavation respectively, indicating stable slopes. Picture C is taken from test pit 1 showing a large boulder in the moraine material. Picture A are taken by NPRA (2013a) and B and C by Langåker (2013).

### 3.3 Topography

The topography above the planned Joberget tunnel alignment is illustrated in Figure 5. Joberget is a steep sided mountain, but relative flat at the top. The overburden is around 600 m at its highest and 5 m at its lowest.

The Southeastern entrance of Joberget tunnel located near Holven is covered by soil deposits. A talus slope stretches some 120 m above the planned tunnel entrance, terminating at a approximately 300 m high vertical rock wall. The slope angle is approximately 30° (NPRA, 2013a).

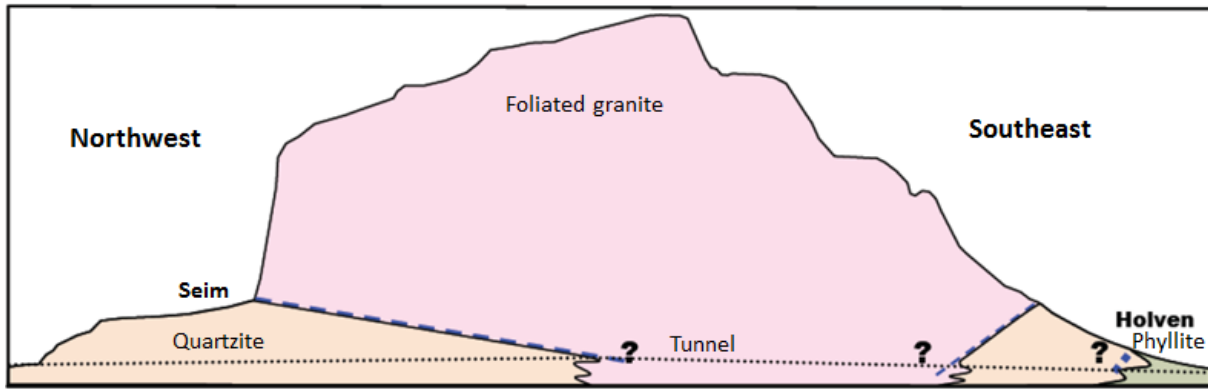


Figure 5: Longitudinal profile of Joberget tunnel with possible rock boundaries (NPRA, 2013a).

### 3.4 Hydrology

No lakes are found in the immediate distance to Joberget tunnel. Streaming water was observed above test pit 3 during permeability testing in August 2013. Hydraulic conductivity,  $k$  found from sieve analysis and permeability tests varies between  $10^{-4}$ - $10^{-8}$  m/s. These hydraulic conductivity values are typical measures for glacial till, silt, loess and silty sand as indicated by Figure 6. The ground water table is estimated to be approximately 10 m below surface, but will vary with the season due to raining and melt water. Sudden increases in ground water level is also possible, due to common periods of heavy rainfall (Sweco, 2013b).

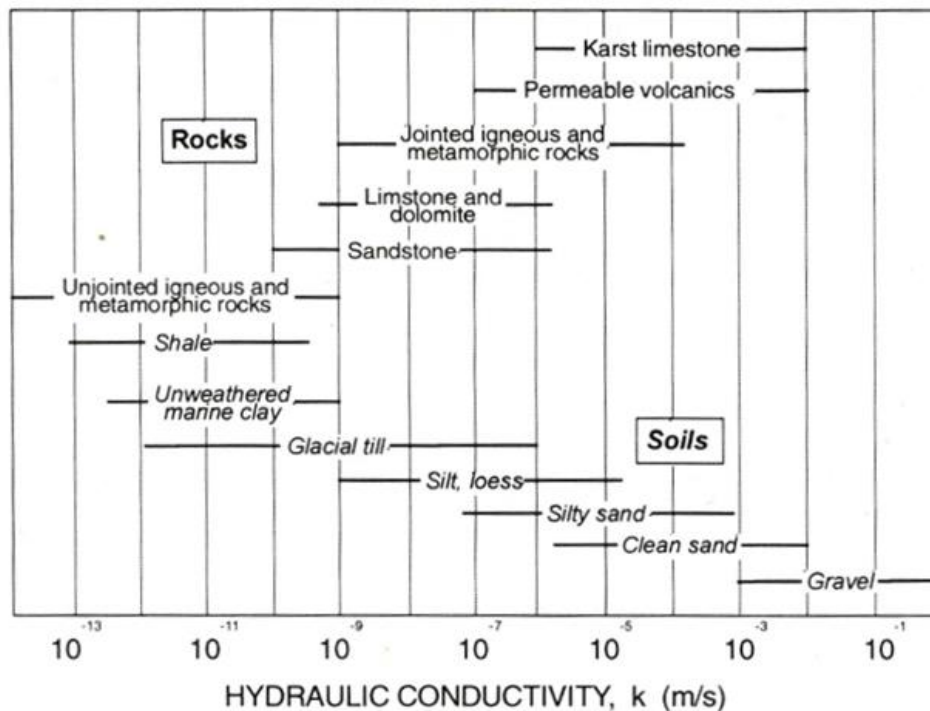
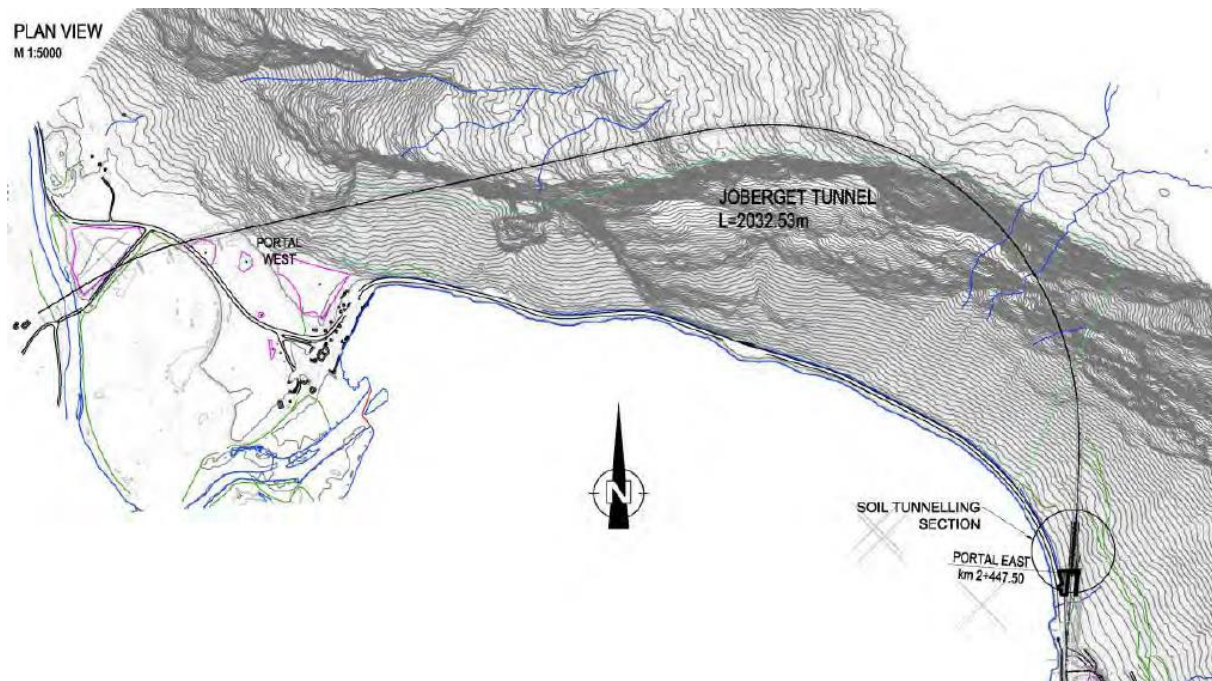


Figure 6: Typical hydraulic conductivity of rocks and soils (Freeze and Cherry, 1979).



## 4 Joberget soil tunneling section

Approximately 80 m, from profile 2437 to profile 2357 (Appendix A1), from the southwestern entrance of the tunnel will be excavated partly in soil and partly in rock. This tunnel section is planned as a soil tunnel, using the pipe umbrella support method. Figure 7 shows a plan view of project site with the tunnel alignment and the soil tunneling section. Joberget tunnel is designed as a T9.5 road tunnel. According to Handbook 021 by the NPRA (2010) about road tunnels in Norway, T9.5 is defined as a road tunnel with a total base width of 9.5 m. The general cross section of the soil tunnel designed by iC-Consulenten (2013) can be seen in Figure 8. Excavation of the soil tunneling section is planned to start autumn 2014.



**Figure 7: Plan view of project site showing tunnel alignment and soil tunneling section (iC-Consulenten, 2013).**

### 4.1 Excavation and support

The pipe umbrella support method together with careful excavations, additional face support, drainage and monitoring, will be carried out to avoid collapse during and after excavation and to ensure secure tunneling. Excavation of the tunnel face will be divided in approximately 5.3 m high top heading and approximately 3 m high bench as is indicated in Figure 7. The top heading will be excavated every meter and the bench every four meters. Permanent support of inner and outer lining is installed after every round length of 1 m (Sweco and iC-Consulenten, 2013).

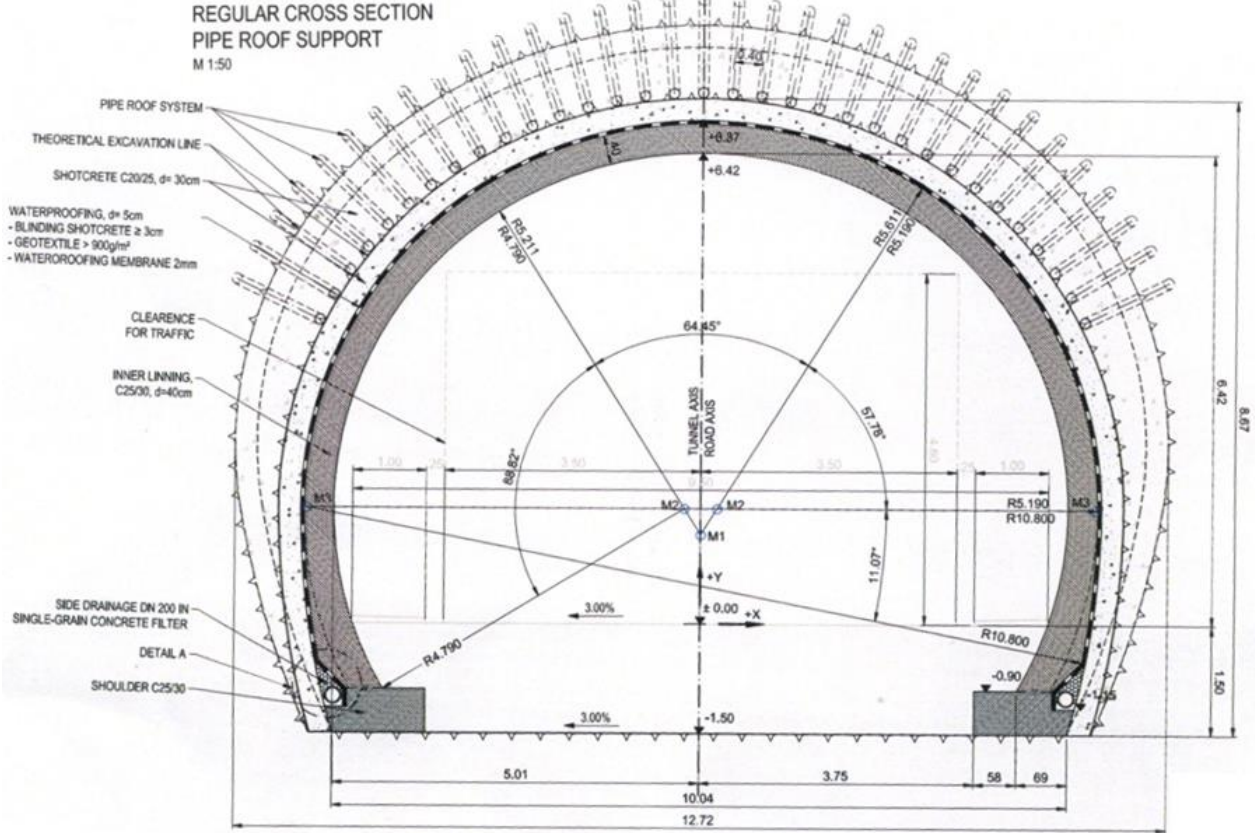
### 4.1.1 Pipe umbrella method

The pipe umbrella method is a primary support method carried out to allow safe excavations during tunneling. Perforated pipes are installed in the tunnel face periphery and injected with grout to stiffen the ground resulting in an “umbrella” above the area to be excavated (Wang and Jia, 2009).

A pipe umbrella with 15 m long pipes will be installed from tunnel face within an angle of 130° of the tunnel crown, as shown in the cross section in Figure 8. The description of the steel pipes selected in the pipe umbrella design is presented in Table 1. The pipes are perforated and will be grouted with concrete following installation.

**Table 1: Characteristics of the steel pipes proposed for the pipe umbrella section in Joberget soil tunnel (iC-Consulenten, 2013).**

<b>Steel pipe</b>	
Length	15 m
Outer diameter	114 mm / 140 mm
Wall thickness	6.3 mm/ 8.0 mm
Overlap	3 m
Inclination	5°
Distance between pipes	0.4 m
Steel grade	S355
<b>Concrete</b>	
Concrete strength class	C 25/30



**Figure 8: Conceptual design of the general cross section of Joberget soil tunnel with primary and inner lining and the pipe umbrella section within an angle of 130° in tunnel crown (iC-Consulenten, 2013).**

The longitudinal section in Figure 9 shows a pipe umbrella section, with a pipe overlap of 3 m. This overlap is designed to ensure proper foundation length and transfer loads from supported areas to less critical areas. The installation angle for the steel pipes of 5° to the tunnel axis, is chosen to make overlapping possible (Sweco and iC-Consulenten, 2013).

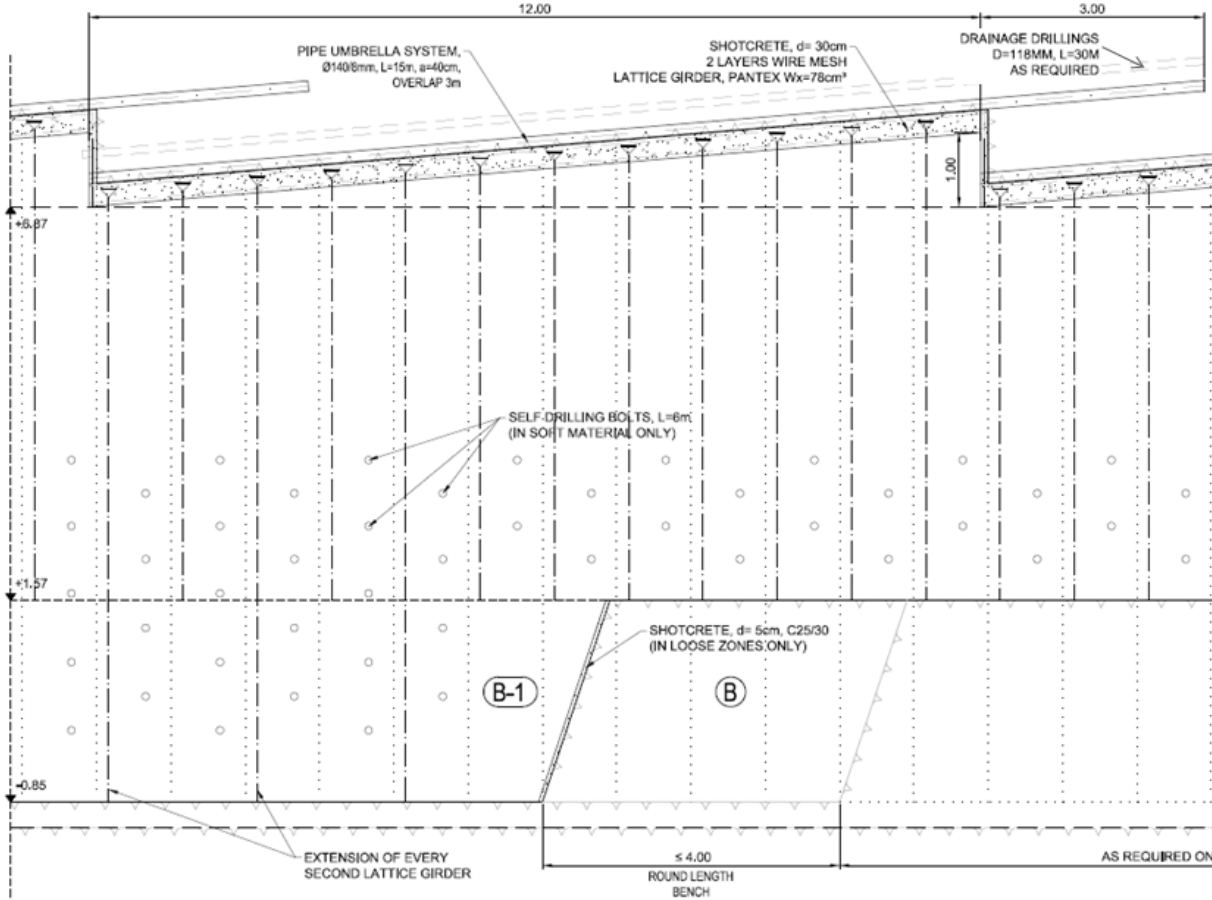


Figure 9: A section of the conceptual design of the longitudinal section of Joberet soil tunnel showing a pipe umbrella system with 15 m long pipes and an overlap of 3 m (iC-Consulenten, 2013).

4.1.2 Tunnel face support

Face bolts, being the most reliable and cost-effective support element, are often used in combination with the pipe umbrella system, to stabilize the tunnel face (Volkman and Schubert, 2009).

10 m long face bolts of threaded, coupled tube-type bolts with self-drilling bits such as Ischebeck, in combination with 10 cm shotcrete and wire mesh, will be installed to support tunnel face. If the moraine is found to have insufficient strength during tunneling, a pocket-excavation with further division of tunnel face can be performed. The soil will be excavated with a strong backhoe, such as a tunnel excavation Liebherr 944. Blasting will be performed when excavating in bedrock. Continuous working with 24 hours 7 days a week is recommended to avoid pore water pressure built up and the need for additional support of tunnel face (Sweco and iC-Consulenten, 2013).

### 4.1.3 Primary and inner lining

A minimum of 30 cm of shotcrete with two layers of wire mesh (K257) in top heading and bench is estimated as the required primary lining. At any construction joints, wire mesh will be overlapped in longitudinal and radial direction. After every round length, a lattice girder is installed. Tunnel invert is most certain located in rock and therefore no structural invert is required.

Installation of inner lining takes place when the outer lining is still active. The thickness of the inner lining is varying from 40 cm in the top head to 60 cm at the abutment of inner lining with a rock foundation, as seen in Figure 8 (iC Consulenten 2013).

### 4.1.4 Drainage

Permeable layers inside the moraine or rock encountered during tunneling can result in water seepage. To ensure proper drainage in the Joberget soil tunneling section, a permanent drainage system will be located between the shotcrete and inner lining. This system consists of a continuous fibre cloth layer and local, by perforated material in stripes. An impermeable membrane of fibre cloth will be installed between primary lining and inner lining. Drainage water will be led into a drainage system of perforated pipes installed parallel to the pipe umbrella or through half-pipes in the entrance area of the tunnel. In worst case, use of vertical drainage holes with an installed suction pump drilled from surface to control water ingress is also under consideration (Sweco and iC-Consulenten, 2013).

### 4.1.5 Monitoring

The influence on stability conditions and deformations is difficult to observe because the pipe umbrella support method is primarily working ahead of the primary lining. Deformation measurements, before, during and after excavations, are therefore crucial and is often related to successive tunneling (Volkman and Schubert, 2008).

Convergence bolts that measure displacements will be installed in the cross section of Joberget soil tunnel and at the surface. The monitoring procedure is described in Table 2.

**Table 2: Planned monitoring procedure during construction of Joberget soil tunnel (iC-Consulenten, 2013).**

Interval of monitoring cross section	Monitoring interval <i>This may be changed by field engineer</i>	
	Distance to face	Intervals
Tunnel		
5 – 10 m	< 30 m	Daily
Surface		
10 m	< 60 m	Every second day
	> 60 m	Weekly

### 4.1.6 Spiling

If the moraine material turns out to be strong and stable with no weak and erodible pockets during construction, pipe umbrella may be replaced by spiling. Use of 3 m long Ø 50 mm Tubespiles with c/c 20 – 40 cm is suggested (Sweco 2013a).



## 5 Laboratory work

Shear Box testing, Sieve and Density analysis were carried out at the geological engineering and rock mechanical laboratory at NTNU/SINTEF by Langåker (2013). The tests were conducted on samples taken from a depth of 2-3 m. Due to large boulders and a high degree of packing, samples were inherently disturbed. The samples were collected above the local level of ground water which is approximately 10 m below surface, from the site of the planned Joberget soil tunnel.

To get a better understanding of the soil material at Joberget, triaxial testing was carried out at the laboratory of pavement technology, Department of Civil and Transport Engineering at NTNU, March 2014. The aim of the triaxial testing was to obtain and analyse the elasticity and strength of the material. Additionally, the results from the triaxial testing were used to confirm the results obtained from the shear box test.

Based on observations from site visit, background study and previous laboratory testing, the material is evaluated as an over-consolidated sub-glacial moraine (Langåker, 2013).

### 5.1 Material classification

Langåker (2013) carried out a material classification of the soil material located at Joberget based on grain size distribution curves. Figure 10 shows average grain size and gradation as a function of depositing condition for all material tested at Joberget with regard to drill hole number and ID. The location of the boreholes can be seen in Appendix A3.  $S_0$  and  $M_d$  are calculated from grain size distribution curves provided by the NPRA (2013b). Included is the calculation from the grain size distribution curve of the material tested at the NTNU/SINTEF laboratory by Langåker (2013). All calculations are presented in Appendix A4. As expected, the material is classified as moraine material. The major part of the material is plotted as moraine sand despite the presence of clay and silt in the material.

Drill holes 6, 57 and 62 are not representative for the moraine material as they are taken approximately 100 m south of the tunnel entrance (Sweco, 2013b)

All calculations are based on data from manually reading of the grain size distribution curves and the figures may therefore inherit some uncertainties.

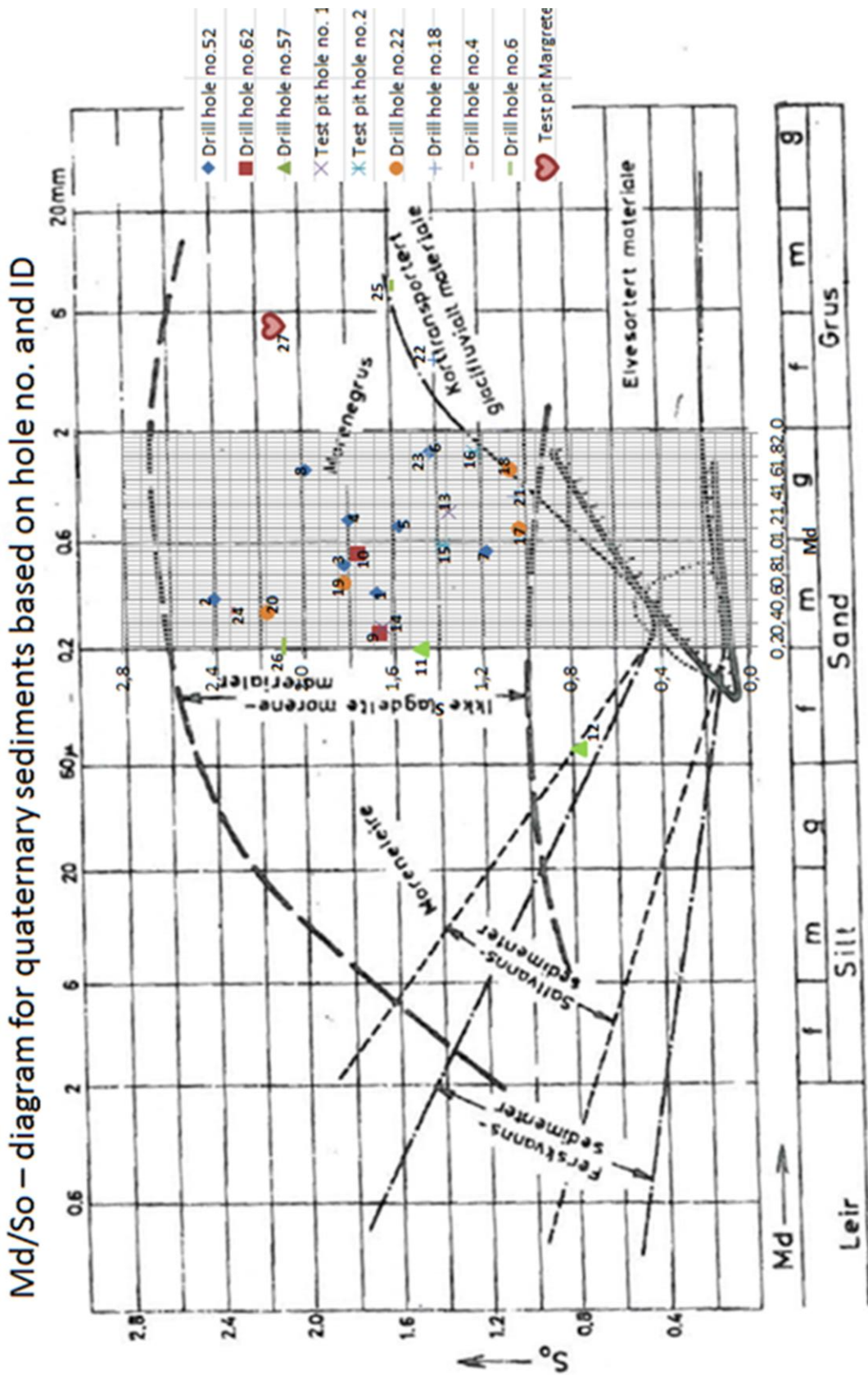


Figure 10: Average grain size and gradation as a function of depositing condition for all material tested at Joberget with regard to drill hole number and ID. Location of drill holes are presented in Appendix A4 and calculations are presented in Appendix A4. The figure is modified after Nilsen and Broch (2011).



## 5.2 Laboratory results from Shear Box testing, Density and Sieve analysis

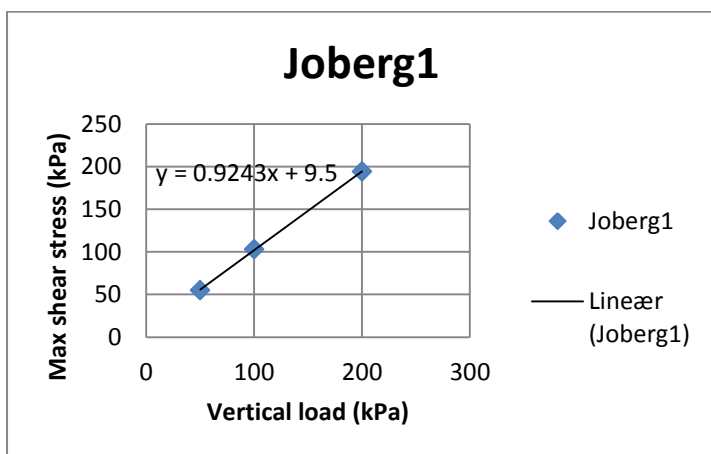
Figures and tables presented in this chapter are taken from the project assignment conducted by Langåker (2013).

### 5.2.1 Shear Box testing

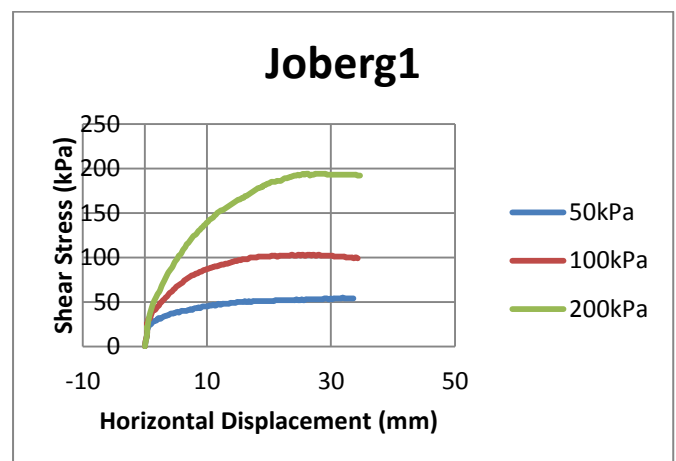
Shear box testing is performed according to the ASTM standard D3080/D3080 - 11. The shear tests measurements with The Large Scale Shear Box, Model SB2010 for two samples in laboratory dry and water saturated condition are directly presented in Figures 12, 14, 16 and 18. Vertical load versus maximum shear stress measurements are plotted with a linear approximation curve to find the cohesion and friction angles for the two different samples and are showed in Figures 11, 13, 15 and 17. The calculated friction angles and cohesions are presented in Table 3.

**Table 3: Friction angles and cohesions for two different samples, Joberg1 and Joberg2 in laboratory-dry and water saturated condition.**

Sample	Condition	Cohesion[kPa]	Friction angle [°]
Joberg1	Laboratory-dry	9.5	42.7
Joberg2	Laboratory-dry	15	42.5
JobergW1	Water saturated	20	39.5
JobergW2	Water saturated	15	38.9



**Figure 11: Vertical load (kPa) versus maximum shear stress (kPa) based on shear test results for sample Joberg1 in laboratory-dry condition.**



**Figure 12: Shear tests measurements for sample Joberg1 in laboratory-dry condition.**

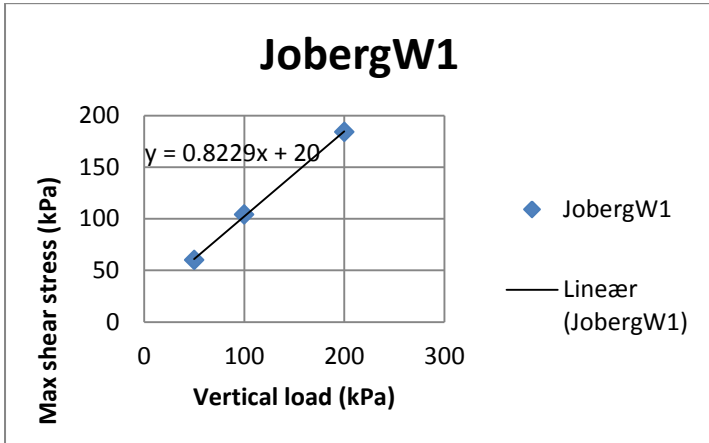


Figure 13: Vertical load (kPa) versus maximum shear stress (kPa) based on shear test results for sample JobergW1 in water saturated condition.

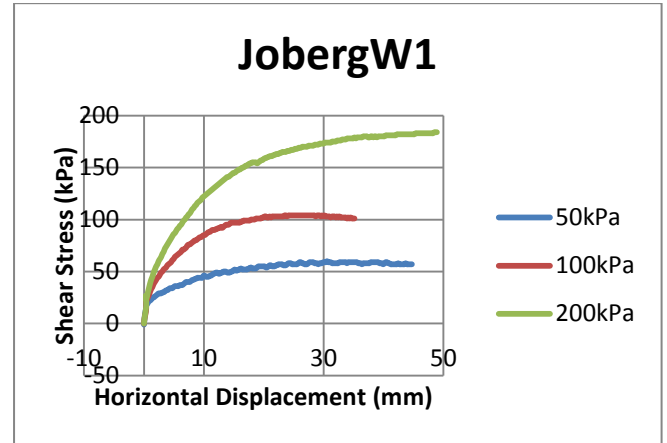


Figure 14: Shear tests measurements for sample JobergW1 in water saturated condition.

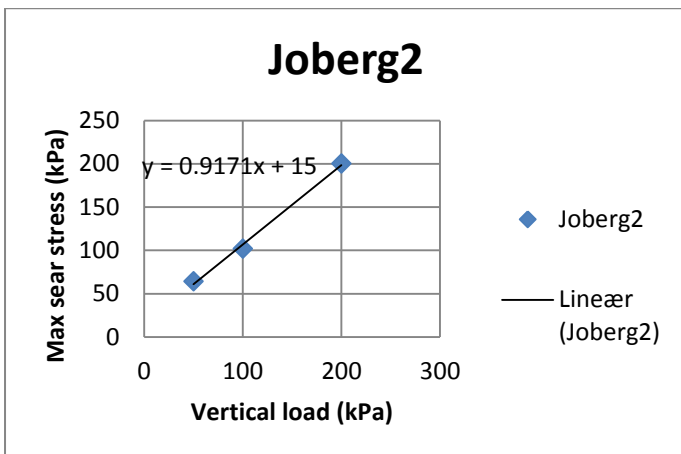


Figure 15: Vertical load (kPa) versus maximum shear stress (kPa) based on shear test results for sample Joberg2 in laboratory-dry condition.

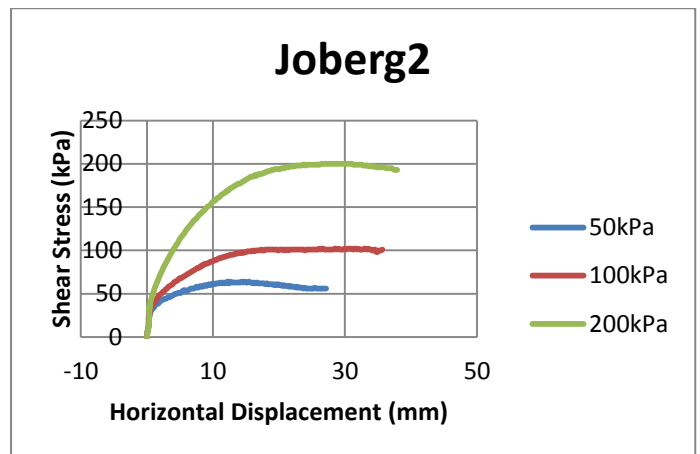


Figure 16: Shear tests measurements for sample Joberg2 in laboratory-dry condition.

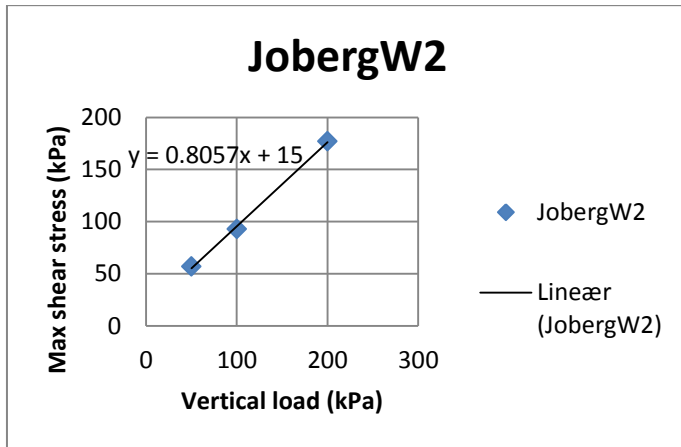


Figure 17: Vertical load (kPa) versus maximum shear stress (kPa) based on shear test results for sample JobergW2 in water saturated condition.

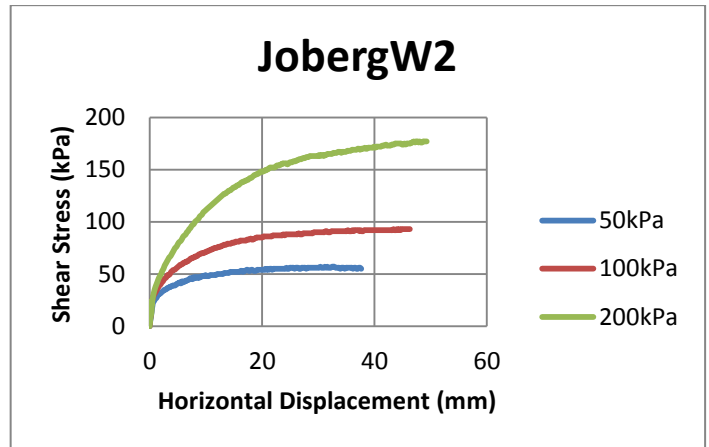


Figure 18: Shear tests measurements for sample JobergW2 in water saturated condition.

### 5.2.2 Density analysis

The unit weight,  $\gamma$  and water content,  $\theta_d$  were found from a test sample of water saturated material.

$$\gamma = 21.7 \text{ kN/m}^3$$

$$\theta_d = 9.2 \%$$

### 5.2.3 Sieve analysis

Sieve analysis is performed according to the standard NS-EN 933-1 (1998). The grain size distribution curve carried out on one soil material sample from Joberget is presented in Figure 19.

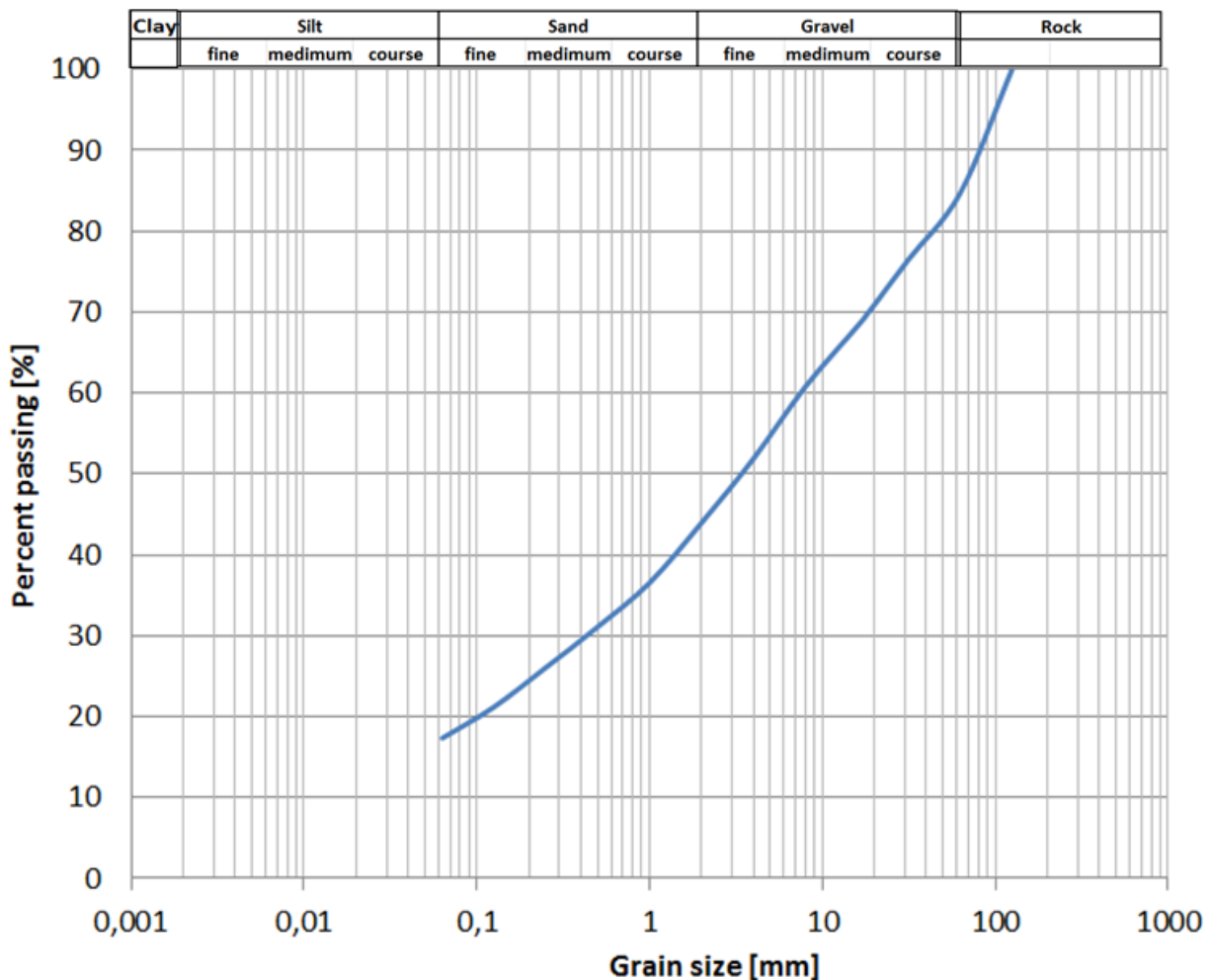


Figure 19: Grain size distribution curve found with a sieve analysis.

### 5.3 Triaxial testing

There are three primary triaxial tests which can be conducted in the laboratory. These are the Unconsolidated Undrained test (UU), the Consolidated Undrained test (CU) and the Consolidated Drained test (CD). The CD test is performed in this study to simulate the stress paths followed by soil elements in the tunnel that fails under drained conditions. Additionally, drained triaxial tests are conventionally performed on coarse sands and gravel because these soils normally behave drained in situ (Nordal, 2013).

The triaxial testing is performed according to the ASTM standard D7181 – 11.

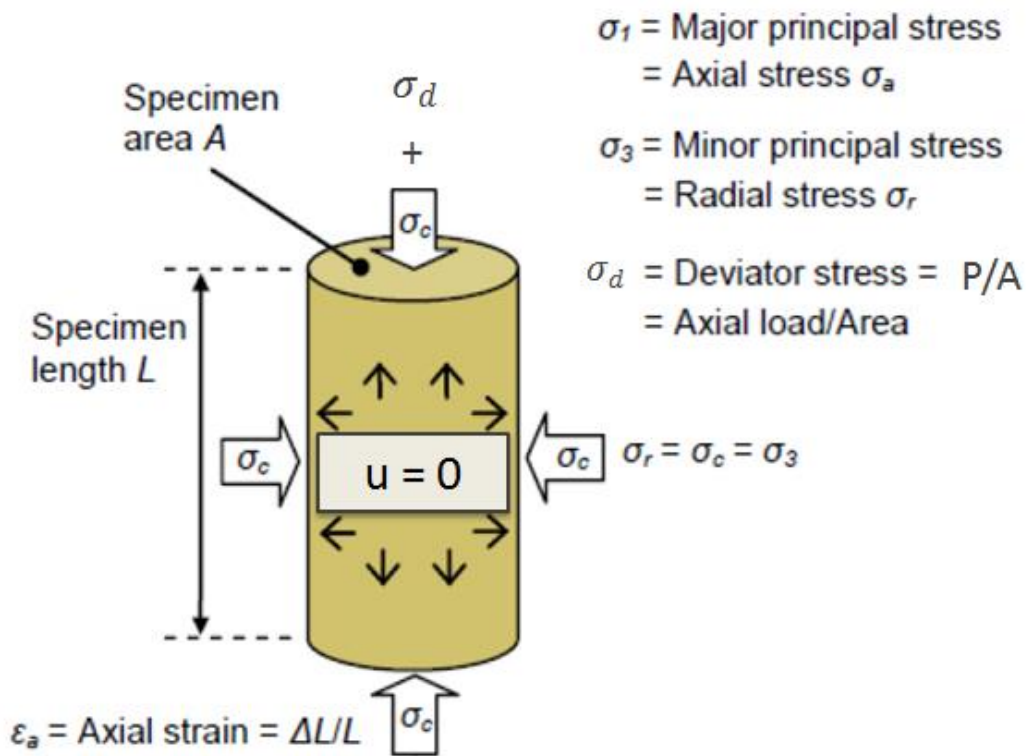
#### 5.3.1 Theory

Strength and stress-strain relationship of a cylindrical specimen of an intact or a reconstituted soil is determined with the triaxial test. The specimen is consolidated, subjected to a confining pressure and loaded axially with a constant rate while axial load, axial and radial strain are measured constantly. It is important in a CD test to apply the axial load with a very slow rate, to ensure dissipation of excess pore water pressures (ASTM, 2011b).

The soil specimen is saturated and compacted allowing the soil response to be observed under conditions that approximate those in situ. The specimen is 150 mm in diameter and 220 mm in height following compaction.

The confining stress  $\sigma_c$ , equal to the radial stress  $\sigma_r$  and the minor principal stress  $\sigma_3$ , is applied by pressurising cell fluid or air. By applying an axial load to the soil, a deviator stress,  $\sigma_d$  (principal stress difference) is generated, given in Equation 1. The specimen stress state during triaxial compression can be seen in Figure 20.

$$\sigma_d = \sigma_a - \sigma_c = \sigma_1 - \sigma_3 \tag{1}$$



**Figure 20: Stresses applied to a soil specimen during triaxial compression. The figure is modified after Rees (n.d.).**

Time of failure may include the peak deviator stress, observation of constant stress and excess pore pressure/volume change or a specific value of axial strain being reached. At least three tests with different confining pressure should be performed on each soil specimen (Rees, n.d.).

The modulus of elasticity or Young’s modulus, E is defined as the ratio of axial stress change,  $\Delta\sigma$  to axial strain change,  $\Delta\epsilon_a$  given in Equation 2. E is specific for every material and defines the ability of elastic deformation of a material (Myrvang, 2001). The value of E can be found from the slope of a tangent or secant to the curve plotted in a stress-strain diagram.

Commonly, the average stiffness,  $E_{50}$  at 50 % of peak strength is calculated, illustrated in Figure 21 (Nordal, 2013).

$$E = \frac{\Delta\sigma}{\Delta\epsilon_a} \quad (2)$$

$$\epsilon_a = \frac{\Delta l}{l_0} \quad (2.1)$$

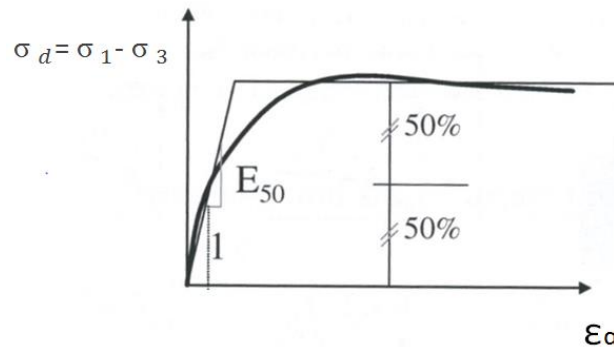
$\Delta l$  = change in axial length

$l_0$  = original axial length

$$\sigma = \frac{P}{A_0} \quad (2.2)$$

$A_0$  = initial cross-sectional area

$P$  = applied axial load

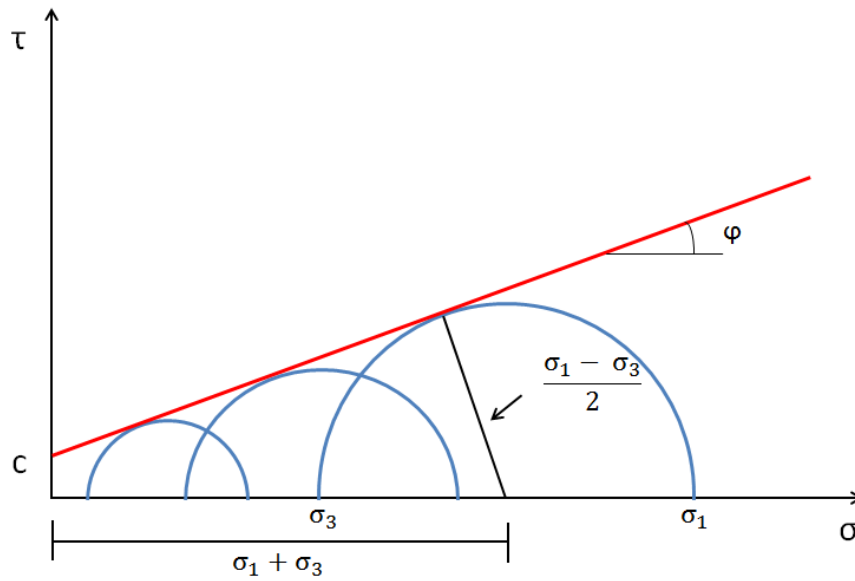


**Figure 21: Defining average stiffness,  $E_{50}$  on the curve half way to failure of a drained triaxial test on sand (Nordal, 2013).**

When a cylinder is compressed axially, it will expand radially (Gercek, 2007). This phenomenon is material dependent and known as the *Poissons effect*, defined by Poisson's ratio. Poisson's ratio,  $\nu$  is the negative of the ratio of radial strain,  $\epsilon_r$  to axial strain,  $\epsilon_a$  given in Equation 3. For most common rock materials the Poisson's ratio ranges from 0.0 to 0.5, where 0.5 is the ratio of a perfectly incompressible material.

$$\nu = - \frac{\Delta\epsilon_r}{\Delta\epsilon_a} \quad (3)$$

When plotting normal stress versus shear stress, Mohr circles can be constructed from the principal stresses measured at failure. The circles are drawn with a radius of one half of the deviator stress at failure, with the center at one half of the sum of the major and minor principal stresses. When three Mohr-circles are drawn, the Mohr-Coulomb failure envelope can be plotted intersecting the periphery of the circles as illustrated in Figure 22. The intercept of the Mohr-Coulomb failure envelope on the shear stress axis is defined as the cohesion. The friction angle can be found from the angle of the failure envelope, illustrated in Figure 22 (Rahardjo et al., 2004)



**Figure 22: Mohr failure envelope in red indicating cohesion,  $c$  and friction angle,  $\phi$ . The figure is modified after Nordal (2013).**

### 5.3.2 Working method

The consolidated drained triaxial tests are performed on reconstituted test specimens. Firstly, the soil material was sieved with a 31.5 mm sieve, following standard procedure of the largest particle size being smaller than 1/5 of the total specimen. The material less than 31.5 mm was used to prepare the test specimens with a water content of 5 % and a unit weight of  $21.7 \text{ kN/m}^3$  in order to be similar to its in situ condition. One test specimen was divided in five equal portions, sealed in plastic bags and left overnight to allow for equalization of water content of the soil. The material was subsequently moved from the plastic bags into the cylinder in five layers. Every layer was compacted with vibration amplitude of 5, meaning 0.5 mm motion, in 20 seconds. The vibration apparatus used for compacting can be seen in Figure 23.



**Figure 23: Second layer of material under compaction with a vibration apparatus.**

To provide drainage at each ends, a base and porous disc were installed on the bottom of the specimen and a top-cap and a porous disc on the top of the specimen. The material in the cylinder was transferred into a rubber membrane by an apparatus, seen in Figure 24 together with a vacuum producing suction, seen in Figure 25. The rubber membrane protects against leakage and makes radial deformation possible. The membrane was sealed to the top-cap and the base with rubber O-rings to prevent specimen having contact with cell fluid (ASTM, 2011b).





**Figure 24: The laboratory technician demonstrates how the material was transferred from the cylinder into the rubber membrane.**



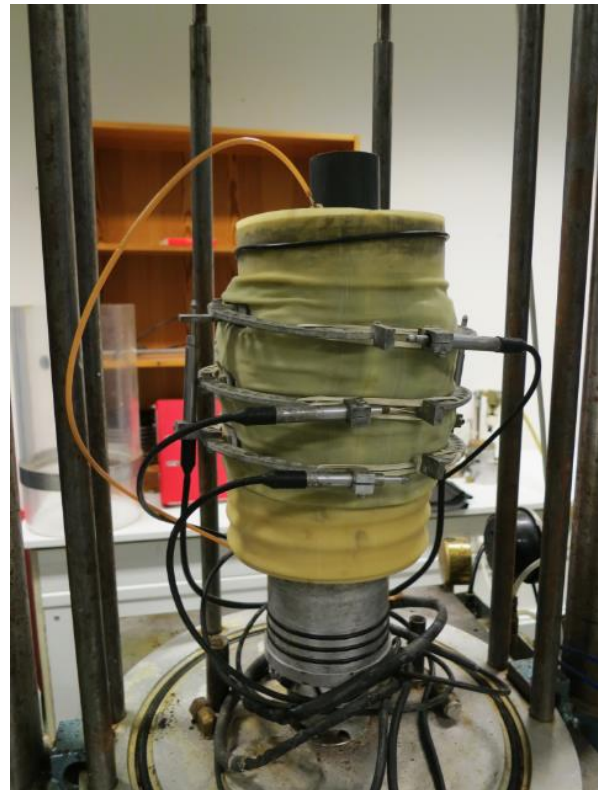
**Figure 25: Together with vacuum the material was slowly screwed into the rubber membrane. The black O-rings were placed at the top and the bottom.**

The test specimen was placed inside the triaxial apparatus as shown in Figure 26. Two axial Linear Variable Displacement Transducers (LVDT), were installed at each side of the specimen. One radial LVDT was installed in the middle of the specimen, and two radial LVDT were installed 50 mm from the middle. When all LVDTs were calibrated with a custom-built data program by Einar Værnes (Hoff, 2014), the cylindrical specimen was encased by a chamber and consolidated under a selected isotropic confining pressure. While the specimen was subjected to a confining pressure, the axial load piston was brought into contact with top-cap.

The specimen was loaded axially with a constant rate of approximately  $d\sigma/dt = 0.12$  kPa/min for the tests with confining pressures of 50 kPa and 100 kPa. With a reasonable assumption that tests under higher confining pressure may take more load, the rate was increased to  $d\sigma/dt = 0.16$  kPa/min for the test with confining pressure of 150 kPa. Strain and stresses were constantly measured by a PC controller until a assumed failure (ASTM, 2011b). An example of a test specimen at failure can be seen in Figure 27.



**Figure 26:** The triaxial apparatus, Møyfrid showing the test specimen inside the chamber with installed LVDTs . This test specimen is constantly loaded with a confining pressure of 50 kPa.



**Figure 27:** An example of a test specimen at failure.

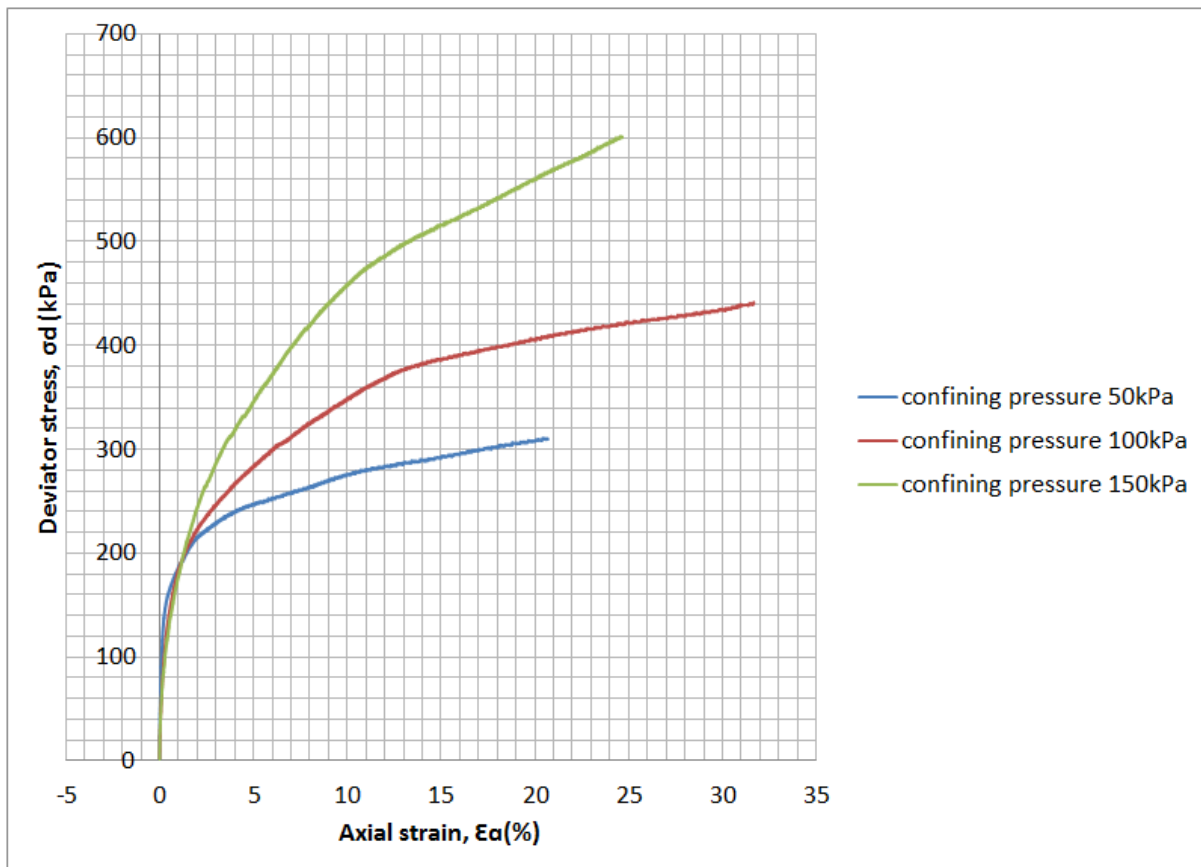
Three tests were performed on three different test specimens with confining pressures of 50 kPa, 100 kPa and 150 kPa. Air pressure was applied during the test with confining pressure at 50 kPa. To achieve higher confining stresses, pressurised cell fluid was used.

A graph based on strain versus deviator stress was carried out and the Young's modulus,  $E$  was found from selected secants of 2% strain on the each graph. The Poisson's ratio was found from the measurements of the radial and axial strain. Finally, the Mohr failure envelope was found from the construction of three Mohr circles and friction angle and cohesion was estimated.

### 5.3.3 Results

- ***Young's Modulus***

The measured axial strain is plotted versus the applied deviator stress for the three triaxial tests with different confining pressure of 50 kPa, 100 kPa and 150 kPa shown in Figure 28. Usually, the mean values of the axial LVDTs are used to carry out this graph. During testing, only one axial LVDT for every test was in position the whole time to measure axial strain. Hence, this axial LVDT is used, instead of the mean value, to carry out the stress-strain graphs.



**Figure 28: Stress-strain graphs from three triaxial tests with different confining pressures.**

The calculated values of the Young's modulus from the three tests with different confining pressure are presented in Table 4. The values of  $E$  are found from the slope of the secant of 2% strain for each triaxial test defined in the stress-strain graphs in Figures 29, 30 and 31.

**Table 4: Young's modulus,  $E$  for different confining pressures.**

Confining pressure [kPa]	$E(2\%)$ [MPa]
50	10.7
100	11.2
150	12.2

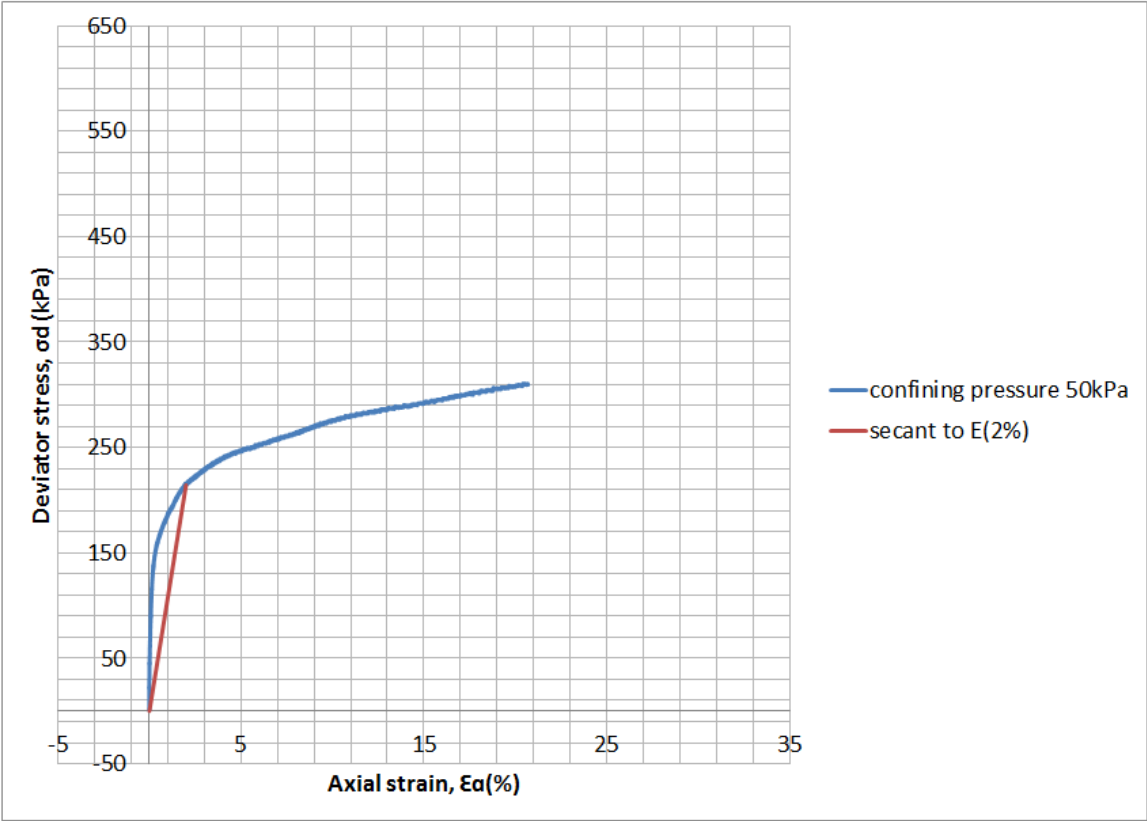


Figure 29: Stress-strain graph of the triaxial test with confining pressure of 50 kPa. The red line defines the secant to 2% strain used in the calculation of  $E(2\%)$ .

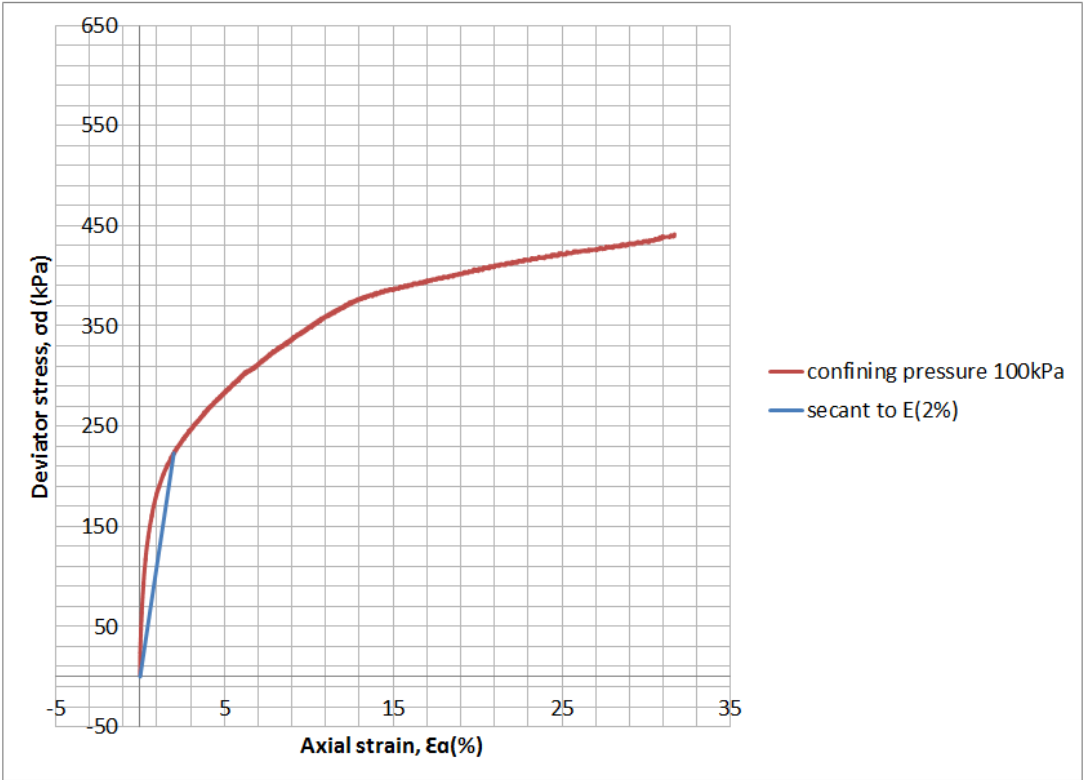
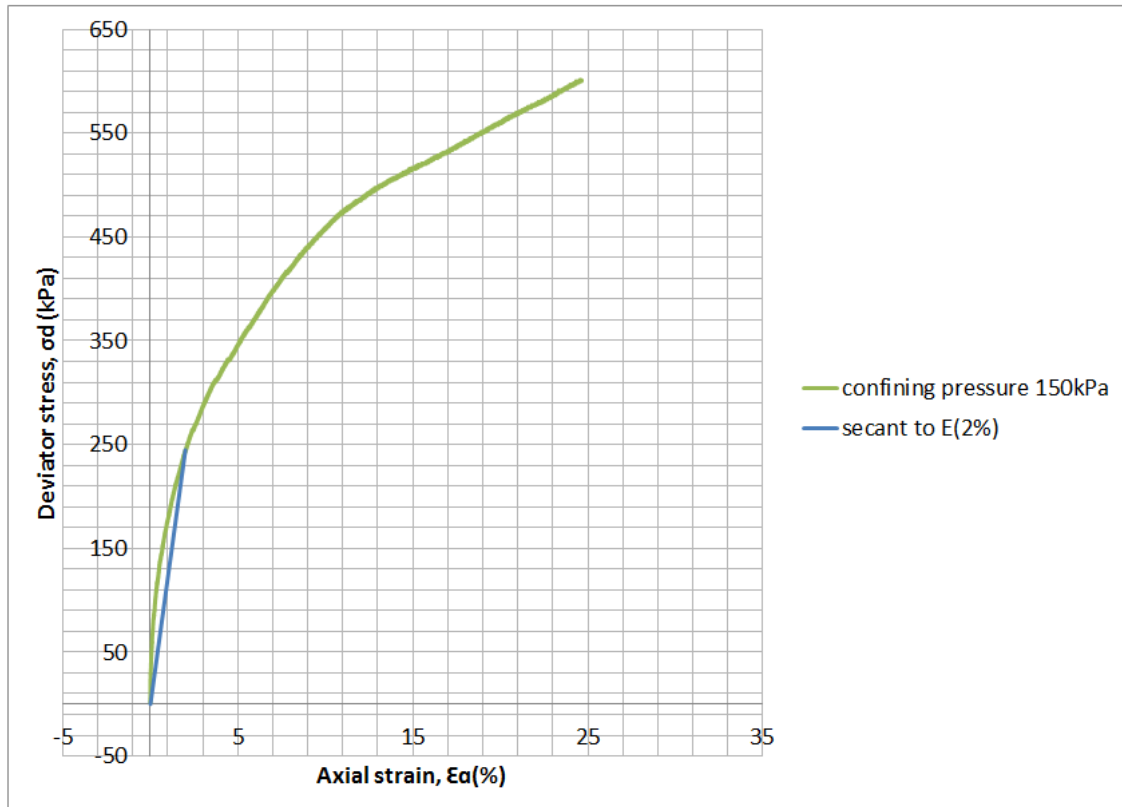


Figure 30: Stress-strain graph of the triaxial test with confining pressure of 100 kPa. The blue line defines the secant to 2% strain used in the calculation of  $E(2\%)$ .



**Figure 31: Stress-strain graph of the triaxial test with confining pressure of 150 kPa. The blue line defines the secant to 2% strain used in the calculation of  $E(2\%)$ .**

- ***Poisson's Ratio***

Calculations of Poisson's ratio show considerable variations. Very few values lay within the range 0.0 to 0.5 and no reasonable Poisson's ratio are found for the interesting strain at 2%. Hence, no useful results for the Poisson's ratio were able to be obtained from these triaxial tests.

- ***Mohr Coulomb***

Mohr circles can be constructed from the principal stresses measured at failure. Since there are no obvious failures seen from the stress-strain graphs in Figure 28, a deformation of 10 % is chosen to find the Mohr circles. Calculations of the Mohr circles are presented in Table 5. The x and y values give the intercept of the circles centum on the normal stress axis. Together with the radius, these values are used to find coordinates on the circumference of the circles for every 10<sup>th</sup> degree with trigonometry, presented in Appendix A2.

**Table 5: Mohr circle calculations.**

<b>Confining pressure [kPa]</b>	<b><math>\sigma_1</math> [kPa]</b>	<b><math>\sigma_3</math> [kPa]</b>	<b>x [kPa]</b>	<b>y [kPa]</b>	<b>Radius [kPa]</b>	<b><math>\sigma_1 - \sigma_3</math> [kPa]</b>
<b>50</b>	270.3	50	160.2	0	110.2	220.3
<b>100</b>	343.1	100	221.5	0	121.5	243.1
<b>150</b>	447.4	150	298.7	0	148.7	297.4

The Mohr failure envelope is difficult to fit, as no possible line intersected the periphery of all the circles. The best fit of the Mohr failure envelope together with the calculated cohesion and friction angle is seen in Figure 32. A red dotted line is drawn in the figure to show another possible failure envelope which may corresponds better to the material.

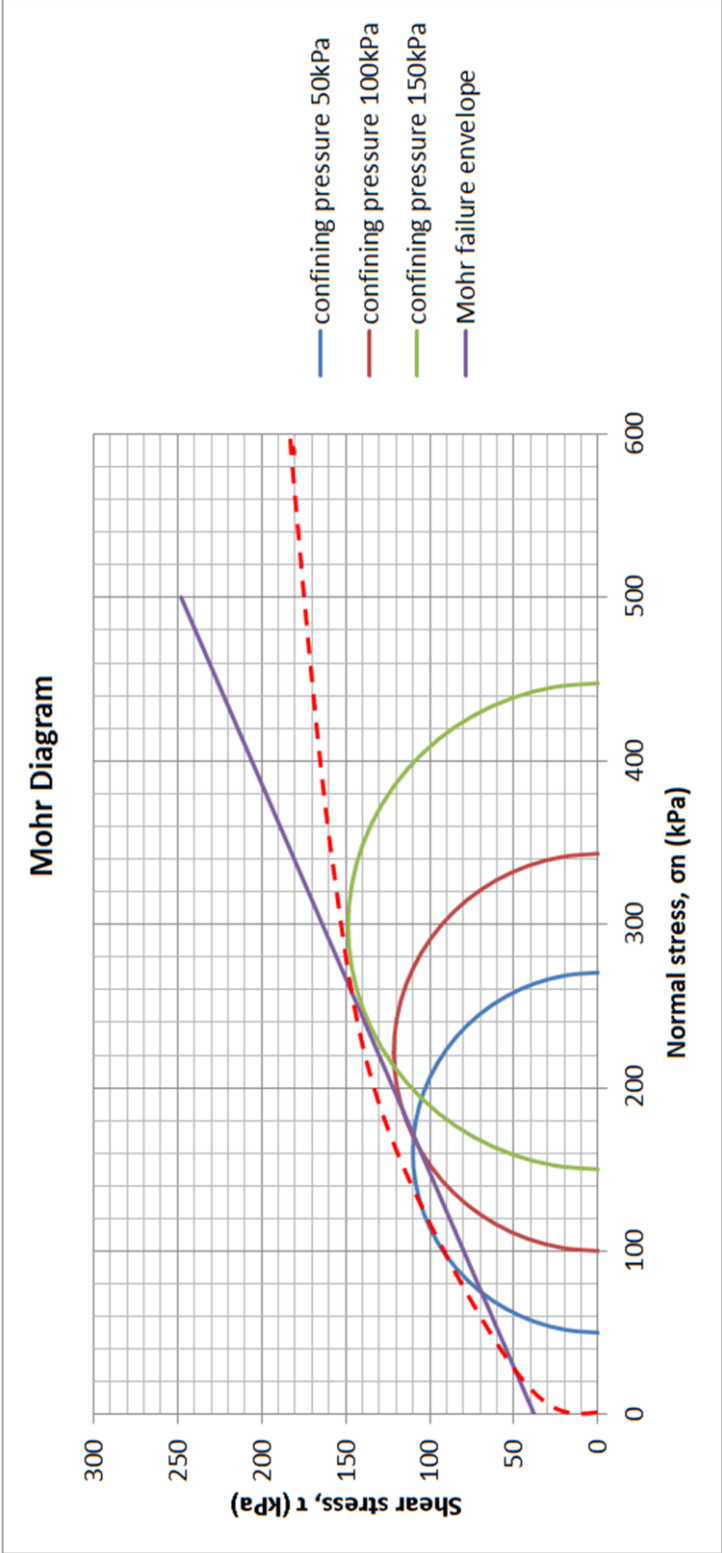
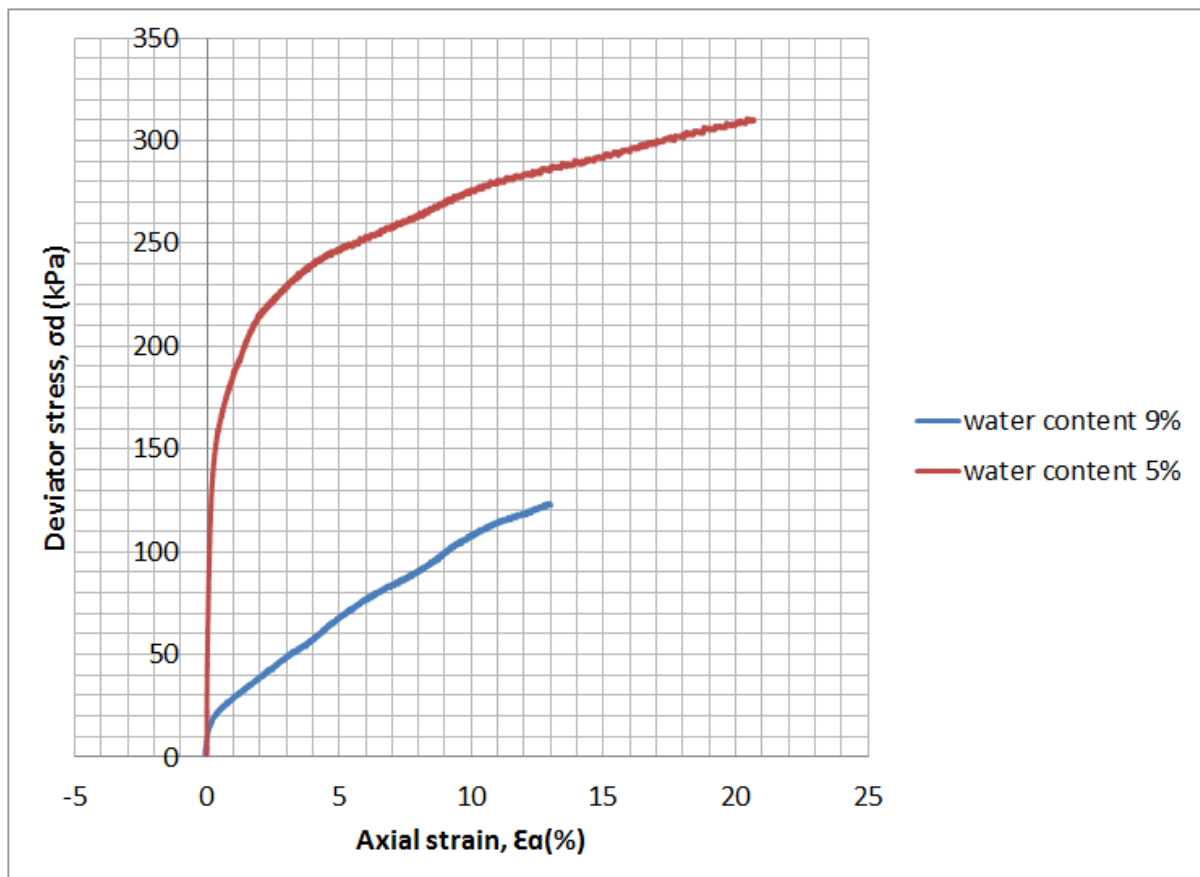


Figure 32: Mohr diagram with calculated Mohr circles and the fitted Mohr failure envelope. The red dotted line is an assumed failure envelope.

- **Water content**

Due to limited information about the water content in the moraine material at Joberget, it was difficult to find the required water content for the triaxial tests. Langåker (2013) implies a water content of 9.2 % found from one reconstituted sample during density analysis. Hence, the first triaxial test at 50 kPa confining pressure was carried out with a water content of 9%. Based on recommendations from Gaut (2014) and Brattli (2014), a new water content of 5 % was chosen and used in the rest of the triaxial tests. The stress and strain measurements from two triaxial tests at a confining pressure of 50 kPa with different water contents of 5 % and 9 % is shown in Figure 33.



**Figure 33: Stress-strain graphs of two triaxial tests at confining pressure of 50 kPa with different water content of 5% and 9%.**



## 5.4 Discussion

### 5.4.1 Soil Characteristics

The shape of the grain size distribution curve of the soil indicates a poorly sorted and highly heterogeneous material, typical for moraine materials. The unit weight of the soil was found to be approximately  $21.7 \text{ kN/m}^3$ . Commonly, a unit weight of  $20 \text{ kN/m}^3$  is assumed for soil materials. The soil at Joberget has a high packing degree, resulting in low porosity and high unit weight. Therefore, a unit weight higher than the general assumption for soil materials is considered to be a good estimate.

### 5.4.2 Elasticity

The elasticity of the moraine material at Joberget is measured with the triaxial test and defined by Young's modulus and Poisson's ratio.

Generally in soil mechanics, Young's modulus is found at 50% of the peak strength in a stress-strain curve. Since there is no peak strength revealed in the stress-strain curves obtained from the triaxial tests,  $E$  is calculated for a selected strain of 2 %. The strain of 2 % was selected based on an assumption made by Sakurai (1983) about 2 % being the critical strain before adequate support is needed. The average value of  $E$  found at 2 % strain is  $11.4 \pm 0.6 \text{ MPa}$  which is similar to a loose sandy soil, with estimated  $E$  of 10-50 MPa (Zhu, 2012). Bearing in mind that the material is an over-consolidated moraine material with big boulders that will increase the stiffness, a higher estimate of Young's modulus is more likely such as estimated  $E$  for gravel soil of 70-170 MPa (Zhu, 2012).

$E$  increases with increasing confining pressure. This is logical since interlocking of particles improves, resulting in increasing strength and stiffness. However, the increase at 2% strain is very little in comparison to possible  $E$ -values at higher strain rates. The soil material tested responds rapidly on consolidation due to the material characteristics. The short term displacements in this study may therefore be more relevant than the long term displacements.

No reasonable Poisson's ratios are obtained from the triaxial testing. In practice it is often difficult to determine Poisson's ratio from the axial strain and radial strain. The reason for this might be the uncertainties in the measured radial strain. Some typical ranges of Poisson's ratio for granular soils are given by Gercek (2007). The moraine material can be compared to granular soil of sand and gravel with Poisson's ratio ranging from 0.15 - 0.35.

### 5.4.3 Strength

The main mechanical properties of a soil used in stability analysis are the strength parameters, friction angle and cohesion (Lebourg et al., 2004).

The average friction angle and cohesion for material tested in the shear box in water saturated condition are  $39,2^\circ \pm 0,3^\circ$  and  $17.5 \pm 2.5 \text{ kPa}$  respectively. The average values of internal friction angle and cohesion for lateral moraine materials may vary from  $20^\circ - 36^\circ$  and  $0 - 80 \text{ kPa}$  respectively, confirming the great variability of mechanical properties (Lebourg et al., 2004). Since the material at Joberget is classified as an over-consolidated sub-glacial moraine,

the friction angle may be higher due to heavy consolidation resulting in a higher degree of packing.

The Mohr Coulomb failure criterion is carried out to find the friction angle and the cohesion from the triaxial test. Since the curve in the stress-strain diagram most likely would have increased after the test was stopped, no failure from the curve was possible to find. Instead, stresses at 10 % strain were used in the construction of the Mohr circles. This strain was chosen being after the breaking point of the graphs and closer to failure. At higher strains, increased cross section may change the initial stress calculated, resulting in errors in measurements.

The best fit of the Mohr failure envelope intersects the periphery of two circles and crossing one circle. It should be emphasized that Mohr Coulomb failure criterion is a simplification of the reality. Hence, it is difficult to find a line that perfectly intersects every circle periphery. From the best fitted Mohr failure envelope, the friction and cohesion was estimated to be approximately  $23^\circ$  and 38 kPa respectively.

Firstly, based on the fact that overconsolidated moraines possess high friction angles, the average friction angle obtained from the shear box test is assumed to be more realistic than the friction angle obtained from the triaxial test. Secondly, the repeating results make the shear box test results more reliable. Finally, the strength parameters found with the triaxial test are found with the simplified Mohr Coulomb failure criterion which may provide uncertain results due to the simplification of reality.

The soil obtains no real tensile strength, even though the cohesion indicates so. According to Hoff (2014) the failure line will reach zero when the confining pressure reaches zero and the friction angle at low stresses are generally higher than those at lower stresses. This is shown by the red dotted line in Figure 32.

#### **5.4.4 Water content**

The first triaxial test was carried out with a water content of 9 % based on result from the project assignment by Langåker (2013). The test results gave too low strength and stiffness based on what is normally estimated for overconsolidated moraine materials. According to Gaut (2014) and Brattli (2014) water content depends on the degree of packing and the grain size distribution of the material. Generally, it is assumed that the water content of sand varies between 3 – 8 %. Since the moraine material at Joberget also contains gravel and holds a high degree of packing, a water content of 5 % was assumed in order to be more realistic. The triaxial results confirmed this assumption, providing more reasonable estimates of the elasticity.

According to Nilsen and Palmstrøm (2000) the main effect of water is the reduction of material strength. The effect of water on the soil material is very well illustrated in Figure 33, indicating a great reduction in strength for small changes in water content. Extra care regarding water inflow during tunneling should therefore be taken. It should also be emphasized that the material tested are collected above the ground water table and higher water content may occur.

### 5.4.5 Sources of error

A source of error to take into account is the manual work, performed to obtain in situ conditions for the laboratory tests. It is impossible to reconstruct a soil sample identical to in situ condition. This deviation may produce uncertainties when applying the test results to describe the in situ condition. For example, in the preparation of triaxial test samples, sieving may change the initial material due to some material being excluded from the test sample. Also, compaction by vibration may produce errors in the results, due to a possible non-uniform density with more fines at the bottom of the sample.

The fact that the size of a material sample is only a small portion of the moraine material situated at Joberget, is another important source of error. Moraines are generally unsorted and heterogeneous materials, characterized by rock particles of all sizes. The Lithology, petrography and the spatial distribution of blocks in the moraine are also heterogeneous. Thus, a large sample is often necessary to achieve representative results of a moraine (Lebourg et al., 2004)

Further laboratory tests should be carried out to achieve more confidence in the test results. Due to limited capacity of the laboratory, this was not possible in this study. However, with most results being comparable to similar test results presented in literature, the laboratory results provide a good picture of the mechanical factors and the characteristics of the sub-glacial moraine at Joberget.



## 6 Stability analysis in soil tunneling

Stability analysis of the tunnel and surroundings in both construction and permanent phase, are important in soil tunneling. Such analysis can be used to avoid collapses due to excessive deformations or failure of supporting structures. Tunnel stability may depend on in situ stresses, strength and stiffness of soil and strength and stiffness of the support (Nordal, 2013).

Stability in tunneling is strongly connected to a required level of safety and will vary with the use of excavation and support (Nilsen and Palmstrøm, 2000). The stability of an underground construction is evaluated during the design process. There are four different geotechnical design methods recommended in Eurocode 7 (Polimac, 2007):

- *Design by calculation*
- *Design by Prescriptive Measures*
- *Design using load tests and test on experimental models*
- *Design using the Observational Method*

The design method based on calculations is the most common method carried out for stability analysis in geotechnical projects, and is performed in this study. The design method by prescriptive measures is understood as a method based on experiences and normal practise. According to Eurocode 7, this method should only be used if calculations are inaccessible or unnecessary. The design method based on load tests and experimental models is barely used in geotechnical problems in Norway. The final method, the observational method is more commonly used for checking results and predictions in the geotechnical design than as an independent design, and is basically based on monitoring during excavation (Nilsen et al., 2011).

The *design by calculation* method may be categorised in the following methods (Nilsen et al., 2011):

- *Analytical methods*: Simple mathematical calculation methods like limit equilibrium.
- *Semi-empirical methods*: Failure criterions such as Hoek-Brown or Mohr-Coulomb based on systematization of collected data, which can be applied in analytical or numerical methods. Also, methods based on empirical experiences are included such as rock mass classification systems like the Q- and the RMR-system.
- *Numerical methods*: Use of software programs like Phase<sup>2</sup> to simulate engineering geological problems.

The analytical methods based on limit equilibrium are more commonly carried out for slope stability and will therefore not be discussed in this thesis. However, the semi-empirical method and the numerical method can be used to evaluate the stability in the Joberget soil tunneling section.

## 6.1 Support analysis for tunneling in weak rock masses

Rock support is provided to improve stability during and after tunneling, and is designed based on in situ ground condition. Generally, the support is divided in primary support, installed to ensure safe working condition and permanent support, installed to meet the requirements of the project life time (Nilsen and Palmstrøm, 2000).

Misjudgements in the design of support systems for tunneling in weak rock masses may lead to very costly failures due to sudden and uncontrolled collapses. Hence, tunneling in weak rock masses such as soil is inherently challenging. Support systems should in addition to have sufficient capacity, be installed in a sequence that does not allow uncontrolled deformation. Also, probe hole drillings should be made mandatory ahead of the advancing face when weak rock masses are suspected (Hoek, 1999).

In order to understand the rock-support interaction in weak rock masses, it is recommended by Hoek (2007a) to examine basic concepts of how the surrounding rock mass deforms and how the support systems acts to control this deformation. Because soft material has ductile behaviour, deformation can be a good indicator for tunnel instability.

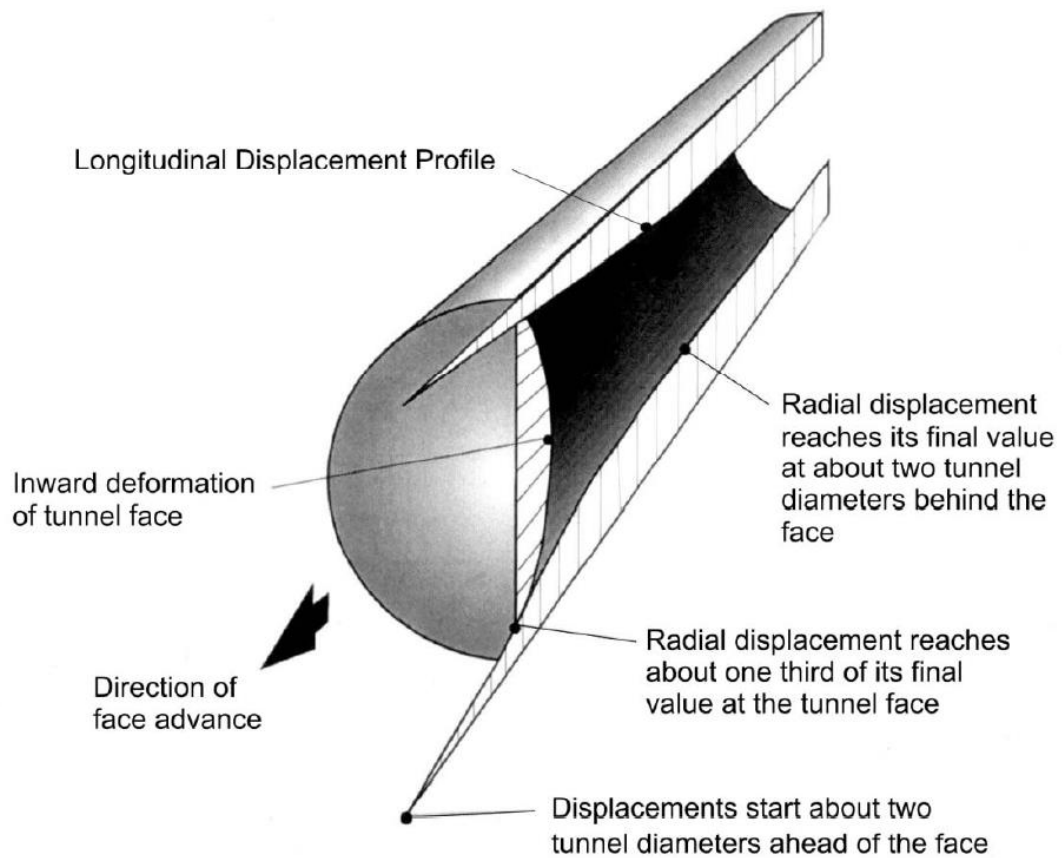
### 6.1.1 Critical strain

Tunnel strain is defined by the ratio of tunnel convergence to tunnel diameter. Sakurai (1983) suggested that the stability of tunnels can be found on the basis of the strain in the surrounding rock mass. A critical strain of approximately 2 %, represents the boundary between stable tunnels that require minimal support and unstable tunnel that require special consideration for support designs. This concept has proved to correspond well with many practical tunnel problems and is a good indication that tunnel stability problems increase with increasing strain level (Hoek, 1999).

### 6.1.2 Tunnel deformation and rock-support interactions

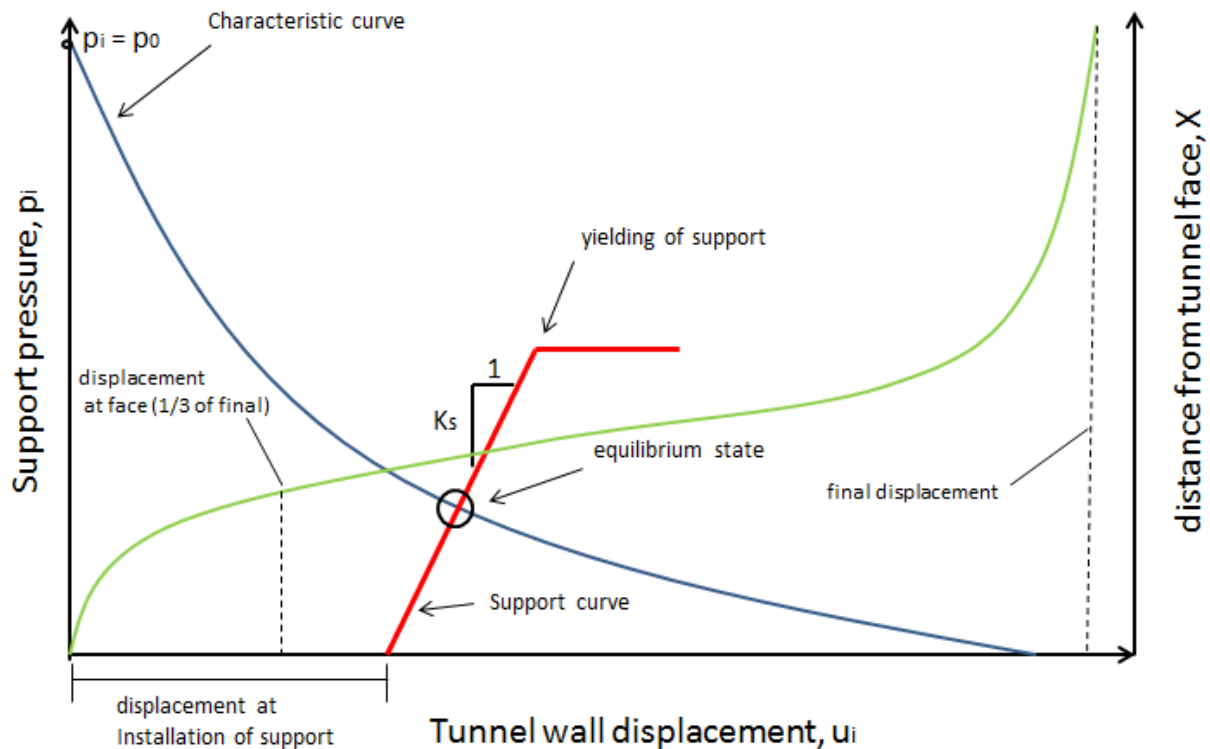
A three-dimensional finite element analysis of tunnel deformation, based on the assumption of a circular tunnel subjected to a hydrostatic stress field where the horizontal stresses equals the vertical stresses, is presented in Figure 34. According to Hoek (1999), the assumption of a hydrostatic stress field is reasonable in a weak rock mass, since it has already undergone failure. Therefore, it is incapable of sustaining significant stress differences.

It is indicated in Figure 34, that elastic deformation of the rock mass starts about two tunnel diameters ahead of the tunnel face and reaches its maximum at about two tunnel diameters behind the face. This is based on the assumption that deformation occurs immediately upon excavation of the face, and that the surrounding homogeneous weak rock mass behaves as an elastic-perfectly plastic material (Hoek, 2007a).



**Figure 34: Elastic deformation in the rock mass surrounding an advancing tunnel (Hoek, 2007a).**

The relationship between internal support pressure,  $p_i$  and tunnel deformation,  $u_i$  is generally presented by a characteristic curve of the rock mass and the support curve in Figure 35.  $p_i$  depends upon the stiffness,  $K_s$ , the maximum load bearing capacity of the support and the distance from the face at the time of installation. Figure 35 shows that the support pressure increases with increasing deformation, until an equilibrium state where a support pressure is established between the tunnel wall and support elements. The curve is based on the assumption that the rock at the tunnel face provides an initial support pressure equal to the in situ stress,  $p_0$ . It is also assumed that the surrounding rock mass fails with no increase in volume. This is a reasonable assumption, since weak rock masses are likely to crush rather than fail in a dilatant manner. The longitudinal displacement profile included in Figure 35, allows tunnel wall displacement at a given distance behind the face to be determined (Hoek, 2007a).



**Figure 35: Rock-support interaction plot with the blue characteristic curve, red rock support curve and green longitudinal displacement profile. It is assumed that the rock at the tunnel face provides an initial support pressure equal to the in situ stress,  $p_0$ . The figure is modified after Hoek (2007a).**

The rock-support interaction analysis may be a useful tool for understanding the process of rock mass deformation around an advancing tunnel and the response of the support installed. Due to the many assumptions made in the characteristic curve, it should be used as a very crude first estimate of possible support requirements and not to investigate details of excavation and support. In cases with difficult tunneling conditions such as for soil tunneling, excavation details are required to analyse possible failures and may be provided by more comprehensive analysis, like numerical analysis (Hoek, 2007a).



## 7 Empirical analysis

### 7.1 Experiences with soil tunneling

Soil is known as a weak, water bearing and unstable excavation material which may lead to problems during tunneling. Instability of the face, unsupported span and water leakage are typical problems in soil tunneling. Hence, additional measures to ensure stable condition during tunneling and to reduce construction induced deformations are necessary (Volkman and Schubert, 2008). Different measures like spiling, grouting, jet-grouting, artificial ground freezing and pipe umbrella are commonly used during soil tunneling.

Based on experiences from tunneling in weakness zones in Norway and international soil tunneling evaluated in a literature study by Langåker (2013), a summary of the characteristic of the different support methods are given in Table 6. The choice of support method depends on geotechnical characteristics of the soil together with safety, costs and benefits of intervention. These values are considered through six different parameters in the Table 6. The flexibility shows how well a method adapts to various geological conditions and is related to field of application. The ease of installation is based on the machine dimension, type and cost and the need for specialised workers.

**Table 6: Comparison of different support methods commonly used in soil tunneling based on the evaluation of six different parameters. The figure is modified after Pelizza and Peila (1993) and is presented in project assignment by Langåker (2013).**

Support methods	Flexibility	Feasibility	Ease of installation	Speed of installation	Field of application	Monitoring
<b>Grouting</b>	Medium (require suitable ground)	Medium (necessary to carry out tests)	Medium	Low	Sand, gravel	Possible to difficult
<b>Jet grouting</b>	Medium	Medium	Difficult	Medium	Various soils (difficult in soil with boulders)	Difficult
<b>Spiling</b>	High	High	Easy	High	Various soils (from moraine to hard rock)	Possible
<b>Pipe umbrella</b>	Very high	High	Easy to medium	High	Various soils (from moraine to hard rock)	Possible
<b>Freezing</b>	Medium (require saturated ground)	Medium	Difficult	Medium	Saturated soil	Possible to difficult

In addition to the support methods described in Table 6, a common procedure in soil tunneling is the use of shorter round lengths and partial face excavations. This is performed to

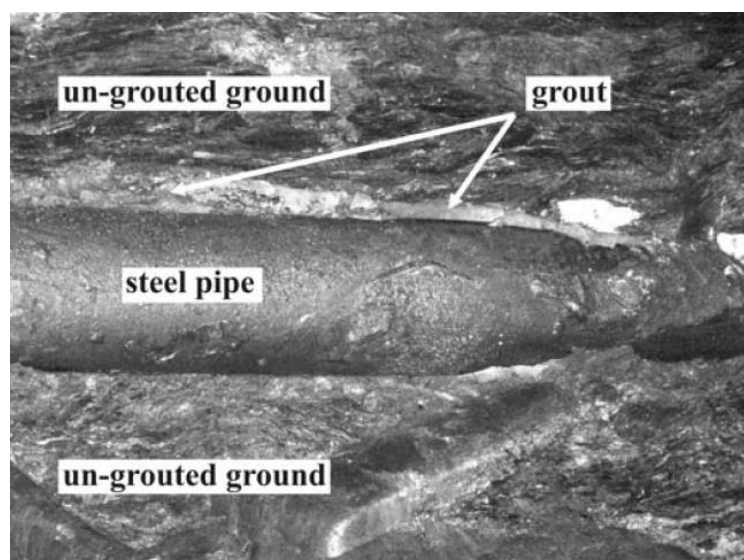
achieve better control of instability and to apply support faster due to a limited stand-up time (NFF, 2008). Partial face excavations and shorter round lengths rely on the fact that smaller faces and shorter span require less support. Also, the total stability is easier to control (Hoek, 2001).

### 7.1.1 Spiling versus Pipe Umbrella

The proposed pipe umbrella and the alternative spiling method for Joberget tunnel are feasible in various ground conditions and are less cost- and time consuming compared to the other primary support methods mentioned in Table 6. The pipe umbrella method and spiling are similar in many ways, but in difficult ground condition the pipe umbrella has several advantages. The pipes are often installed simultaneously with case-drilling method to prevent collapsing boreholes. With a larger pipe diameter, the steel pipes are stiffer and can take larger and heavier loads than the spile bolts. Drilling is more accurate and a bore length of 15-20 m without deviation is possible. The greatest advantage lies in the possibility to apply grout through the steel pipes and the surrounding material (NFF, 2008).

The grout is used to fill the pipe, the gap between the pipes and the open pores in soil or joints in rock that surround the pipes. This is shown in Figure 36. A grouted pipe can carry larger and heavier loads than an ungrouted pipe, and can better ensure that the tunnel cross section remains un-deformed. Grouted pipes also have an increases flexural strength and a 15 % decrease in flexural strength has been shown for pipes without grout filling (Volkman and Schubert, 2008). Grout in the gaps between the pipes, increases the load transmission between the ground and support. As a result, grout improves ground properties such as stiffness and strength.

A proper foundation length ahead of construction is important when traversing difficult ground conditions. The shorter and less stiff spiling bolt often become overloaded in such conditions. The pipe umbrella method is therefore preferred if sudden, unexpected changes in the ground may occur or if it is a mixed face condition (Volkman and Schubert, 2009).



**Figure 36: Grouted gap between the un-grouted ground and the steel pipe (Volkman and Schubert, 2009).**

### 7.1.2 The significance of water

During the summer of 2013, the pipe umbrella method was successfully carried out for the first time in a moraine section in the Holmestrand tunnel in Norway. However, there were some difficulties with instability due to the ingress of water during construction (Drageset, 2013).

The presence of water may cause serious stability problems during tunneling, particularly in weak rock masses. The effect of ground water on stability is strength reduction due to the physical deterioration of the components of the rock mass and the reduction of effective confining stress due to pore water pressure. The tunnel acts as a drain during construction (Hoek, 2001). A lowering of the ground water table may occur which can result in severe ground settlements on the surface. Additionally, drilling and charging can become difficult, whilst pumping will increase cost and roads may be damaged.

Water inflow into tunnels is often difficult to predict. If there are some uncertainties regarding water leakage, probe hole drilling ahead of the tunnel face and pre-grouting should be carried out. Grouting is performed to reduce permeability and prevent water leakage by sealing the weak rock mass. A sufficient counter-pressure may then be established (Nilsen and Palmstrøm, 2000).

## 7.2 Rock mass classification

Rock mass classification systems are beneficial during preliminary design stage of the project, when little detailed information is available. The classification systems can be used as a check list to ensure that all relevant information has been considered. More importantly, they can be used to determine rock mass strength and deformations and provide initial estimates of support requirements. However, considerable caution must be taken due to the limited detailed information available. According to Hoek (2007b), it is recommended to use at least two classification methods in early project stages.

The two most common rock mass classification systems are the Q-system and the RMR-system. These systems take geological, geometric and design parameters into account when estimating a value of the rock mass quality (Hoek, 2007b).

The Q-system and the RMR-system are applicable for field mapping and for classification of rock masses around underground openings. Estimations from field mapping are more uncertain than those mapped in underground openings due to difficulty with estimating parameters from surface. The reliability of the results of the field mapping will depend on available outcrops and the fact that the rock mass near the surface is often weaker due to weathering. Although this is true, some outcrops in Norway may look less jointed and weak due to former glacier abrasion and plucking that smoothens and polish the bedrock (NGI, 2013).

Jobberget soil tunnel consists of moraine and alternated phyllite. Since soil is a weaker and more challenging excavation material, and is situated in the tunnel heading where support measures are most important, only the Q- and RMR-value for the soil is evaluated in this study.

### 7.2.1 The Q-system

An analysis of a large number of case histories of underground excavations by Barton et al. (1974) revealed a useful correlation between the amount and type of permanent support and the rock mass characteristics, with respect to tunnel stability. The Tunneling Quality Index (Q) was proposed, being a function of six rock mass parameters, defined in Equation 4. Since the introduction of the Q-system, the system has been continuously improved and updated to keep up with the development of new knowledge, experiences and new support measures.

Based on estimation of the rock mass parameters in Equation 4, a Q-value for the rock mass can be found. Ratings for the six Q-system parameters are presented in Appendix A5 and are used in the equation to find the Q-value. The numerical value of Q varies on a logarithmic scale from 0.001 (exceptionally poor quality squeezing-ground) up to 1000 (exceptionally good and unjointed quality rock) (Barton et al., 1974). The Q-values are also related to different types and amount of permanent support and may in addition to be a rock mass quality documentation, be a guideline to rock support design decisions (NGI, 2013).

$$Q = \frac{RQD}{J_n} \times \frac{J_r}{J_a} \times \frac{J_w}{SRF} \quad (4)$$

*RQD = Rock Quality Designation*

*J<sub>n</sub> = Joint set number*

*J<sub>r</sub> = Joint roughness number*

*J<sub>a</sub> = Joint alteration number*

*J<sub>w</sub> = Joint water reduction factor*

*SRF = Stress Reduction Factor*

#### 7.2.1.1 Q-value for Joberget soil tunnel

The Q-value for the soil material in Joberget soil tunnel is estimated from field mapping during the pre-investigation stage. The estimated ranging of the parameters in the Q-system together with the calculated Q-value for the soil at Joberget is presented in Table 7.

**Table 7: Estimated ratings of the parameters in the Q-system to obtain the Q-value of Joberget soil tunnel.**

Parameter	Definition	Rating	Comment
RQD	Percentage of the sum of the length between natural joints of all core pieces more than 10 cm long (or core diameter x 2) in the total core length.	10	Weakly consolidated strongly weathered non-cohesive material that can be defined as soil should have a RQD-value of 10. In cohesive and soft material such as clay, the RQD-value should also be 10 because the material act as a weakness zone compared to the surrounding rock <sup>1</sup> .
J <sub>n</sub>	Joint set number	20	Soil is comparable to <i>Crushed, earth like rock</i> . <sup>2</sup>
J <sub>r</sub>	Joint roughness number	1	For soft rocks without joints a J <sub>r</sub> value of 1 should be given, if the material can be classified as soil <sup>1</sup> .
J <sub>a</sub>	Joint alteration number	8	<i>Zones or bands of clay, disintegrated or crushed rock, medium or low over-consolidated or softening fillings</i> . <sup>2</sup> This value is found to be the best approximation, since there are no joints in the soil.
J <sub>w</sub>	Water reduction factor	0.66	<i>Medium inflow with occasional outwash of joint filling</i> . <sup>2</sup> Assuming that the rock mass is drained or that grouting is carried out before excavations.
SRF	Strength Reduction Factor. Describes the relation between stress and rock strength around an underground opening.	10	Where the soil can be associated with a broad weakness zone where the rock support must be designed as an individual support without taking the quality of the side rock into account, SRF should be 10 <sup>1</sup> .
<b>Q-value</b>		<b>0.00413</b>	<i>Exceptionally poee rock mass</i> <sup>3</sup>
<b>Support requirement</b>			
	Excavating Support Ratio (ESR)	1	ESR value of 1 is commonly used for road tunnels to ensure high level of safety <sup>1</sup> .
	Excavation span	9.5 m	Chosen based on the planned T9.5 tunnel dimension
	Equivalent dimension	9.5	
	<b>Support category</b>	<b>9</b>	<i>Special evaluation</i> <sup>4</sup> .

<sup>1</sup> (NGI, 2013)<sup>2</sup> Ratings obtained from the Q-system in Appendix A5<sup>3</sup> Support chart in Figure 37<sup>4</sup> Support chart description in Appendix A5

When using the Q-system to evaluate the support requirements, an equivalent dimension based on safety requirements and the dimensions, is required and is given in Equation 5. The safety requirements are expressed by an Excavation Support Ratio, ESR. The value of ESR ranges from 0.5 to 5 and low ESR values indicate high level of safety while higher ESR values indicate lower level of safety. With the calculated Q-value and equivalent dimension of Joberget soil tunnel in Table 7, a guideline for the design of permanent support can be found, presented in the support chart in Figure 37. The support recommendations given in the chart may in difficult cases be increased in the amount or type of support (NGI, 2013).

$$\text{Equivalent dimension} = \frac{\text{excavation span or height (m)}}{\text{ESR}} \tag{5}$$

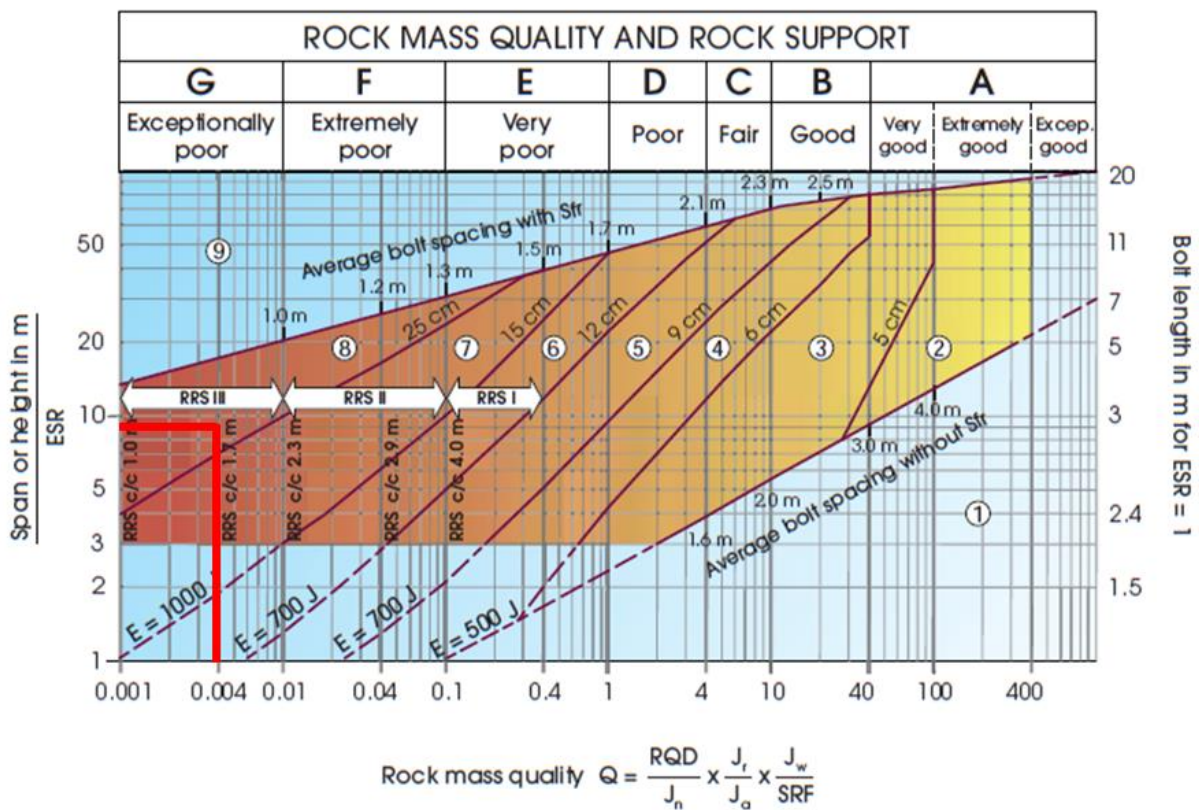


Figure 37: Support chart based on the Q-system and the type of construction. The estimated Q-value of 0.004 and equivalent dimension of 9.5 of Joberget soil tunnel is illustrated in red, indicating an exceptionally poor rock mass quality and a support category 9 implying special evaluation (Appendix A5). The figure is modified after NGI (2013).

### 7.2.2 The RMR-system

In 1976 Bieniawski presented the first details about the rock mass classification system, Rock Mass Rating (RMR). As for the Q-system, RMR is based on case records and has been refined due to examination of new case records. Six parameters are used in the RMR-system to classify a rock mass. The RMR-system including ratings for each of the six parameters is presented in Appendix A6. The ratings from each parameter are summed up to give a value of RMR. The different parameters are listed below.

- The uniaxial compressive strength of rock
- Rock Quality Designation (RQD)
- Spacing of discontinuities
- Ground water condition
- Orientation of discontinuities.

Bieniawski published in 1989 a set of guidelines for excavation and support of 10 m span rock tunnels in accordance with the RMR system, presented in Appendix A6. It should be noted that the guidelines have been published for a 10 m span horseshoe shaped tunnel, constructed with drill and blast method, in a rock mass subjected to a vertical stress  $< 25\text{MPa}$  equivalent to a depth  $< 900$  m below surface (Hoek, 2007b).

#### 7.2.2.1 RMR-value for Joberget Soil tunnel

It is difficult to find values for the discontinuity parameters required in the RMR-system when the material investigated is soil with no discontinuities. According to Zhu (2012) the uniaxial compressive strength for stiff soils varies between 100-200 kPa. By using the assumed values of the parameters in the Q-system, a RMR-value of  $< 20$  is found reasonable and indicates very poor rock.

The guidelines for excavation and support in appendix A6 indicate multiple drift with 0.5-1.5 m advance in top heading and installation of support concurrently with excavation. The support consist of systematic bolting c/c 1-1.5 with wire mesh, shotcrete in crown, sides and face and ribs spaced 0.75 m with steel lagging and spiling if required (Hoek, 2007b).

### 7.3 Evaluation of Joberget soil tunnel based on empirical analysis

The soil at Joberget is classified as a very poor rock mass in the RMR-system and as an exceptionally poor rock mass in the Q-system. Short round lengths, partial face excavations and spiling with bar ribs are suggested for poor rock mass in the RMR system. This corresponds well to the excavation procedure and the alternative support method, spiling proposed for the soil tunnel in Joberget. Special evaluation is suggested concerning rock support of the exceptionally poor rock mass in the Q-system.

Experiences with soil tunneling emphasize the pipe umbrella method as a favorable primary support method in soil tunneling. The pipe umbrella support method is especially carried out during tunneling in soil or weak rock masses, at mixed face conditions and at shallow overburdens (Oke et al., 2013). This is similar to the condition situated at Joberget. Hence, the pipe umbrella method is assumed to be a good support method in Joberget soil tunnel,

especially if it is little distance between the arches and lattice girders. Lattice girders distribute loads better by obtaining a constant pressure arch in the tunnel (NFF, 2008).

The most important advantage of the pipe umbrella method lies in the possibility of grouting through the perforated pipes to increase the flexural strength of the pipes, improve ground stability and prevent leakage. The long and overlapping pipes will give proper foundation length and transfer loads from supported areas to less critical areas. The opportunity of installing the pipes with cased-drilling is also advantageous.

Due to the limited detailed information available at Joberget, results from the classifications systems should only be used as an indication of stability and required support. It should also be kept in mind that the Q-system is based on case histories where only a few of the case histories are derived from very soft rock excavations. Therefore, it is recommended that the Q-values from such rock types should be handled with care and combined with numerical simulations and convergence measurements (NGI, 2013).

The design of the pipe umbrella at Joberget is developed based on experiences from the Holmestrand tunnel, international tunnel projects and site investigations. Even though there is little experience with tunneling based on pipe umbrella in Norway, international tunnels show good results with the use of pipe umbrella method carried out in similar conditions as for Joberget tunnel. With careful excavations, a continuous construction period, continuous monitoring, a well prepared drainage plan, detailed preliminary investigation, risk analysis and a proper stability analysis, soil tunneling at Joberget is considered to be feasible.



## 8 Numerical analysis

The purpose of numerical modelling in engineering geology is to understand all processes that occur in the rock mass as a result of engineering actions. Stability problems and support measures can be analysed with numerical modelling. Also, the effects of engineering actions, such as time when support is introduced, can be studied. Therefore, numerical modelling is an essential component in engineering geology projects. It is important to keep in mind that the reliability of the input parameters represents the greatest limitation of a numerical model. It is therefore recommended to analyse the effect of changing essential input parameters in a parameter study (Jing, 2003).

Numerical modelling means division of rock mass into a large number of individual elements. There are two main categories of numerical modeling, the continuous models and the discontinuous models. In cases where for example single joints will strongly influence the structural behaviour of a model and control the mechanism of failure, discontinuous models are recommended. If not, continuous models can be performed assuming continuous ground condition. The continuous and discontinuous models are additionally divided in different methods. Most commonly, continuous models are applied and especially the Finite Element Method (FEM) (Nilsen and Palmstrøm, 2000).

Whether the numerical modelling is successful in capturing the rock reality is related to both the type of numerical model and the associated rock mass properties (Jing, 2003).

### 8.1 Finite Element Method (FEM)

The FEM has been the most widely applied numerical method for analysing engineering geological problems, because of its flexibility in handling complex materials and boundary conditions. FEM is a continuous method treating the rock mass as a continuum. A geological problem in FEM is divided into a finite number of internal contiguous elements of regular shapes defined by a fixed number of nodes (points) at the vertices. A set of algebraic equations are produced and solved implicitly resulting in calculated stresses and deformations (Jing, 2003).

### 8.2 Two-dimensional numerical analysis of the pipe umbrella method

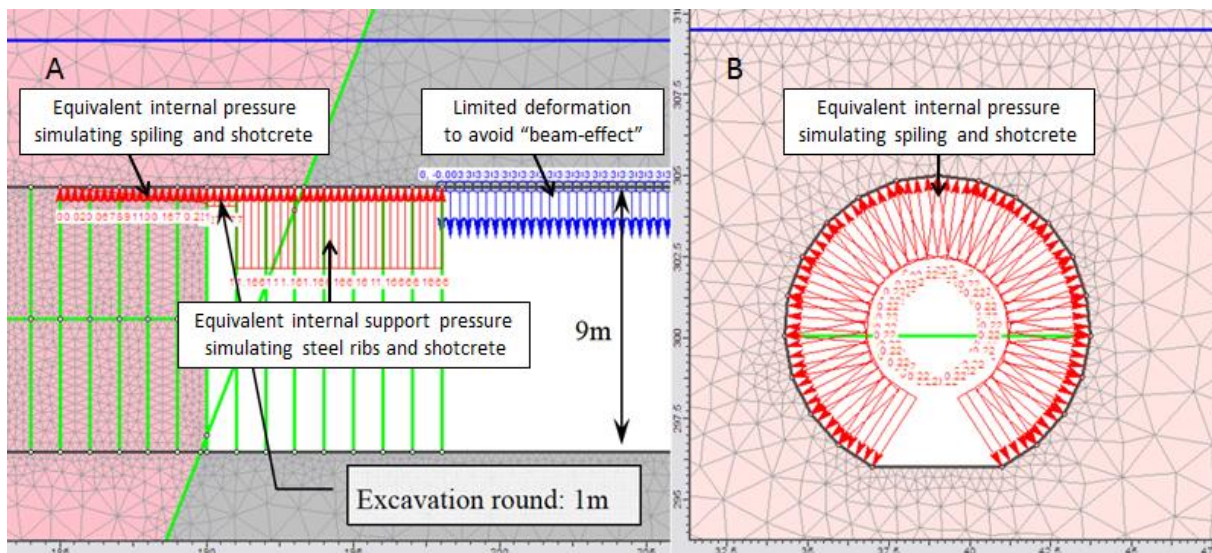
There is no generally accepted method for designing pipe umbrella systems in two-dimensional (2D) numerical modelling. However, two different methods, one with the use of equivalent internal pressure and the other with the use of an improved layer, have been carried out to simulate the pipe umbrella support method. These methods are based on the fact that the pipes form a shell that reduces the gravitational stress acting on the rock mass ahead of the advancing tunnel face (Hoek, 2001).

Both cross sections and longitudinal sections are useful when analysing stability, support and excavation methods in two dimensions. The longitudinal section is especially useful when evaluating spiling or pipe umbrella support methods, since these methods not only provide support at tunnel face, but also pre-reinforce the rock mass ahead of the advancing face. When

modelling the longitudinal section, it is important to consider the “beam effect”. The excavated tunnel in the longitudinal section can be compared to a “beam” fixed at both ends subjected to self-gravity loading. This is known as the “beam effect” and creates unrealistically high displacements in tunnel roof. In three dimensions, the walls of the tunnel will act to reduce this “beam effect”. In two dimensions, the cross section with walls can be used to find the appropriate displacement of tunnel roof. This displacement is assigned to the longitudinal section as a displacement limit (Trinh and Broch, 2008).

### 8.2.1 Equivalent internal pressure

Trinh and Broch (2008) have proposed a method to analyse support measures with spiling bolts, steel ribs and shotcrete, in a two dimensional numerical model by the use of equivalent internal pressures. The equivalent internal pressures can be obtained from the program, RocSupport. RocSupport provided by Rocscience Inc. is computer software used for estimating deformations of circular, or near circular tunnels in weak rock and visualizing tunnel interaction with various support systems (Rocscience, 2009). The rock support analysis is based on the Characteristic curve, described in chapter 6.1.2. Figure 38, modified after Trinh and Broch (2008) show an example of how equivalent internal pressure is used to simulate support measures of spiling, steel ribs and shotcrete in a 2D numerical model. The support pressure provided by the spiling bolts and the shotcrete is found with the cross section in model B in Figure 38. The equivalent internal pressure of spiling was applied to the front end and gradually reduced to zero at the rear end of the spiling bolt, as illustrated in model A, Figure 38.

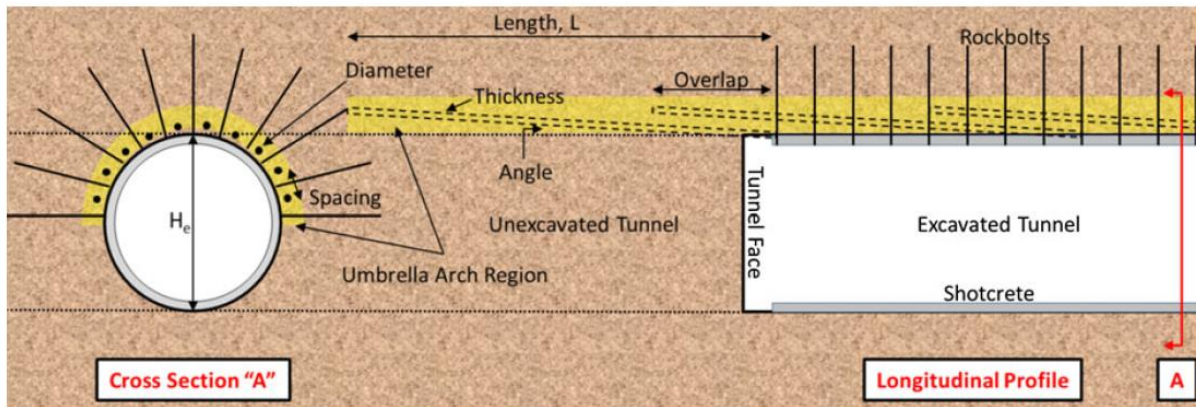


**Figure 38: A. Longitudinal model of proposed excavation and support. B. Cross section with estimated internal pressure provided by spiling bolts and shotcrete applied in the longitudinal section. The figure is modified after Trinh and Broch (2008).**

### 8.2.2 Improved material layer

Hoek (2001) describes a method of simulating pipe umbrella support in two dimension with a zone of improved rock mass properties. An improved material layer is created in the tunnel roof of the cross section and longitudinal section as illustrated in Figure 39. The properties of this improved layer are estimated with a weighted average (based on a cross sectional area)

for the strength and deformation properties of the steel pipes, the grout filling and the original rock mass. This method does not correctly represent the three dimensional bending strength of the pipe umbrella. Although this is true, observations of tunnels constructed with pipe umbrella designs confirm that the improved strength estimates are reasonable.



**Figure 39: Illustration of pipe umbrella with design parameters. The yellow shaded region defines where the pipe umbrella is located and indicates how the improved layer in a two dimensional analysis will look like (Oke et al., 2013).**

### 8.3 2D- versus 3D-numerical analysis

The most correct way of modelling pipe umbrella systems is with three-dimensional (3D) numerical analysis in which the pipes are installed as structural elements embedded in the rock mass (Hoek, 2001). Hence, more details around the supporting effect of the pipes can be analysed in a 3D model. This can be used to evaluate the design of the pipe umbrella system regarding pipe dimension, stiffness and spacing that satisfy both stability and performance requirements. Also, the behaviour of the important tunnel face reinforced with longitudinal pipes can be investigated with a 3D analysis (Yoo, 2002).

With reasonable estimations of rock mass and support properties, 2D numerical modelling may be carried out to analyse complicated tunneling issues, such as spiling or pipe umbrella. The model will most likely provide a good base for tunneling design process. Additionally, 2D numerical methods are easier to implement and understand. However, details about the support measure can only be conducted with a 3D numerical analysis (Trinh et al., 2010).



## 9 Basics and procedure of the numerical modelling

The numerical model does not have to be complete and perfect, it only has to be adequate for the purpose (Jing, 2003). Keeping this in mind, a simple, but realistic numerical model for the soil tunneling section in Joberget tunnel is developed.

The numerical modelling of Joberget soil tunnel is performed with a 2D continuous model based on FEM. This model is chosen based on the assumption that the soil and rock at Joberget is fairly homogenous and continuous, with no significant features affecting the stability. When performing numerical modelling in two dimensions, a simplification of the reality is performed and may provide uncertainty in the results. However, 2D numerical models have shown reasonable estimates of stability in rock masses and are easier to implement and understand.

Numerical modelling in engineering geology is comparable to working with variability and uncertainty, because the geometry and properties of the rock mass components will never be completely known (Jing, 2003). The reliability of the analysis will not be better than the reliability of the input parameters (Nilsen and Palmstrøm, 2000).

The steps of numerical modelling consist of building geometry, choosing material properties, defining boundary and initial condition, computing and then analysing. These steps will be further discussed in this chapter.

### 9.1 Software

#### 9.1.1 Phase<sup>2</sup>

The numerical modelling of Joberget soil tunnel is carried out with Phase<sup>2</sup> version 8.0. Phase<sup>2</sup> is a two-dimensional elasto-plastic finite element program provided by RocScience Inc. The program is commonly used for stress and displacement analysis for underground or surface excavations in rock and soil. Phase<sup>2</sup> offers multi-stage modelling, slope stability analysis, ground water seepage analysis and a wide range of support modelling options. Researchers and engineers use the program for solving geotechnical problems (Rocscience, 2014a).

#### 9.1.2 RocLab

RocLab version 4.0 is a software from Rocscience Inc. used for determining rock mass properties based on the latest version of the generalized Hoek-Brown failure criterion. Reliable estimates of rock mass properties can easily be obtained and the effect of changing the parameters is visualized with failure envelopes. The rock mass strength and deformation parameters found in RocLab can be used as input for numerical programs such as Phase<sup>2</sup> (Rocscience, 2014b).

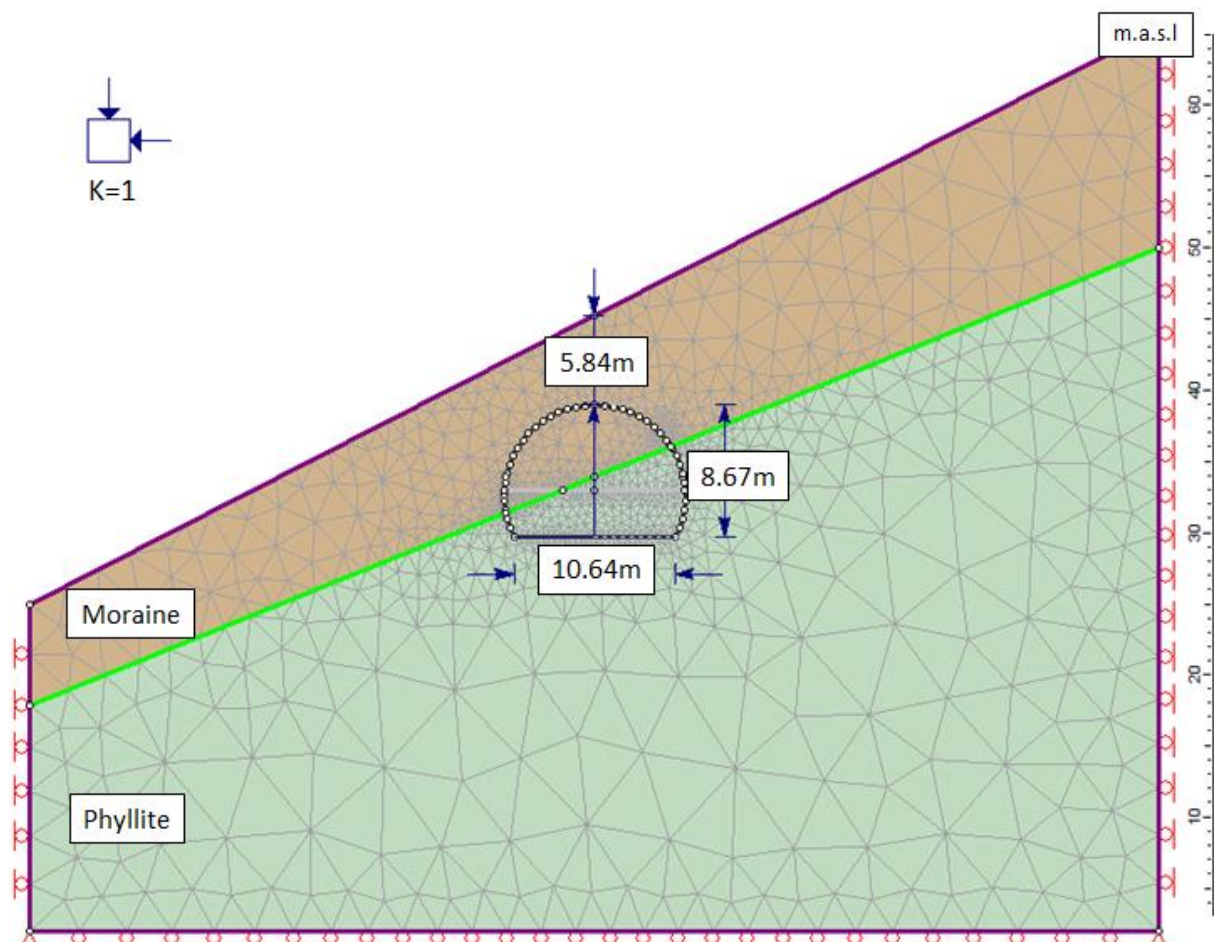
### 9.2 Model set up

Based on conceptual designs and reports by Sweco and iC-Consulenter (2013), one cross section and one longitudinal section of Joberget soil tunnel are modelled in Phase<sup>2</sup>. The

models are a simplification of the reality, including assumed rock mass distribution and actual ground surface.

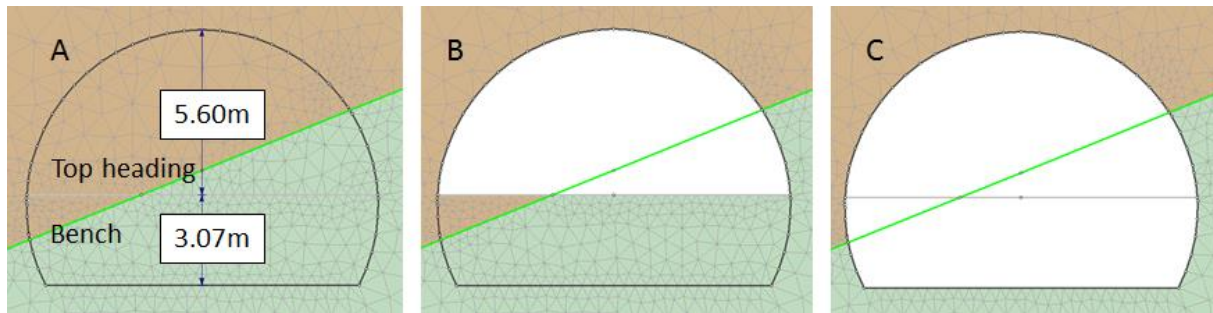
### 9.2.1 Cross section

The model of the cross section can be seen in Figure 40. The first 7-8 m from the southeastern entrance of the Joberget soil tunnel consists of a shotcrete canopy that is difficult to model in Phase<sup>2</sup> and is therefore assumed to be stable. It is estimated that the overburden ranges from 5-17 m. The location of the cross section is chosen to observe the stability at the most critical overburden and at the same time avoiding that the shotcrete canopy will affect the stability support being analysed. Hence, the cross section is taken at approximately 20 m from the southeastern entrance of the planned Joberget soil tunnel, with an overburden of 5.84 m. The exact location of the cross section can be found in the longitudinal section in Figure 42 and in Appendix A1. The width of 10.64 m (10.04 m + 0.6 m lining) and the height of 8.67 m of the tunnel are obtained from the regular cross section in Figure 6. The upper part of the cross section consists of moraine material and the lower part of phyllite. Tunnel invert is planned located at 30 m.a.s.l.



**Figure 40: Cross section with assumed rock mass distribution, proposed tunneling geometry, selected mesh and boundary condition under isotropic field stress,  $K=1$ , with actual ground condition.**

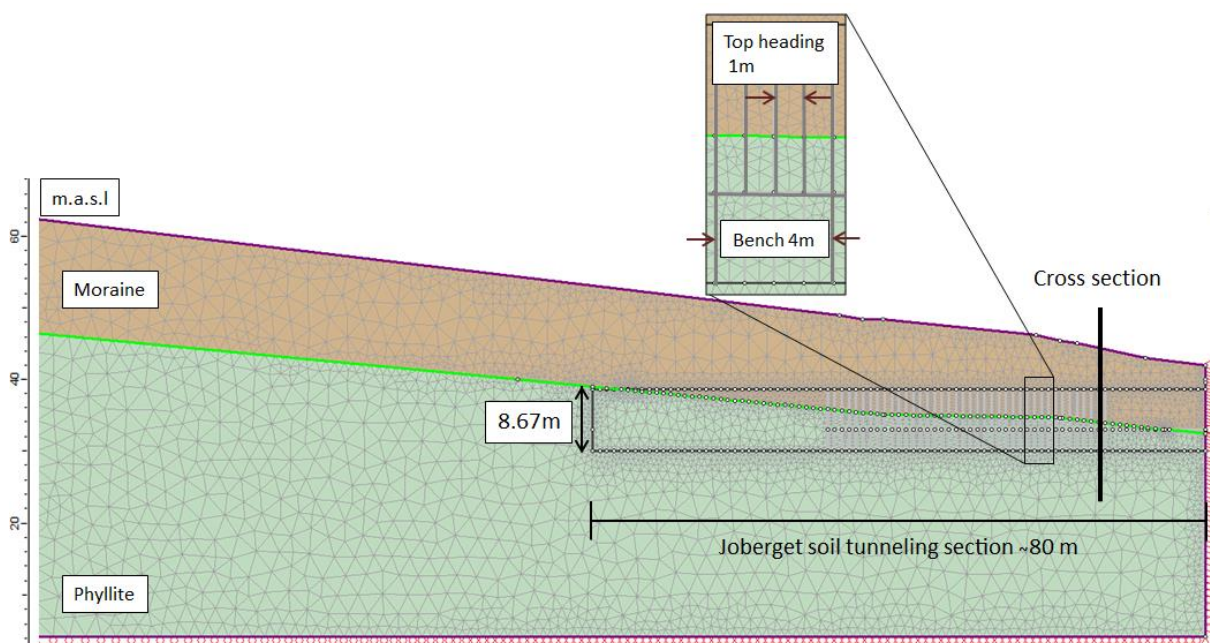
The excavation of the tunnel face will be divided in a top heading with a height of 5.6 m and a bench with a height of 3.07 m as illustrated in model A in Figure 41. To simulate the excavation procedure the cross section is staged as seen in model B and C in Figure 41.



**Figure 41: Illustrates excavation of top heading and bench A. cross section with top heading and bench height B. Excavation of top heading every meter C. Excavation of bench every four meters.**

### 9.2.2 Longitudinal section

Figure 42 shows the assumed longitudinal section of the approximately 80 m long soil tunnel section of Joberget tunnel. The location of the selected cross section in this study is also indicated in the figure. The excavation of the soil tunneling section is performed with short round lengths where the top heading is excavated every meter and the bench is excavated every four meters. This excavation procedure is simulated by stages in the model. The advantage of modelling with stages is the possibility of analysing stability for every excavation step.



**Figure 42: Longitudinal section of the approximately 80 m long soil tunnel at Joberget with the estimated actual ground surface. Selected mesh and boundary condition are included.**

### 9.2.3 Mesh and external boundary

A graded mesh type with 3 noded triangles is chosen for the models. The gradation factor of the mesh is 0.1 and the number of excavation nodes is 100 for the cross section and 400 for the longitudinal section due to being a bigger model. The number of excavation nodes determines directly the discretization of the excavation boundaries, whereas the gradation factor determines the discretization of all the other boundaries in the model (Rocsience, 2014). The mesh is chosen to obtain a detailed analysis especially around the tunnel excavation and at the same time keeping the solution time relatively short. The deformation is simulated with the default tolerance of 0.001 and maximum amount of iteration of 500 (Gaussian type).

The chosen geometry and condition of the external boundary is based on recommendation from (Rocsience, 2014). The boundary surface is estimated from actual ground surface measurements, whereas the other external boundaries are chosen to avoid influencing the results of the numerical analyses. The boundary that makes up the surface is given free restraint. The boundary at the bottom of the model is allowed to restrain horizontally, whereas the vertical boundaries are allowed to restrain vertically. However, the lower corners of the model can restrain both horizontally and vertically.

Selected mesh and boundary conditions are displayed in the longitudinal and cross section in figure 40 and 42 respectively.

### 9.3 Field stress

The initial in situ stress condition prior to excavation is determined by the field stress, and can be defined as a constant or as gravity. Gravity field stress is commonly used for surface or near surface excavations and varies linearly with depth. Since the actual ground surface is modelled in Phase<sup>2</sup>, gravitational field stress is chosen for this analysis. The total stress ratios (horizontal/vertical in plane and out-of-plane) are used to calculate the horizontal components of the gravitational field stress, based on the vertical stress at any point in the model. The relationship between horizontal and vertical stress is given in Equation 6 (Rocsience, 2014). This relationship is known as the coefficient of earth pressure at rest,  $K_0$  for soils that currently exists under the condition of zero horizontal deformation (Mesri and Hayat, 1993).

$$K = \frac{\sigma_H}{\sigma_V} \quad (6)$$

The vertical stress is calculated with Equation 7. When Poisson's ratio of an elastic rock mass is known, the horizontal stress induced by gravity can be estimated with Equation 8 (Nilsen and Palmstrøm, 2000).

$$\sigma_v = \gamma h = \rho g h \quad (7)$$

$\gamma = \text{Unit weight}$   
 $h = \text{Tunnel depth}$

$$\sigma_h = \frac{\nu}{1-\nu} \sigma_v \quad (8)$$

$\nu = \text{Poisson's ratio}$



Vertical stresses in soils can be determined from depth, while horizontal stresses are difficult to establish. Therefore, the magnitude of the horizontal stress is assumed identical to the magnitude of the vertical stress,  $K=1$  which is a common assumption for soils (Hoek, 1999).

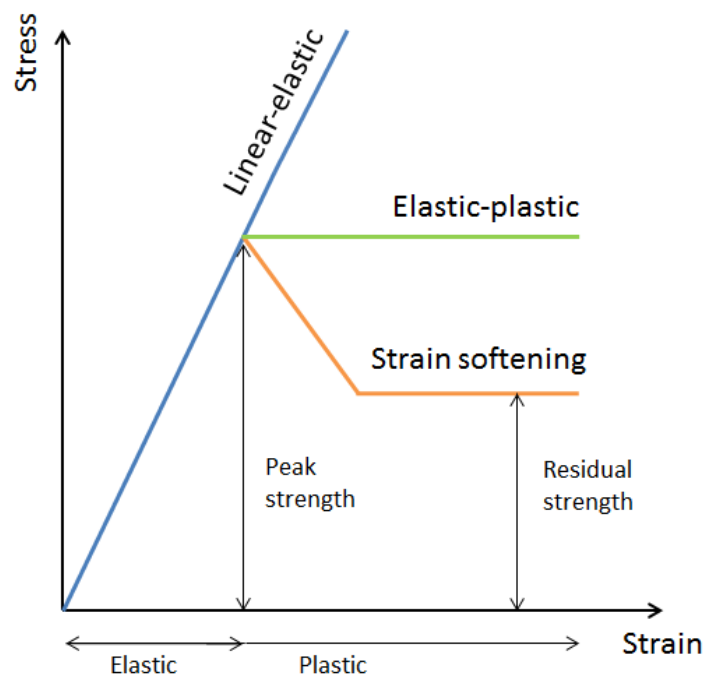
## 9.4 Material properties

The Joberget soil tunnel will be excavated partly in soil and partly in rock. The crown and a significant portion of the tunnel walls, will be located in moraine material, whereas the invert will be located in bedrock. The amount of bedrock in the tunnel cross section will increase with decreasing profile number. Type of bedrock appearing in the sole is uncertain but based on different investigation phyllite is most likely (NPRA, 2013a). Hence, both rock mass and soil properties are estimated for the numerical modelling.

### 9.4.1 Plastic material

An elasto-plastic model accounts for yielding and permanent displacement of the rock mass if it becomes critically stressed during excavation. The material type in Phase<sup>2</sup> is chosen to be plastic allowing yielding of the rock mass to be analysed for Joberget soil tunnel. After yielding rock mass material may still carry some strength, based on rock mass quality and is illustrated in Figure 43. This strength is defined by the residual strength parameters and the dilation parameter.

The dilation parameter is a measure of volume increase during shearing. Generally, low dilation parameters are associated with soft rock and high dilation parameters with brittle rock (Rocsience, 2014).



**Figure 43: Suggested post failure characteristics for different quality rock masses. Strain softening is assumed for the average quality rock mass and elastic-plastic is assumed for very poor quality soft rock mass such as soil. The figure is modified after Hoek (2007c).**

## 9.4.2 Rock mass properties

There are no laboratory tests performed on the rock mass at Joberget. However, some field observations, geological mapping and seismic measurements have been conducted by the (NPRA, 2013a). The rock beneath the moraine material is phyllite, assumed strongly influenced by tectonics.

### 9.4.2.1 Generalized Hoek-Brown

When laboratory testing is not possible, RocLab can be used to determine reliable rock mass properties from estimated intact rock properties. RocLab is based on the generalized Hoek-Brown failure criterion. The criterion was derived from a research on brittle failure of intact rock and on model studies of jointed rock mass behaviour. This failure criterion appears to provide the most reliable results for use as input in numerical analysis for rock engineering and has been applied in many geological projects around the world. The generalized Hoek-Brown failure criterion is defined in Equation 9 (Hoek, 2007c).

$$\sigma_1 = \sigma_3 + \sigma_{ci} \left( m_b \frac{\sigma_3}{\sigma_{ci}} + s \right)^a \quad (9)$$

$\sigma_1$  and  $\sigma_3$  = maximum and minimum principal stresses at failure

$\sigma_{ci}$  = uniaxial compressive strength of the intact rock pieces

$m_b$  = Hoek-Brown constant for the rock mass

$s$  and  $a$  = constants depending upon the rock mass characteristics

The influence of sample size on the rock mass strength is important to consider. Generally, it is assumed that the strength reduces with increasing sample size. The rock mass can be treated as a Hoek-Brown material when the structure analysed is large and the block size is small. Thus, the Hoek-Brown failure criterion assumes isotropic conditions and a homogeneous rock mass (Hoek, 2007c).

In order to determine strength and deformability of rock masses with RocLab, estimations of five rock mass properties are needed and are listed below:

- The uniaxial compressive strength (UCS),  $\sigma_{ci}$
- The Hoek-Brown constant,  $m_i$
- The geological strength index, GSI
- The disturbance factor, D
- The intact deformation modulus,  $E_i$

- ***The uniaxial compressive strength (UCS),  $\sigma_{ci}$***

The uniaxial compressive strength can be determined in RocLab and is based on field estimates given in Table 8.

Phyllite is a foliated rock, showing anisotropic behavior due to closely spaced planes of weakness, cleavage or schistosity. This behaviour causes complications when determining the uniaxial compressive strength. With the use of Table 8, phyllite is found to be a strong rock,

with a uniaxial compressive strength between 50-100 MPa. Since the phyllite at Joberget is assumed to be weak as a result of tectonic influence, the lowest value of 50 MPa is chosen.

**Table 8: Field estimates of uniaxial compressive strength (Hoek, 2007c).**

Grade*	Term	Uniaxial Comp. Strength (MPa)	Point Load Index (MPa)	Field estimate of strength	Examples
R6	Extremely Strong	> 250	>10	Specimen can only be chipped with a geological hammer	Fresh basalt, chert, diabase, gneiss, granite, quartzite
R5	Very strong	100 - 250	4 - 10	Specimen requires many blows of a geological hammer to fracture it	Amphibolite, sandstone, basalt, gabbro, gneiss, granodiorite, limestone, marble, rhyolite, tuff
R4	Strong	50 - 100	2 - 4	Specimen requires more than one blow of a geological hammer to fracture it	Limestone, marble, phyllite, sandstone, schist, shale
R3	Medium strong	25 - 50	1 - 2	Cannot be scraped or peeled with a pocket knife, specimen can be fractured with a single blow from a geological hammer	Claystone, coal, concrete, schist, shale, siltstone
R2	Weak	5 - 25	**	Can be peeled with a pocket knife with difficulty, shallow indentation made by firm blow with point of a geological hammer	Chalk, rocksalt, potash
R1	Very weak	1 - 5	**	Crumbles under firm blows with point of a geological hammer, can be peeled by a pocket knife	Highly weathered or altered rock
R0	Extremely weak	0.25 - 1	**	Indented by thumbnail	Stiff fault gouge

\* Grade according to Brown (1981).

\*\* Point load tests on rocks with a uniaxial compressive strength below 25 MPa are likely to yield highly ambiguous results.

- **The Hoek-Brown constant,  $m_i$**

The  $m_i$  constant varies with rock type and the constant should be determined by statistical analysis of the results of a set of triaxial tests on carefully prepared core samples (Hoek and Brown, 1997). Since no laboratory testing of the phyllite of Joberget is possible,  $m_i$  is also found with RocLab, based on Table 9. The  $m_i$  constant for phyllite is estimated to be  $7 \pm 3$ . The phyllite in Joberget is assumed weak and therefore the lowest value of 4 is chosen.

**Table 9: Values of the Hoek-Brown constant  $m_i$  for intact rock, by rock group. The values in parenthesis are estimated (Hoek, 2007c).**

Rock type	Class	Group	Texture			
			Coarse	Medium	Fine	Very fine
SEDIMENTARY	Clastic		Conglomerates* (21 ± 3)	Sandstones 17 ± 4	Siltstones 7 ± 2	Claystones 4 ± 2
			Breccias (19 ± 5)		Greywackes (18 ± 3)	Shales (6 ± 2) Marls (7 ± 2)
	Non-Clastic	Carbonates	Crystalline Limestone (12 ± 3)	Sparitic Limestones (10 ± 2)	Micritic Limestones (9 ± 2)	Dolomites (9 ± 3)
		Evaporites		Gypsum 8 ± 2	Anhydrite 12 ± 2	
	Organic				Chalk 7 ± 2	
METAMORPHIC	Non Foliated		Marble 9 ± 3	Hornfels (19 ± 4) Metasandstone (19 ± 3)	Quartzites 20 ± 3	
	Slightly foliated		Migmatite (29 ± 3)	Amphibolites 26 ± 6		
	Foliated**		Gneiss 28 ± 5	Schists 12 ± 3	Phyllites (7 ± 3)	Slates 7 ± 4
IGNEOUS	Plutonic	Light	Granite 32 ± 3 Granodiorite (29 ± 3)	Diorite 25 ± 5		
		Dark	Gabbro 27 ± 3 Norite 20 ± 5	Dolerite (16 ± 5)		
	Hypabyssal		Porphyries (20 ± 5)		Diabase (15 ± 5)	Peridotite (25 ± 5)
	Volcanic	Lava		Rhyolite (25 ± 5) Andesite 25 ± 5	Dacite (25 ± 3) Basalt (25 ± 5)	Obsidian (19 ± 3)
		Pyroclastic	Agglomerate (19 ± 3)	Breccia (19 ± 5)	Tuff (13 ± 5)	

\* Conglomerates and breccias may present a wide range of  $m_i$  values depending on the nature of the cementing material and the degree of cementation, so they may range from values similar to sandstone to values used for fine grained sediments.

\*\* These values are for intact rock specimens tested normal to bedding or foliation. The value of  $m_i$  will be significantly different if failure occurs along a weakness plane.

- **The Geological Strength Index, GSI**

The GSI gives the characterisation of blocky rock masses based on interlocking and joint condition. The strength of a jointed rock mass depends on intact rock piece properties and the freedom of the pieces to slide and rotate under different stress condition. The GSI can be used to estimate the reduction in rock mass strength, when discontinuity spacing is small compared to the size of the structure.

The system of estimating the GSI is presented in Figure 44 and is applied for estimating the GSI for phyllite in RocLab. The phyllite is assumed to have a very blocky structure, due to the tectonic history and fair surface conditions, assuming moderately weathered with altered surfaces and hence a GSI value of 45.

The factors  $m_b$ ,  $s$  and  $a$  given as output from RocLab is found with Equations 10,11 and 12 respectively, based on the GSI system influenced by blast damaged (Hoek et al., 2002).

$$m_b = m_i \exp\left(\frac{GSI-100}{28-14D}\right) \quad (10)$$

$$s = \exp\left(\frac{GSI-100}{9-3D}\right) \quad (11)$$

$$a = \frac{1}{2} + \frac{1}{6} \left( e^{-\frac{GSI}{15}} - e^{-\frac{20}{3}} \right) \quad (12)$$

$D =$  disturbance factor

$m_b =$  reduced value of the material constant  $m_i$

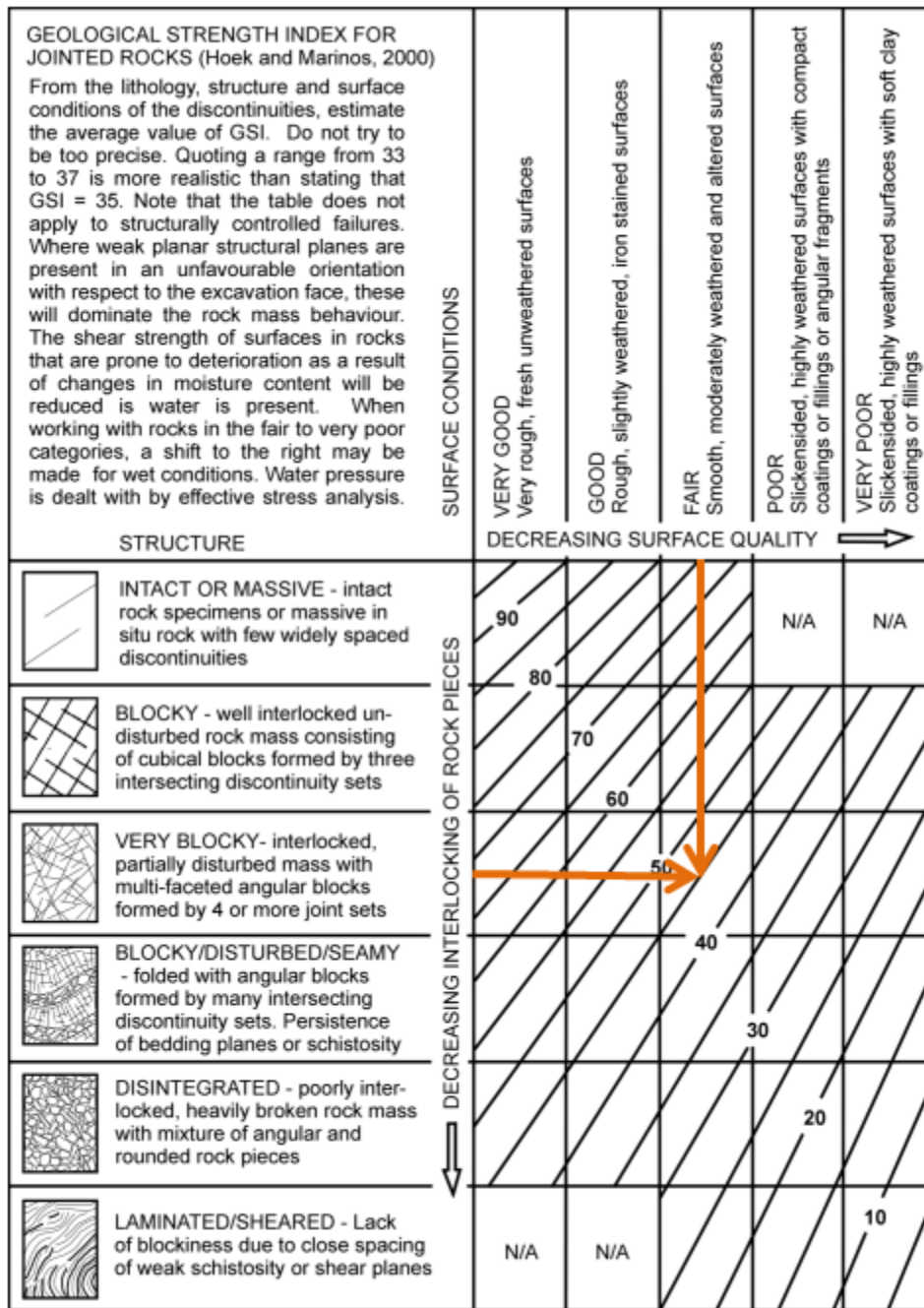



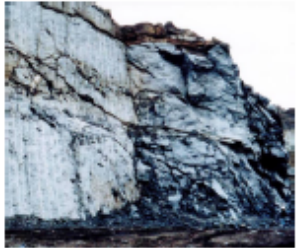



Figure 44: Estimate of Geological Strength Index based on geological description. Orange arrows indicate the assumed GSI for the phyllite at Joberget (Hoek, 2007c).

- *The disturbance factor, D*

The disturbance factor depends on the degree of disturbance due to blast damage and stress relaxation. D varies from 0, for undisturbed in situ rock masses to 1, for very disturbed rock masses. The factor is only applied to the blast damage zone and not to the entire rock mass to avoid misleading results (Hoek, 2007c). Guidelines for the choice of appropriate values for D are given in Table 10. D is assumed to be 0 for excavation of Joberget tunnel since the tunnel will be mechanically excavated in poor quality rock masses, most likely resulting in minimal disturbance to the surrounding rock mass.

**Table 10: Guidelines for estimating the disturbance factor, D (Hoek, 2007c).**

Appearance of rock mass	Description of rock mass	Suggested value of <i>D</i>
	Excellent quality controlled blasting or excavation by Tunnel Boring Machine results in minimal disturbance to the confined rock mass surrounding a tunnel.	$D = 0$
	Mechanical or hand excavation in poor quality rock masses (no blasting) results in minimal disturbance to the surrounding rock mass.  Where squeezing problems result in significant floor heave, disturbance can be severe unless a temporary invert, as shown in the photograph, is placed.	$D = 0$  $D = 0.5$ No invert
	Very poor quality blasting in a hard rock tunnel results in severe local damage, extending 2 or 3 m, in the surrounding rock mass.	$D = 0.8$
	Small scale blasting in civil engineering slopes results in modest rock mass damage, particularly if controlled blasting is used as shown on the left hand side of the photograph. However, stress relief results in some disturbance.	$D = 0.7$ Good blasting  $D = 1.0$ Poor blasting
	Very large open pit mine slopes suffer significant disturbance due to heavy production blasting and also due to stress relief from overburden removal.  In some softer rocks excavation can be carried out by ripping and dozing and the degree of damage to the slopes is less.	$D = 1.0$ Production blasting  $D = 0.7$ Mechanical excavation

- **Intact deformation modulus,  $E_i$**

Based on data from a large number of in situ measurements, from underground constructions in China and Taiwan, a relationship for the rock mass deformation modulus,  $E_{rm}$  is proposed by Hoek and Diederichs (2006). The relationship is found from the connection between the intact deformation modulus,  $E_i$ , GSI and  $D$  and is given in Equation 13

$$E_{rm} = E_i \left( 0.02 + \frac{1 - \frac{D}{2}}{1 + e^{\left( \frac{60 + 15D - GSI}{11} \right)}} \right) \quad (13)$$

When there are no values of the intact deformation modulus available or undisturbed sampling for  $E_i$  measurements is difficult, the modulus ratio MR proposed by Deere (1968), can be used and is given in Equation 14. Even when measurements of  $E_i$  are available, their reliability is suspect due to specimen damage. Damages of specimen has a lower impact on the strength, hence intact rock strength is considered more reliable (Hoek and Diederichs, 2006). The MR can be found in RocLab and is based on Table 11 showing guidelines for finding the appropriate MR. The mean value of 425 is chosen as MR for phyllite.

$$MR = \frac{E_i}{\sigma_{ci}} \quad (14)$$



**Table 11: Guidelines for the selection of MR values based on Deere (1968) and Palmstrøm and Singh (2001) in (Hoek, 2007c).**

	Class	Group	Texture			
			Coarse	Medium	Fine	Very fine
SEDIMENTARY	Clastic		Conglomerates 300-400	Sandstones 200-350	Siltstones 350-400	Claystones 200-300
			Breccias 230-350		Greywackes 350	Shales 150-250 * Marls 150-200
	Non-Clastic	Carbonates	Crystalline Limestone 400-600	Sparitic Limestones 600-800	Micritic Limestones 800-1000	Dolomites 350-500
		Evaporites		Gypsum (350)**	Anhydrite (350)**	
Organic					Chalk 1000+	
METAMORPHIC	Non Foliated		Marble 700-1000	Hornfels 400-700 Metasandstone 200-300	Quartzites 300-450	
	Slightly foliated		Migmatite 350-400	Amphibolites 400-500	Gneiss 300-750*	
	Foliated*			Schists 250-1100*	Phyllites /Mica Schist 300-800*	Slates 400-600*
IGNEOUS	Plutonic	Light	Granite+ 300-550 Granodiorite+ 400-450	Diorite+ 300-350		
		Dark	Gabbro 400-500 Norte 350-400	Dolerite 300-400		
	Hypabyssal		Porphyries (400)**		Diabase 300-350	Peridotite 250-300
	Volcanic	Lava		Rhyolite 300-500 Andesite 300-500	Dacite 350-450 Basalt 250-450	
		Pyroclastic	Agglomerate 400-600	Volcanic breccia (500) **	Tuff 200-400	

\* Highly anisotropic rocks: the value of MR will be significantly different if normal strain and/or loading occurs parallel (high MR) or perpendicular (low MR) to a weakness plane. Uniaxial test loading direction should be equivalent to field application.

+ Felsic Granitoids: Coarse Grained or Altered (high MR), fined grained (low MR).

\*\* No data available, estimated on the basis of geological logic.

The peak values of the parameters in the generalized Hoek-Brown failure criterion obtained from estimated rock mass parameters in RocLab are presented in Table 12 and in Appendix A7.

**Table 12: Input and output estimated in RocLab to obtain the peak values of the parameters in the generalized Hoek-Brown failure criterion needed in the numerical model.**

	Parameter	Symbol	Value
<b>Input</b>	Uniaxial Compressive Strength (UCS)	$\sigma_{ci}$ [MPa]	50
	The Hoek-Brown constant	$m_i$	4
	Geological Strength Index (GSI)	GSI	45
	Disturbance factor	D	0
	Modulus ratio	MR	425
<b>Output</b>	Hoek-Brown constant for rock mass	$m_b$	0.561
	Hoek-Brown constants depending upon the rock mass characteristics	s	0.0022
		a	0.508
		$E_{rm}$ [MPa]	4753

- **Residual parameters**

Phyllite may be estimated as an average quality rock mass with Strain-softening post failure characteristics, illustrated in Figure 43. A relationship between the GSI and the residual strength parameters is proposed by Cai et al. (2007) where residual strength parameters for jointed intermediate rocks ( $40 < \text{GSI} < 50$ ) such as assumed for phyllite, is approximately half the peak value. The residual strength parameters for the phyllite are calculated based on this proposal and is presented in Table 13 together with the other input parameters for the phyllite required in Phase<sup>2</sup>.

The dilation angle for phyllite is chosen to be 0 assuming no volume increase during shearing.

**Table 13: Estimated peak and residual values of the material properties for the phyllite used as input to Phase<sup>2</sup>.**

Parameter	Unit	Young's Modulus	Poisson ratio	UCS	Hoek Brown constants		
Symbol	$\gamma$ [MN/m <sup>3</sup> ]	$E_{rm}$ [MPa]	$\nu$	$\sigma_{ci}$ [MPa]	$m_b$	s	a
<b>Peak</b>	0.027 <sup>1</sup>	4753 <sup>1</sup>	0.26 <sup>1</sup>	50 <sup>2</sup>	0.561 <sup>2</sup>	0.0022 <sup>2</sup>	0.5081 <sup>2</sup>
<b>Residual</b>					0.2805 <sup>3</sup>	0.0011 <sup>3</sup>	0.2541 <sup>3</sup>

<sup>1</sup> (Zhao, 2014)

<sup>2</sup> RocLab (Rocscience, 2014b)

<sup>3</sup> (Cai et al., 2007)

### 9.4.3 Soil properties

Proper simulation of soil behaviour requires an adequate soil model and high quality soil parameters. Both simple and more advanced models exist. The advantage of a simple model is the limited number of input parameters and that it is easier to understand, but they may be too crude (Nordal, 2013).

#### 9.4.3.1 Mohr Coulomb

The linearly elastic, perfectly plastic Mohr Coulomb model is a simple and well defined soil model. Strength is controlled by Mohr Coulomb criterion and stiffness is controlled by Hooke's law. The stiffness parameters are the Young's Modulus and the Poisson's ratio. The Mohr Coulomb criterion is by far the most important criterion concerning the strength of soils. The criterion is expressed in terms of stress components and material properties and is given in Equation 15. The cohesion and the friction coefficient are considered as curve fitting parameters to approximately fit a straight line to experimental results as shown in Figure 22 (Nordal, 2013).

$$\tau_f = c + \sigma \tan \varphi \quad (15)$$

Soil is a complex material and does not behave like an isotropic, linearly elastic material. Therefore, simplification is necessary and demands careful engineering judgement during parameter selection (Nordal, 2013). The soil at Joberget is modelled as a Mohr-Coulomb material and characterized by its cohesion and friction angle throughout this study.

The soil properties used in the numerical model are found from laboratory testing and presented in Table 14.

- **Residual parameters**

From the stress-strain graphs obtained during laboratory testing, no obvious failure was detected. Therefore, the soil is assumed elastic-plastic and a general stress-strain graph of an elastic-plastic material is illustrated in figure 43. For an ideally elastic-plastic material, the strength parameters are defined equal to the peak parameters. The residual parameters together with the other material parameter required in Phase<sup>2</sup> are presented in Table 14 (Rocsience, 2014).

**Table 14: Estimated peak and residual values for the moraine material properties used as input to Phase<sup>2</sup>.**

Parameter	Unit weight	Young's Modulus	Poisson's ratio	Tensile strength	Friction angle	Cohesion
Symbol	$\gamma$ [MN/m <sup>3</sup> ]	$E_{rm}$ [MPa]	$\nu$	$\sigma_t$ [MPa]	$\phi$ [°]	$c$ [MPa]
<b>Peak</b>	0.022 <sup>1</sup>	50 <sup>2</sup>	0.35 <sup>3</sup>	0 <sup>4</sup>	39 <sup>1</sup>	0.017 <sup>1</sup>
<b>Residual</b>					39 <sup>1</sup>	0.017 <sup>1</sup>

<sup>1</sup> (Langåker, 2013)

<sup>2</sup> Mean E of dense sand assumed representing the over-consolidated moraine (Zhu, 2012)

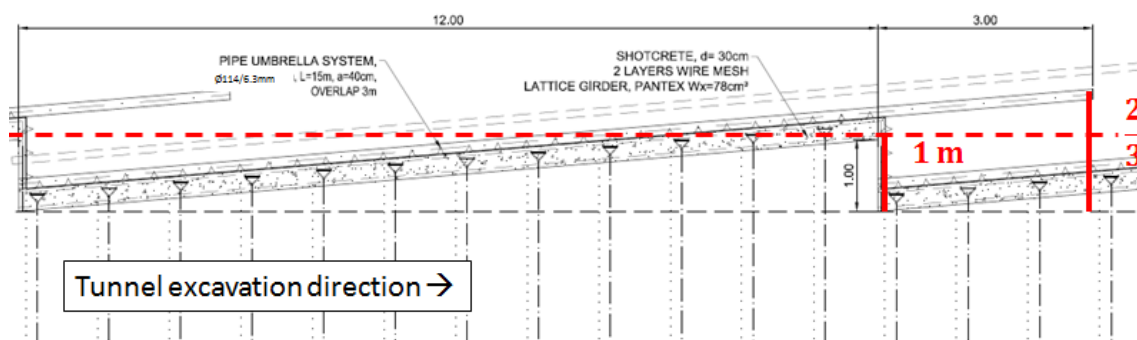
<sup>3</sup> (Gercek, 2007)

<sup>4</sup> Selected value based on an accepted assumption that moraine material possess no tensile strength (Hoff, 2014)

## 9.5 Support

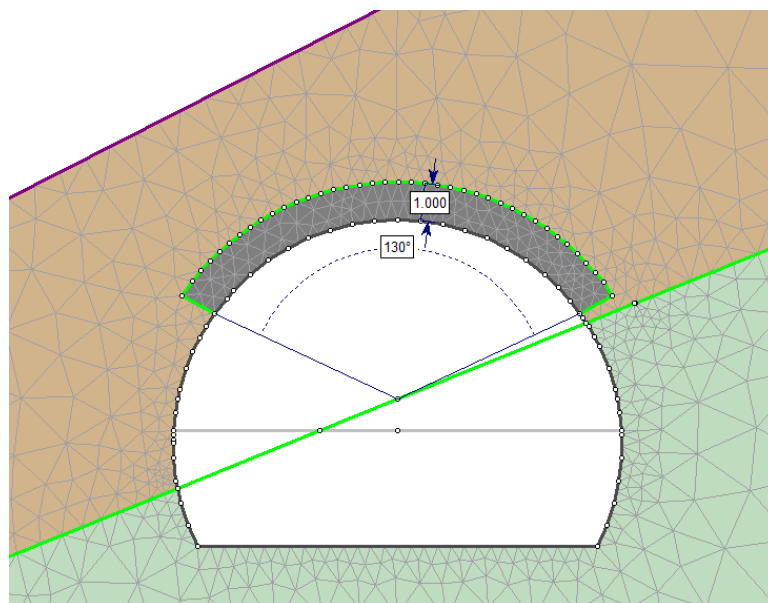
### 9.5.1 Pipe umbrella

According to Hoek (2001), a zone of improved material above the tunnel crown can be used to simulate the pipe umbrella support. The layer is defined as an arch above the excavated tunnel face. The height and the width of the pipe umbrella improved layer are determined from the drawings by iC-Consulenten (2013). The height of a general cross section is estimated from the longitudinal section. Since the pipes are overlapping and installed with an angle, the distribution of the improved layer will vary with length of the pipe umbrella section. To keep the model simple, 1 m being 2/3 of the height at the end of the pipe is assumed possessing the same strength when taking the overlapping of the pipes into account, illustrated in Figure 45.



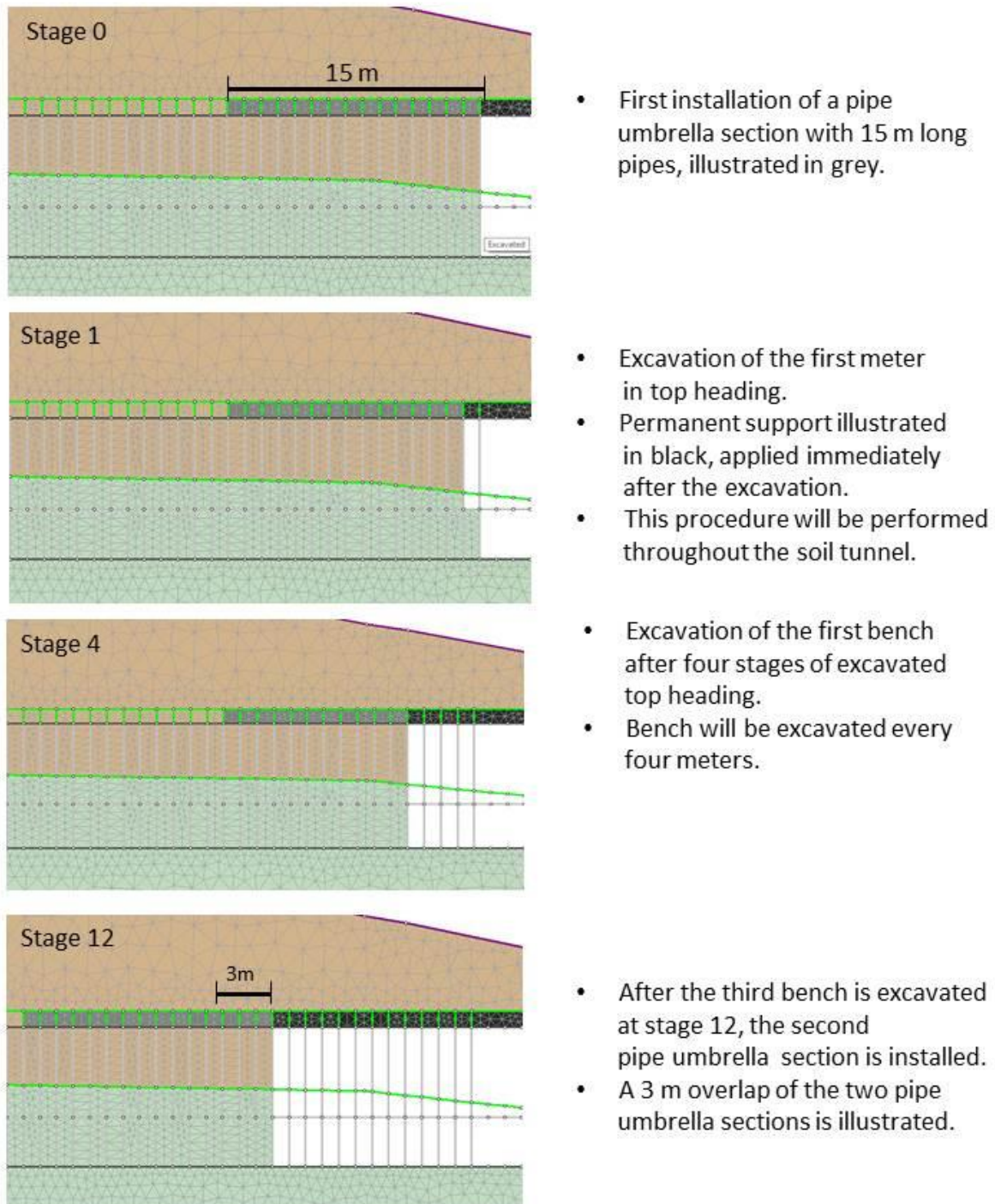
**Figure 45:** Illustration of the assumed pipe umbrella improved layer with a height of 1 m used in the general cross section and longitudinal section numerical model. The figure is cut and modified after a longitudinal section produced by iC-Consulenten (2013). The rest of the figure can be seen in Appendix A1.

The pipe umbrella improved layer is located within an angle of  $130^\circ$  of tunnel crown as illustrated in Figure 46.



**Figure 46:** Cross section with the 1 m thick pipe umbrella improved layer within an angle of  $130^\circ$ .

The pipe umbrella improved layer, together with the proposed installation process of the pipe umbrella improved layer and permanent support in Joberget soil tunnel is described in figure 47. Stage 0 indicates the first pipe umbrella section being analysed and not effected by the shotcrete canopy at tunnel entrance.



**Figure 47: Longitudinal sections with initially planned tunneling support and excavation procedure for Joberget soil tunnel.**

- **Material properties of the pipe umbrella improved layer**

The improved material representing the pipe umbrella support layer consist of steel pipes, grout filling and the original soil. These three components have very different properties which results in difficulties when determining properties of the pipe umbrella improved layer. The material properties of the improved layer are estimated by a weighted average of the strength and the deformation properties of the components, based on a cross sectional area.

A formula of the assumed weighting of the three components is developed and presented in Equation 16. Most of the improved layer consists of soil material. Hence, the soil is given a weighting of 80% of the improved layer. The increasing strength contribution from the steel pipe is assumed to be 1% of the total layer due to the steel pipes cross sectional dimension being small, in comparison to the 1 m thickness of the improved layer. Assuming that the pipes and the soil are perfectly grouted with concrete, 19% of the layer is given material properties of concrete. The calculated values of the material properties of the improved layer are presented in Table 15, including the material properties estimated for each of the three components. Approximations of the values of the improved material layer are performed to fit the other parameters.

$$\text{Pipe umbrella improved layer} = (\text{soil} * 0.8) + (\text{steel pipe} * 0.01) + (\text{concrete} * 0.19) \quad (16)$$

Due to the soil material being a major part of the improved layer, the failure criterion for the improved layer is chosen to be Mohr Coulomb, with a plastic failure type allowing yielding of the pipe umbrella support. Mohr Coulomb strength parameters such as friction angle and cohesion are assumed high for the steel pipes, not indicating any concrete values. The steel pipes do not affect failure, when assuming failure will be initiated in the soil and concrete. However, the stiffness and the tensional strength of the pipe are important parameters to consider for the layer.

By recommendation from Trinh (2014) the residual strength of the improved material layer is assumed being 2/3 of the peak values due to the concrete material and is presented in Table 15.

**Table 15: Material properties based on a weighted average of the material properties of the moraine, steel pipe and concrete, used as input parameters to Phase<sup>2</sup>.**

Parameter	Symbol	Moraine	Steel pipe	Concrete	Improved layer	Residual value
Unit weight	$\gamma$ [MN/m <sup>3</sup> ]	0.022	0.078 <sup>1</sup>	0.023 <sup>1</sup>	0.023	
Young's modulus	$E_{rm}$ [MPa]	50	20000 <sup>1</sup>	31000 <sup>2</sup>	8000	
Poisson's ratio	$\nu$	0.35	0.3 <sup>3</sup>	0.15 <sup>3</sup>	0.3	
Tensile strength	$\sigma_t$ [MPa]	0	400 <sup>1</sup>	5 <sup>1</sup>	5	3.3
Friction angle	$\phi$ [°]	39	High	35 <sup>4</sup>	38	25.3
Cohesion	$c$ [MPa]	0.017	High	5 <sup>4</sup>	1	0.7

<sup>1</sup> (Zhu, 2012)

<sup>2</sup> (iC-Consulenten, 2013)

<sup>3</sup> (Gercek, 2007)

<sup>4</sup> (Ardiaca, 2009)

## 9.5.2 Permanent support

- ***Radial bolts and face bolts***

It is assumed that radial bolts included in the installation of the lattice girders in the permanent support, are counted for in the liner option in Phase2 (Trinh, 2014).

The self-drilling bolts and shotcrete layer suggested as additional face support in the design of Joberget tunnel cannot be included in a 2D numerical model.

- ***Primary and inner lining***

The primary lining and inner lining are applied at every round length. 30 cm of shotcrete with two layers of wire mesh (K257) and 3-bar lattice girders (Pantex 115/20/30) are estimated as the required primary lining for the Joberget soil tunnel. Installation of inner lining takes place when primary lining is still active. The thickness of the inner lining varies from 40 cm in the top head to 60 cm with a rock foundation at the tunnel invert.

To simulate the primary lining and inner lining in the cross section, the Phase<sup>2</sup> standards for liner support are used. Assuming that the primary lining and the inner lining are applied at the same time and possessing the same properties, a liner type of reinforced concrete with the thickness of 0.7 m is applied in the cross section model. Since only one reinforcement type can be included in the liner type, the lattice girder is chosen assumed providing stronger support than the wire mesh. The standard properties of the lattice girder are shown in Figure 48 and the properties of the estimated reinforced concrete liner are presented in Table 16.

Plastic material type is chosen for the liner to make yielding possible. The plastic liner function in Phase<sup>2</sup> is based on different assumptions listed below (Rocsience, 2014):

- The tensile and compressive strengths of the composite liner are computed by weighting the strengths of the reinforcement and concrete according to their area.
- The residual tensile strength of the concrete is assumed to be zero and the residual compressive strength is assumed to be 20 % of peak value
- Both the tensile and compressive strength of the reinforcement are assumed to be perfectly plastic. This implies that the residual tensile strength is equal to the peak tensile strength, and that the residual compressive strength is equal to the peak compressive strength.

**Table 16: Input parameters of the liner used in the cross section in Phase<sup>2</sup>.**

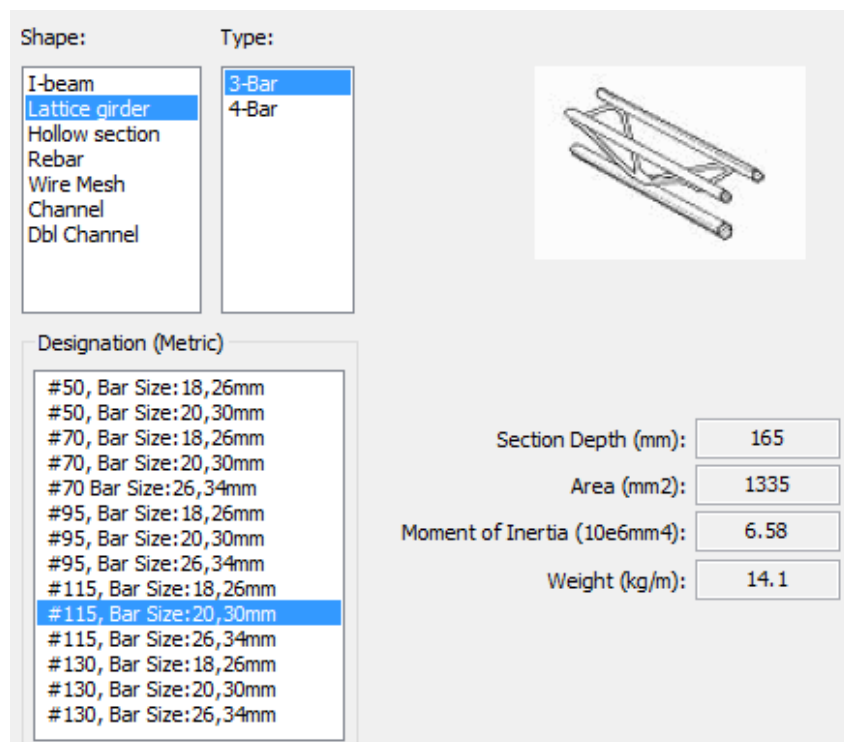
<b>Liner Type: Reinforced Concrete</b>	
<b>Reinforcement</b>	<b>Value</b>
<i>Type: Lattice girder, 3-Bar #115, Bar size:20,30mm</i>	
Spacing [m]	0.4 <sup>1</sup>
Section depth [m]	0.165 <sup>2</sup>
Area [m <sup>2</sup> ]	0.001335 <sup>2</sup>
Moment of Inertia [m <sup>4</sup> ]	6.58e-006 <sup>2</sup>
Young's Modulus [Mpa]	200000 <sup>3</sup>
Poisson's Ratio	0.3 <sup>4</sup>
Compressive strength [Mpa]	250 <sup>3</sup>
Tensile strength [Mpa]	400 <sup>3</sup>
<b>Concrete</b>	
Thickness [m]	0.7 <sup>1</sup>
Young's Modulus (Mpa)	31000 <sup>1</sup>
Poisson's Ratio	0.15 <sup>4</sup>
Compressive strength [MPa]	28 <sup>3</sup>
Tensile strength [MPa]	5 <sup>3</sup>

<sup>1</sup> (iC-Consulenten, 2013)

<sup>2</sup> Phase<sup>2</sup> (Rocsience, 2014)

<sup>3</sup> (Zhu, 2012)

<sup>4</sup> (Gercek, 2007)



**Figure 48: Lattice girder Reinforcement type presented from standard in Phase<sup>2</sup> (Rocsience, 2014).**



The built-in liner function used to model the primary and inner lining in the cross section is not suitable in a longitudinal section (Trinh, 2014). The improved layer method used to simulate the pipe umbrella support is suggested to be applicable to the simulation of the inner and primary lining, in the longitudinal section. An assumed weighted average of concrete and reinforcement is applied to estimate the permanent support-improved layer and is given in Equation 17, based on a cross sectional area. The concrete is weighted to be 9 times more than the weighting of the reinforcement, due to the great difference in the dimension. Approximations of the values of the improved material layer are performed to fit the other parameters.

Given recommendations from Trinh (2014), the residual strength values are assumed being 2/3 of the peak values. The material properties of the improved material layer simulating the permanent support together with estimated properties of concrete and reinforcement is presented in Table 17.

$$\text{Permanent support – improved layer} = (0.9 * \text{concrete}) + (0.1 * \text{reinforcement}) \quad (17)$$

**Table 17: Material properties of the permanent support improved layer based on a weighted average of the material properties of the concrete and reinforcement. The properties of the improved layer are used as input values to Phase<sup>2</sup>.**

Parameter	Symbol	Concrete	Reinforcement	Improved layer	Residual value
Unit weight	$\gamma$ [MN/m <sup>3</sup> ]	0.023	0.078	0.029	
Young's modulus	$E_{rm}$ [MPa]	31000	200000	48000	
Poisson's ratio	$\nu$	0.15	0.3	0.17	
Tensile strength	$\sigma_t$ [MPa]	5	400	45	30
Friction angle	$\phi$ [°]	35	High	35	23.3
Cohesion	$c$ [MPa]	5	High	5	3.3

## 9.6 Ground water

Based on hydrogeological measurements, the groundwater table is assumed located at 10 m below surface level. This can be included in the model by the use of a coupling analysis between ground water analyses and stress-strain analyses in Phase<sup>2</sup>. A steady-state finite element seepage analysis is computed to determine the pore water pressure distribution, based on the ground water boundary condition defined in the model.

Default values in Phase<sup>2</sup> are used for the tolerance and maximum number of iteration. The total head boundary condition is assumed located 10 m below surface at the side external boundaries and an unknown hydraulic boundary condition is defined for the surface. The hydraulic boundary condition of the excavated boundary is zero, due to redistribution of pore water pressure during excavation (Rocsience, 2014)

## 9.7 Stability analyses performed in Phase<sup>2</sup>

A few numerical analyses are carried out to analyse the stability of Joberget soil tunnel. An overview of these analyses is listed below. All analyses are based on interpretation of total displacement defined in Equation 18 to analyse stability. X equals horizontal displacement and Y equals vertical displacement calculated for every node in the model (Rocsience, 2014).

$$\text{Total Displacement} = \sqrt{X^2 + Y^2} \quad (18)$$

### 9.7.1 Support analysis

Different analyses are performed to investigate the stability effect of the initially planned support and excavation methods. The analyses with the both the cross section and longitudinal section are performed on the proposed geometry and excavation procedure of Joberget soil tunnel, if nothing else is stated.

- **Cross section**
  - Cross section of the unrealistic situation with no support to show the need for support measures.
  - Cross section with the pipe umbrella-improved layer.
  - Cross section with an increased zone of the pipe umbrella improved layer.
  - Cross section with pipe umbrella improved layer together with the permanent support lining. The maximum total deformation found in this analysis is transferred to the longitudinal section used to limit deformation and avoid the “beam effect”.
- **Longitudinal section**
  - Longitudinal section with no limit deformation and no support to show the “beam effect”.
  - Longitudinal section with limited deformation and no support.
  - Longitudinal section with the pipe umbrella improved layer.
  - Longitudinal section with the pipe umbrella improved layer and the permanent support improved layer.

### 9.7.2 Ground water analysis

Four analyses are carried out to investigate the effect of changing the location of the ground water table. The ground water analysis is performed on the cross section model.

- No groundwater table assuming dry condition due to appropriate drainage measures.
- Groundwater table at 10 m below surface assuming normal saturated conditions.
- Groundwater table at 5 m below surface assuming highly saturated conditions.
- Groundwater table at surface assuming extremely saturated conditions.

### 9.7.3 Stress analysis

The effect of changing the stresses in the model is investigated with the cross section by four different K-values for the gravity stress field.

- $K = 1$  based on an accepted assumption for weak materials.
- $K = 0.5$  based on an estimated Poisson's ratio and unit weight of the soil and the use of Equation 7 and 8 to find the value of the vertical and the horizontal stress.
- $K = 0.35$  based on experiences with dense sand (Zhu, 2012).
- $K = 0.8$  based on a back analysis performed on a tunnel excavated in glacial, well graded and dense, material in Santiago, Chile (Queiroz et al., 2006).

### 9.7.4 Parameter study of the moraine material

Parameter studies are performed with the cross section model to reveal which material parameters are most important in the stability analysis of Joberget soil tunnel. The model is assumed dry with an isotropic field stress, to better investigate the effect of changing material parameters.

The stability of the tunnel is assumed to mainly depend on the strength of the moraine being situated in the tunnel heading. The phyllite possesses significantly higher strength properties than the moraine and is located in the base of the tunnel. Therefore, varying soil parameters will more likely affect the stability of the model than phyllite parameters. The strength and stiffness of the moraine is investigated by reducing Young's modulus, cohesion and friction angle with 10 %, 30 % and 50 % of the assumed values. Additionally for the Young's modulus the same percent amounts for increase are investigated due to higher value of the E normally estimated for moraine materials.



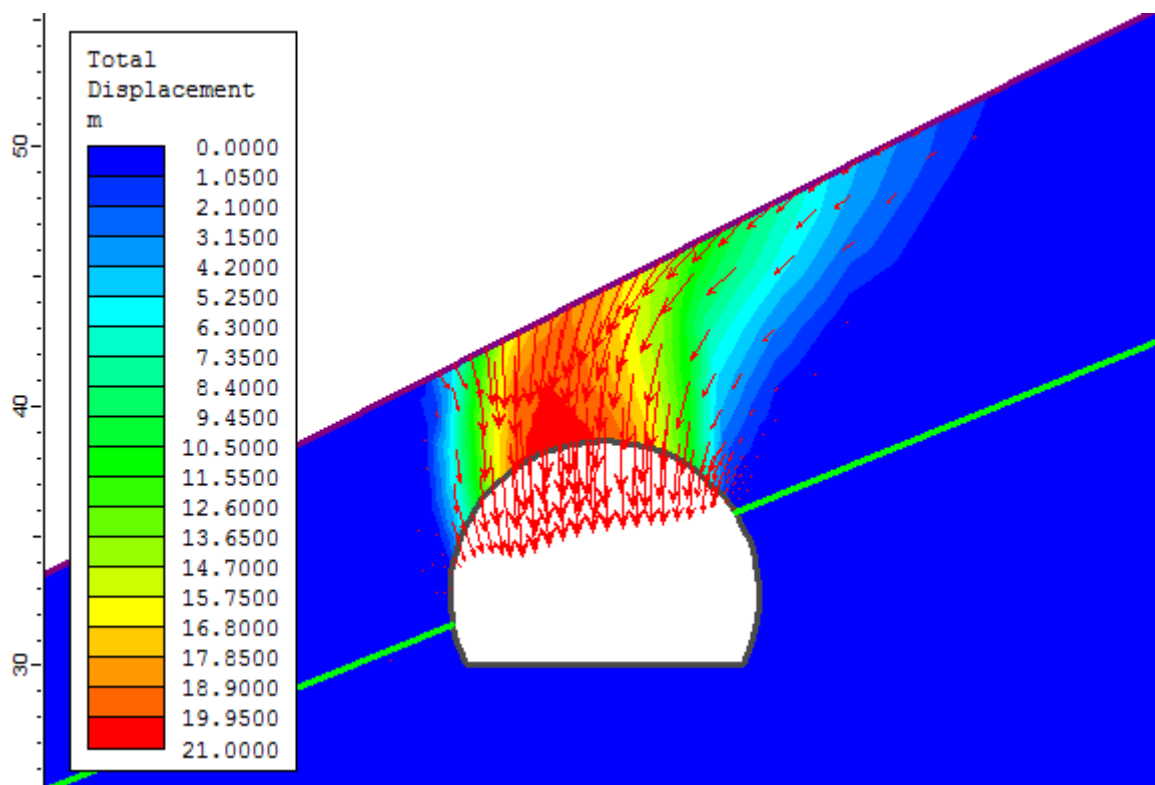
## 10 Results of the numerical analysis

### 10.1 Support analysis

All analyses are performed with isotropic stress condition,  $K=1$ .

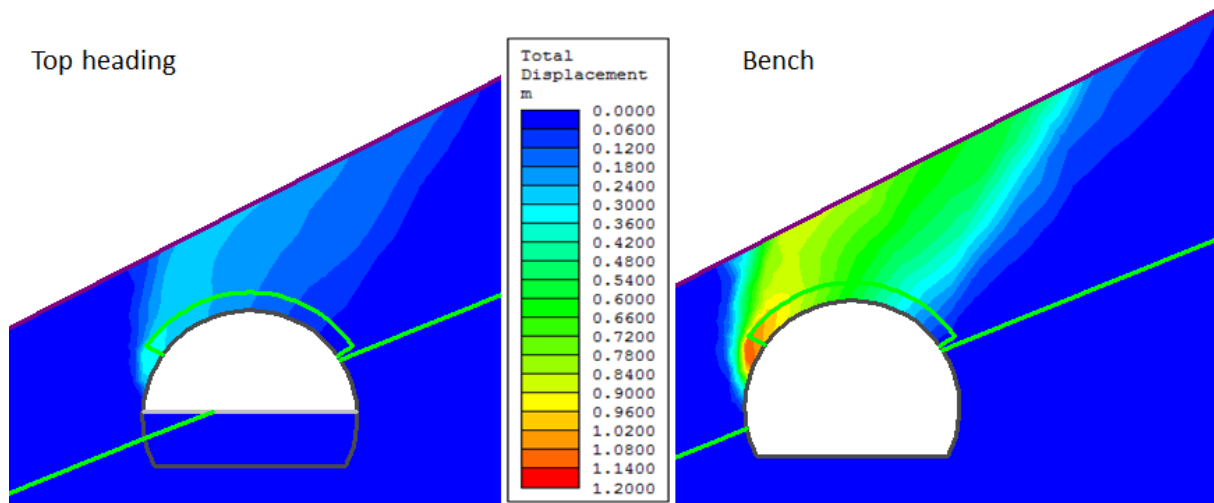
#### 10.1.1 Cross section

Figure 49 shows the total displacement distribution of the unsupported general cross section presenting an unrealistic situation of Joberget soil tunnel. The numerical analysis was not able to converge which indicates failure. The maximum total displacement of an unrealistic value of 20.6 m located in tunnel roof represents an unstable problem.



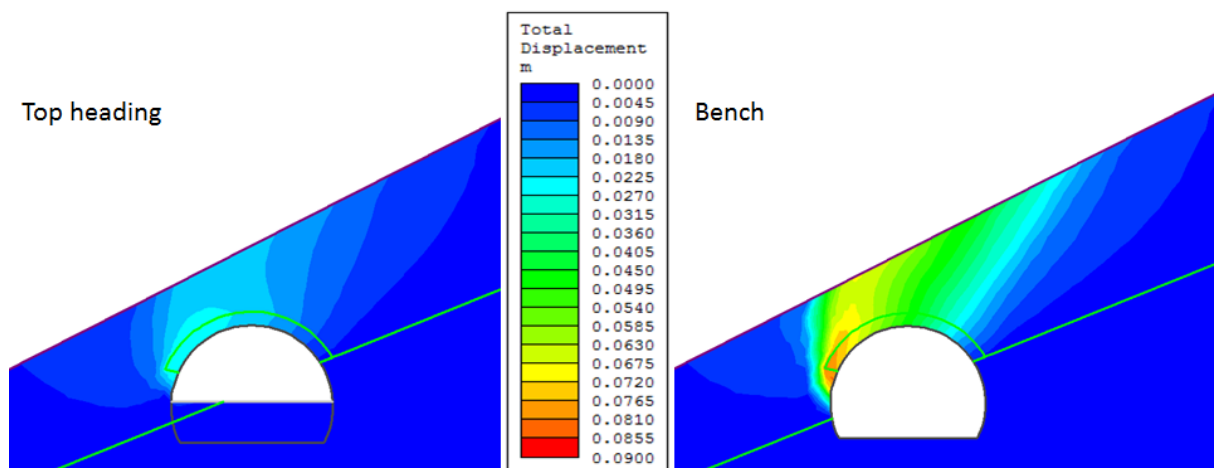
**Figure 49: Interpretation of total displacement of unsupported cross section after excavation of top heading and bench in two stages. Maximum total displacement in tunnel roof is 20.6 m representing an unstable problem. Displacement vectors are displayed to better illustrate the collapsing structure. The tunnel invert is located at 30 m.a.s.l.**

The support effect of the initially planned pipe umbrella improved layer within an angle of  $130^\circ$  in tunnel crown is illustrated in Figure 50. A maximum total displacement of 0.34 m is found in the roof when only top heading is excavated. After the bench is excavated, a higher total maximum displacement of 1.14 m is observed in the roof. The model was not able to converge, indicating an unstable problem.



**Figure 50: Interpretation of cross section with pipe umbrella improved layer within a 130° angle distribution. Maximum total displacement after excavation of top heading is 0.34 m and after bench excavation 1.14 m, indicating a unstable problem.**

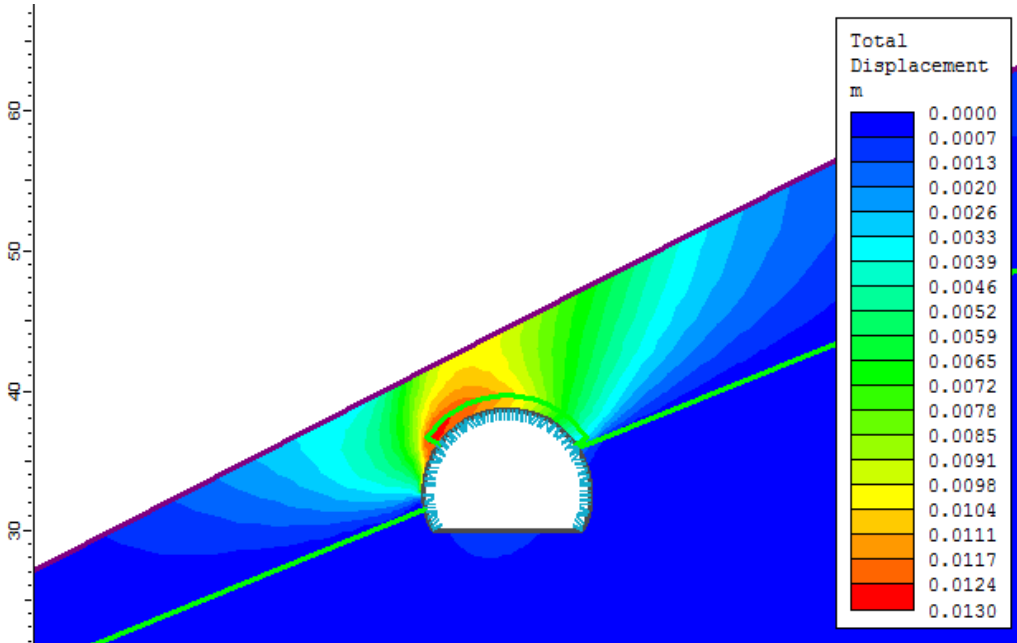
Modelling of a cross section with an increased pipe umbrella improved layer within an angle of 145° in tunnel roof is presented in Figure 51. A maximum total displacement of 0.025 m is observed when top heading is excavated and 0.082 m is observed when the bench is excavated, indicating a stable problem assuming 2 % strain allowance of the tunnel.



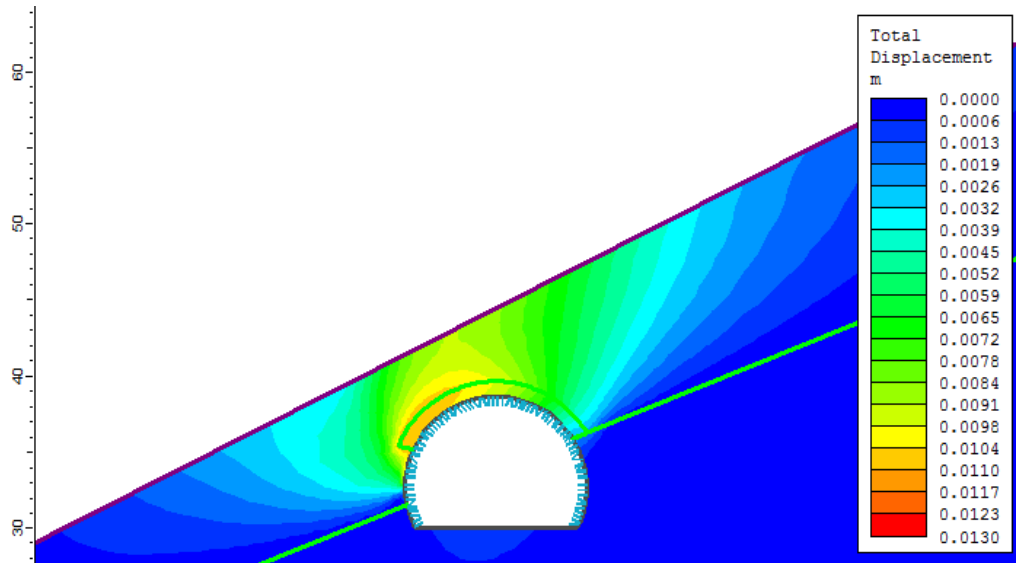
**Figure 51: Interpretation of cross sections with increased pipe umbrella improved layer of 145°. After excavation of top heading, a maximum total displacement of 0.025 m is observed in the tunnel roof and after excavation of bench 0.082 m is observed in the tunnel roof.**

The total displacement of the cross sections with pipe umbrella improved layer and permanent support is shown in Figure 52. Installation of permanent support is performed after top heading is excavated and before and after bench is excavated. A maximum total displacement of 0.013 m is observed with both top heading and bench excavations in the model with a 130°

pipe umbrella layer. Hence, the problem is assumed stable. This displacement is used to limit the vertical displacement, in the assumed stable entrance of the tunnel longitudinal section, to avoid the “beam effect” generating errors in the displacement analyses. The limited displacement is chosen to be 0.02 m. Additionally, the cross section with the increased pipe umbrella improved layer of 145° is also modelled with permanent support showing an even smaller maximum displacement of 0.011 m, presented in Figure 53.



**Figure 52: Interpretation of cross section with the 130° improved pipe umbrella layer and the proposed permanent support. The maximum total displacement is 0.013 m.**

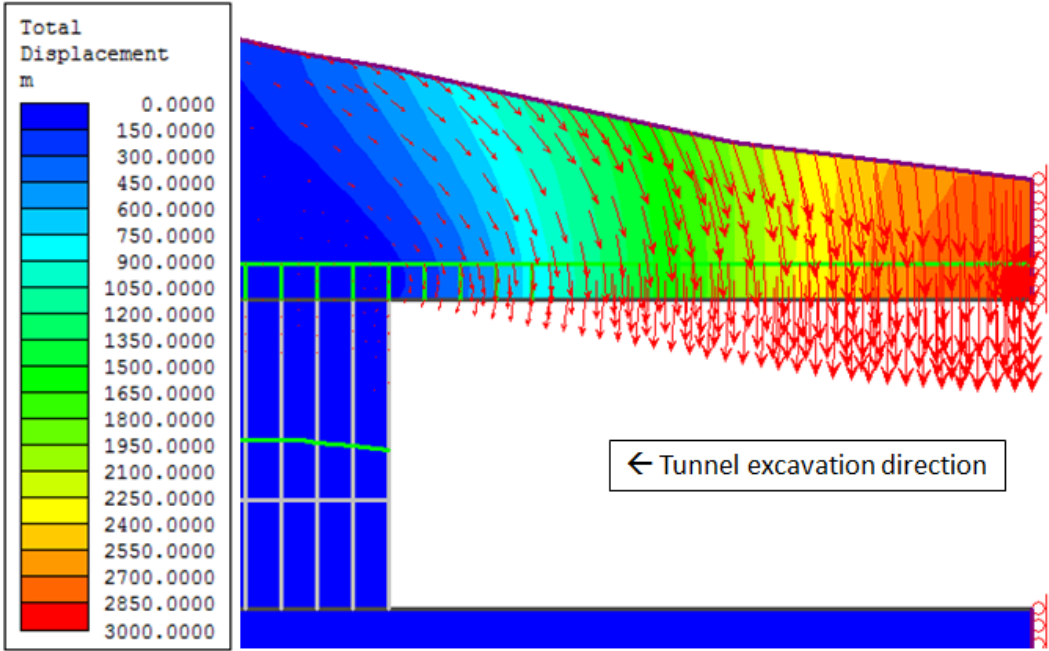


**Figure 53: Interpretation of cross section with the 145° improved pipe umbrella layer and the proposed permanent support 145°. The maximum total displacement is 0.011 m.**

Minor differences between the permanent supported cross section with planned pipe umbrella versus the cross section with advanced umbrella are observed, indicating a very good supporting effect provided by the permanent support.

**10.1.2 Longitudinal section**

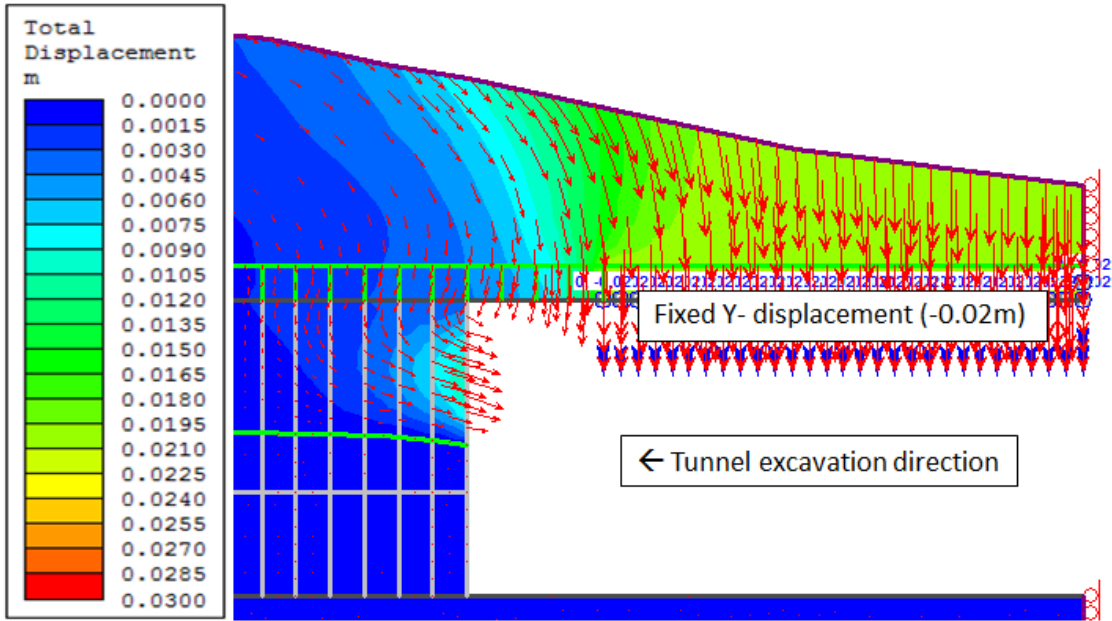
The longitudinal section is modelled without restricted deformation in Figure 54 and with restricted displacement in Figure 55, to illustrate the “beam effect” introduced in chapter 8.2. The “beam effect” is well illustrated in figure 54, showing unrealistic severe displacement values. The displacement in figure 55 is restricted to 0.02 m displacement in the Y-direction, based on the maximum total displacement obtained from the cross section with both primary and permanent support. Hence, this section is assumed stable. The value is negative, indicating the downward direction of the displacement.



**Figure 54: Unrealistic severe displacements after excavation of the first stages of Joberget soil tunnel with the pipe umbrella and the permanent support improved layers when displacements are not limited. The figure illustrates the “beam effect” phenomenon.**

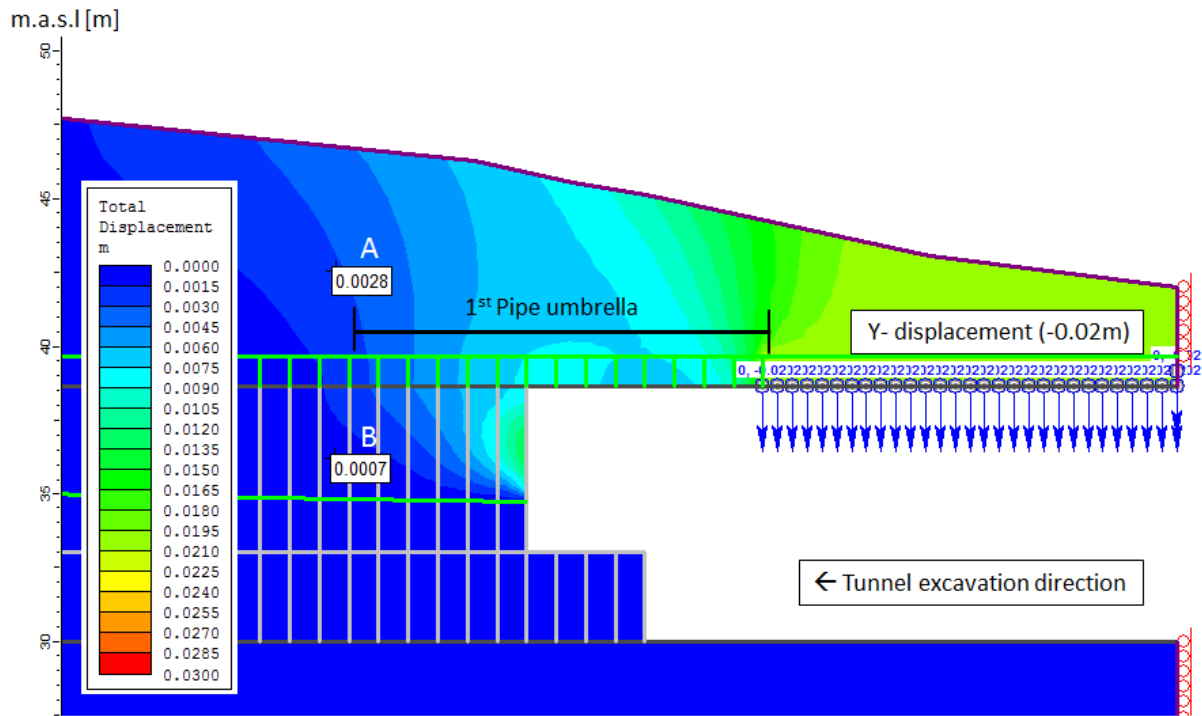
When the “beam effect” is neglected in Figure 55, more reasonable displacement values are observed. Displacements are concentrated in tunnel roof and at the top heading of the tunnel face located in the moraine material layer.



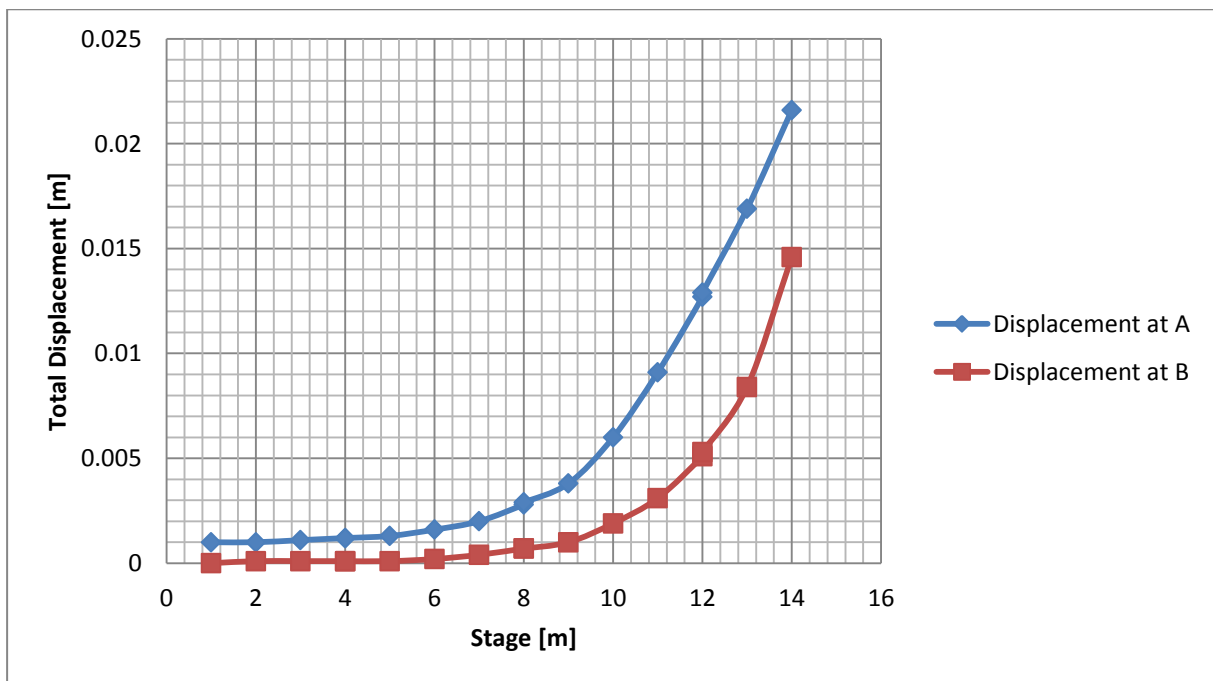


**Figure 55: Total displacements in the longitudinal section with pipe umbrella and permanent support after excavation of the first stages, including restricted displacement of -0.02 m in Y-direction defined from the fully supported cross section analysis.**

Figure 56 shows the longitudinal section with pipe umbrella- and permanent support-improved layer, after excavation of the first 8 m of the pipe umbrella, prior to a bench of 4 m is excavated. Two query points above (A) and under (B) the rear end of the pipe umbrella-improved layer of 15 m, is found after every excavation stage and is presented with graphs in Figure 57. The graphs show the supporting effect of the pipe umbrella advance of the tunnel face.



**Figure 56: Longitudinal section of Joberg soil tunnel showing the first pipe umbrella section simulated with an improved material layer at stage 8. The permanent support improved layer is applied after every stage. The location of the measured displacement above (A) and under the pipes (B) at the end of the pipe umbrella section is indicated in the figure.**



**Figure 57: The total displacement measured above (A) and under (B) the pipe umbrella plotted versus excavated stages of top heading every meter and bench every four meters.**

The maximum total displacement of the first 16 stages in the longitudinal section for three different analyses with, no support, only pipe umbrella support and permanent support together with pipe umbrella, are presented in three graphs in Figure 58 to show the effect of the support. The first tunnel meters are modelled with restricted displacement of -0.02 m in Y-direction for in analyses.

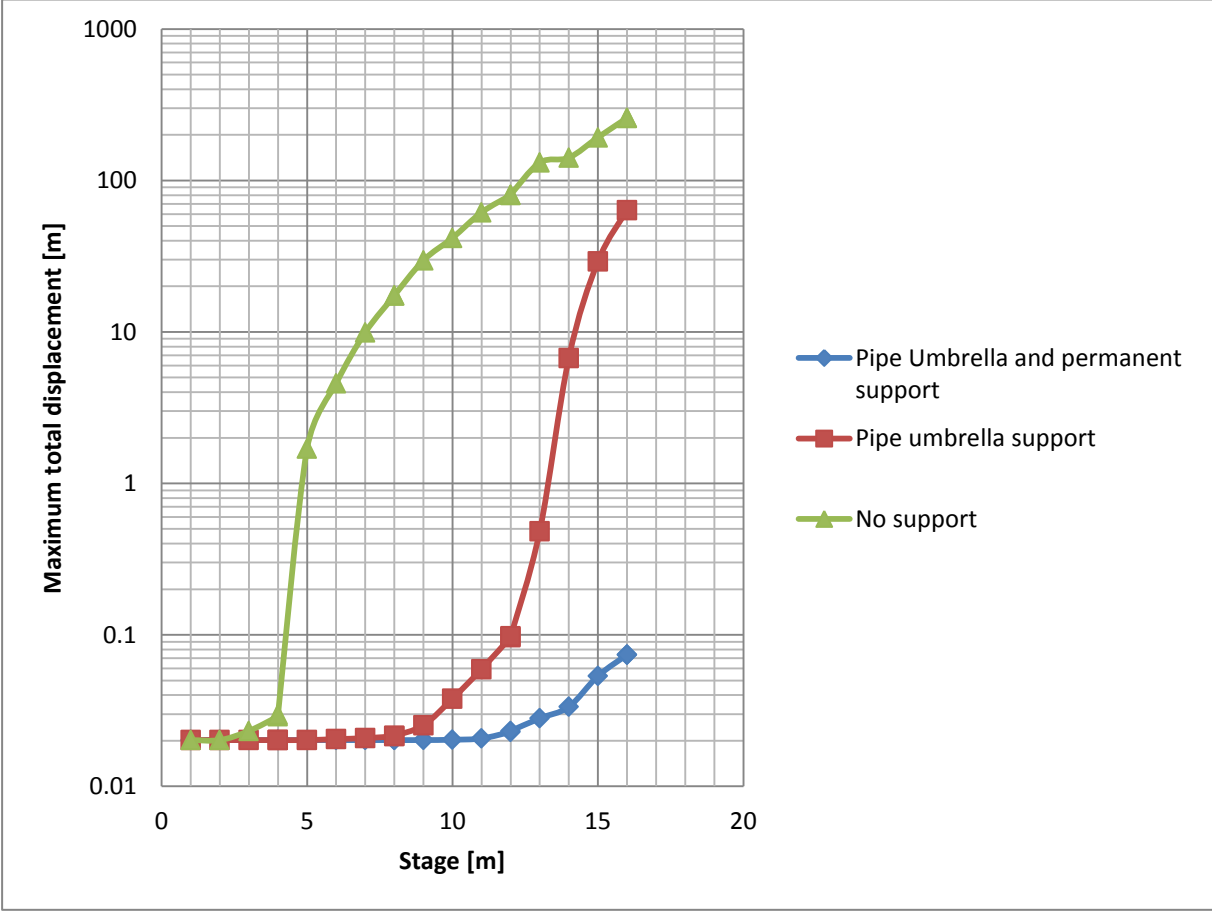


Figure 58: Maximum total displacements of the first 16 stages in the longitudinal section for three different analyses with no support, only pipe umbrella support and permanent support together with pipe umbrella. The first tunnel meters are modelled with restricted displacement of -0.02 m in Y-direction in all analyses.

### 10.2 Stress analysis

Four different K-values of 1, 0.8, 0.5 and 0.35 were investigated and compared based on the interpretation of the total displacement in the cross section and presented in Figure 59

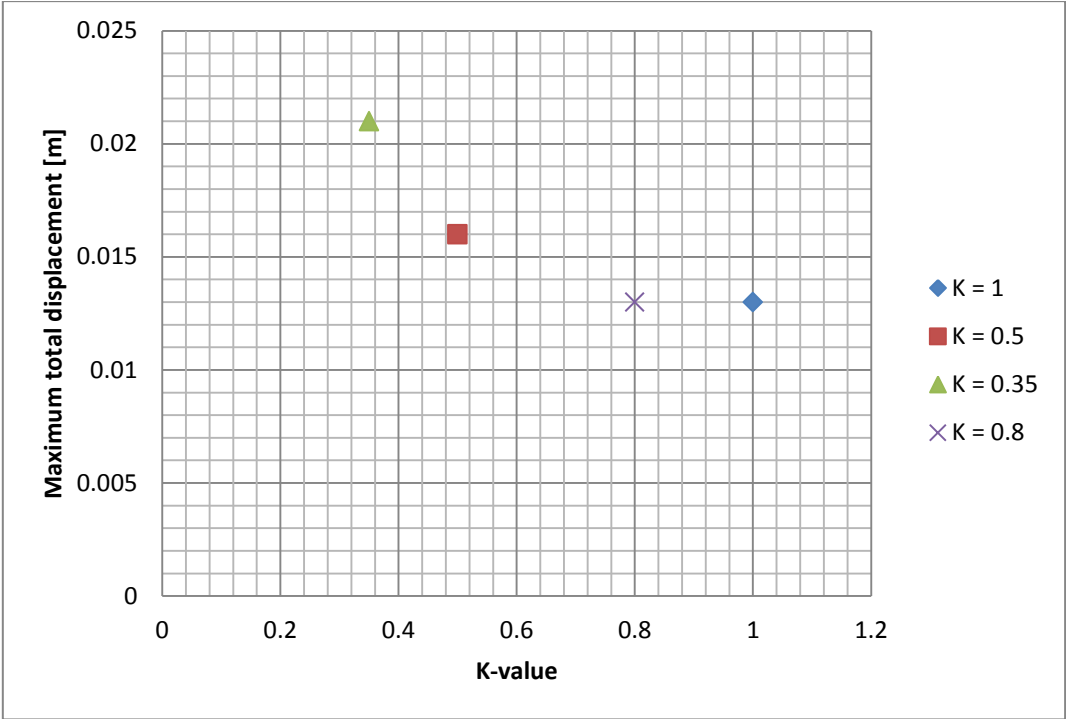


Figure 59: Illustrating the effect of reducing field stress by changing the K-value to 0.8, 0.5 and 0.35.

### 10.3 Ground water analysis

The effect of ground water was investigated with the fully supported cross section model with top heading and bench excavations for four different scenarios based on the elevation of ground water table, listed below:

- No ground water table assuming dry condition or drained condition.
- Ground water table at 10 m below surface assuming normal condition.
- Ground water table at 5 m below surface.
- Ground water table at surface assuming extremely saturated condition.

The influence of changing the groundwater condition on the total maximum displacement is presented in Figure 60. The cross section, with the interpreted total displacement for the ground water table at 10 m is presented in Figure 61 to show the estimated location of the ground water table by Phase<sup>2</sup>.

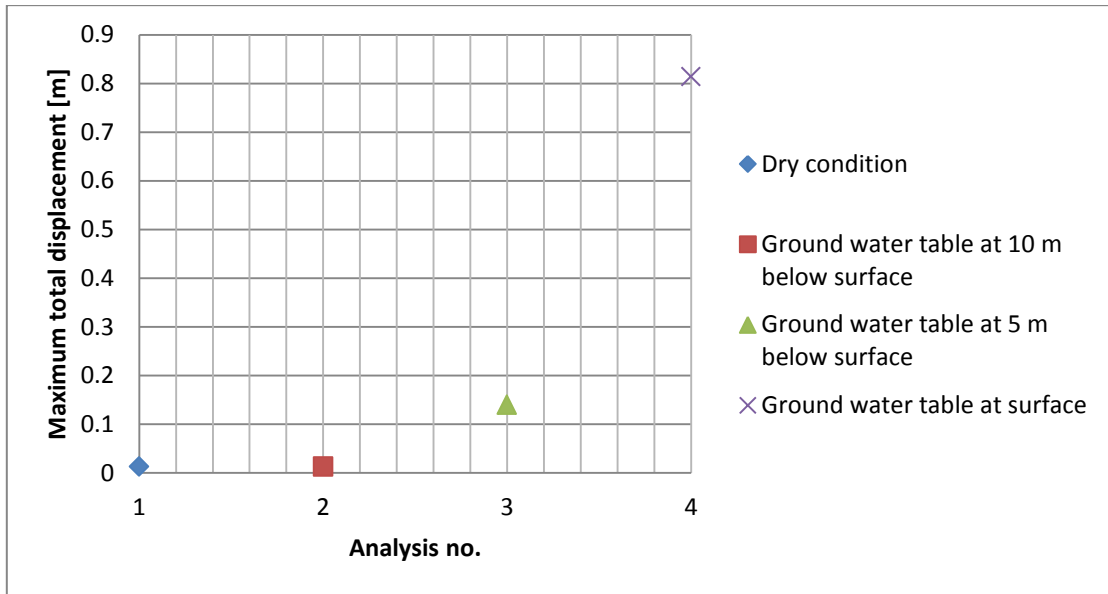


Figure 60: Illustrating the effect of changing the ground water level with the total maximum displacement.

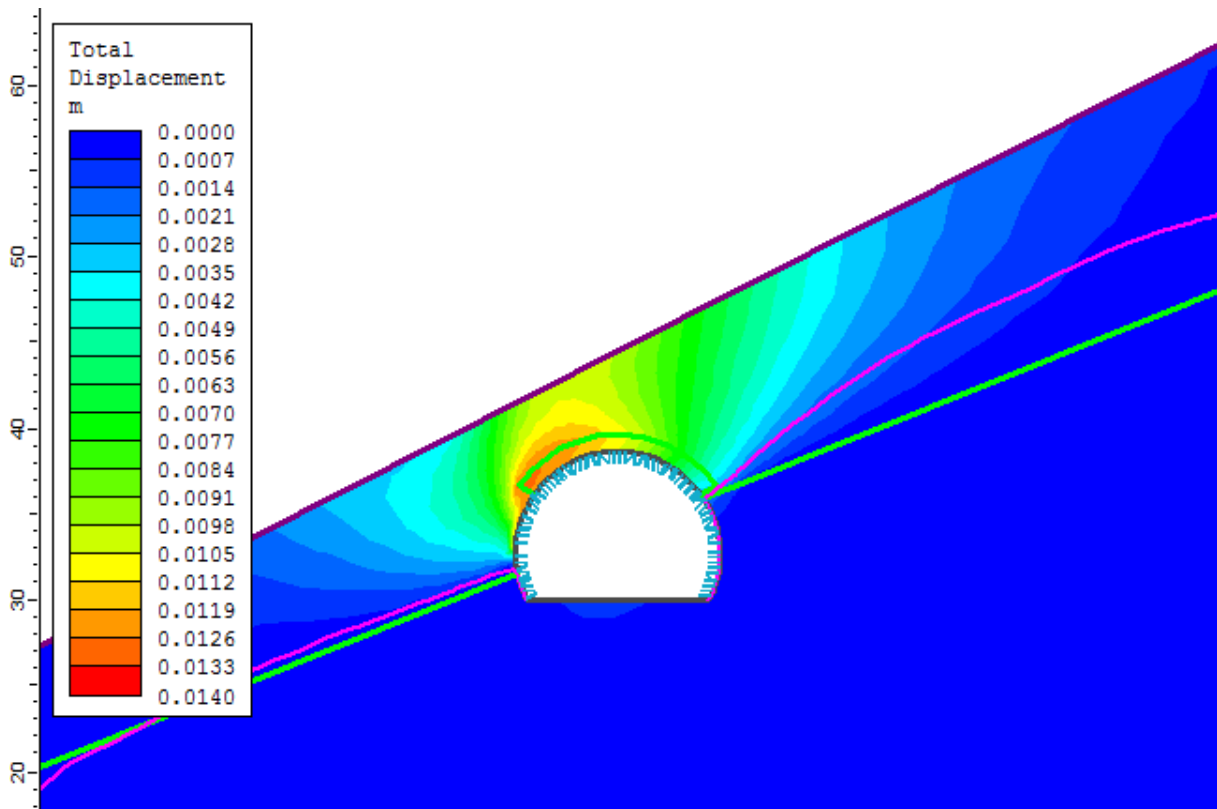
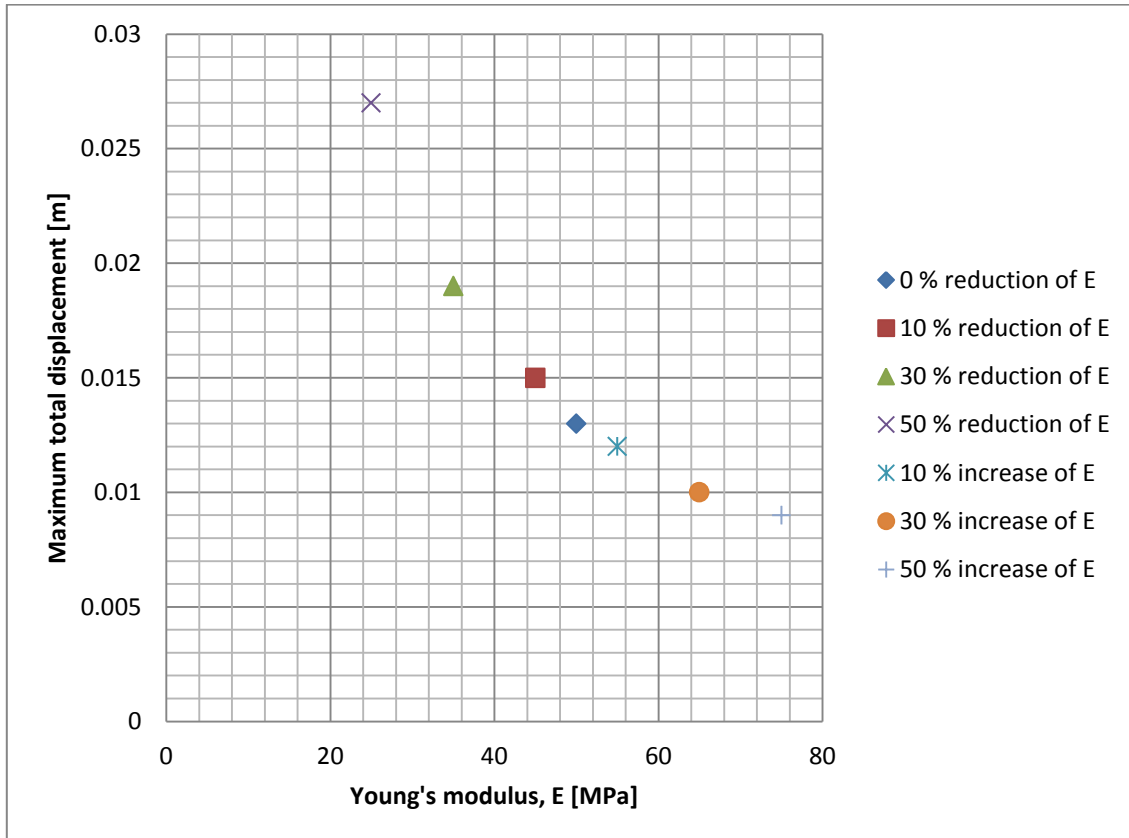


Figure 61: Initial cross section included assumed groundwater table at 10 m below surface. Maximum displacement is 0.013 m for both top heading and bench excavations. Estimated ground water table is illustrated by a pink boundary.

### 10.4 Parameter study of the moraine material

The parameter study is performed by changing one parameter while keeping the others parameters constant. All analyses are performed on the fully supported cross section with hydrostatic field stress condition,  $K=1$ .

The stiffness of the moraine depending on Young's modulus is investigated by reducing and increasing the assumed value of 50 MPa with 10 %, 30 % and 50 %. The influence of changing the parameter is investigated with interpretation of the maximum total displacement and the results is presented in the diagram in Figure 62.



**Figure 62:** Illustrates the influence of changing the assumed Young's modulus, E of the moraine by different percentages.

The strength of the moraine is represented by the friction angle and the cohesion. The influence of changing these parameters one by one is performed with the interpretation of the maximum total displacement. The assumed friction angle of  $39^\circ$  and cohesion of 0.017 MPa are both reduced by 10 %, 30 % and 50 %. The influence of the reduction of the cohesion is presented in Figure 63 and of the friction angle is presented in Figure 64, based on maximum total displacement.

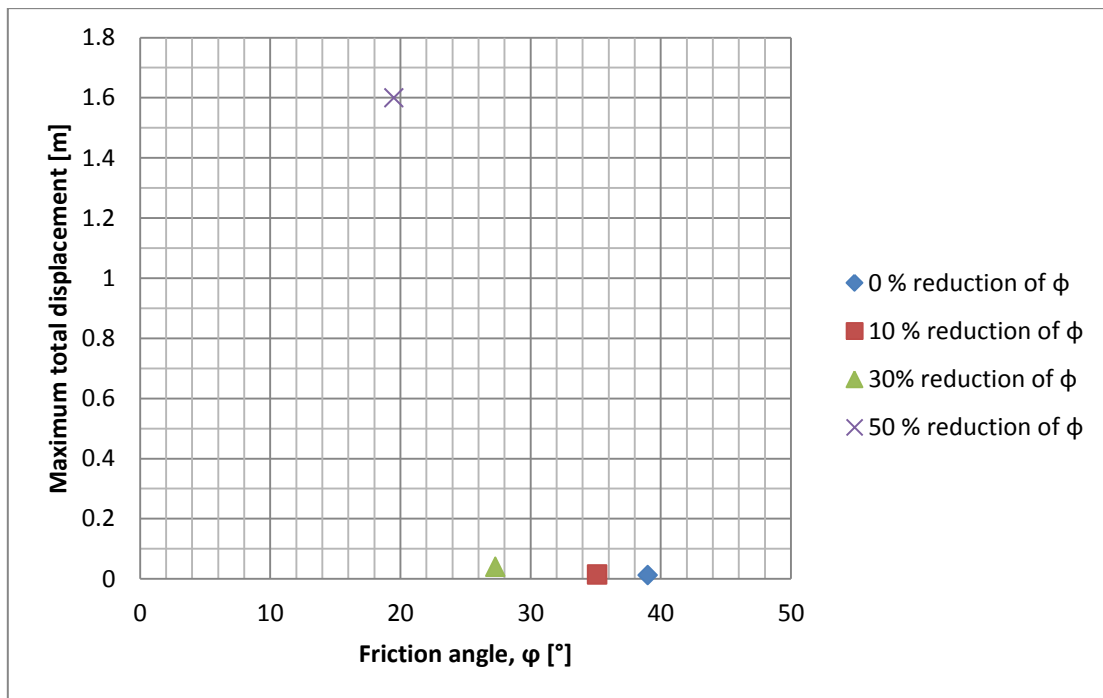


Figure 63: Illustrating the influence of changing the friction angle of the moraine by different percentages.

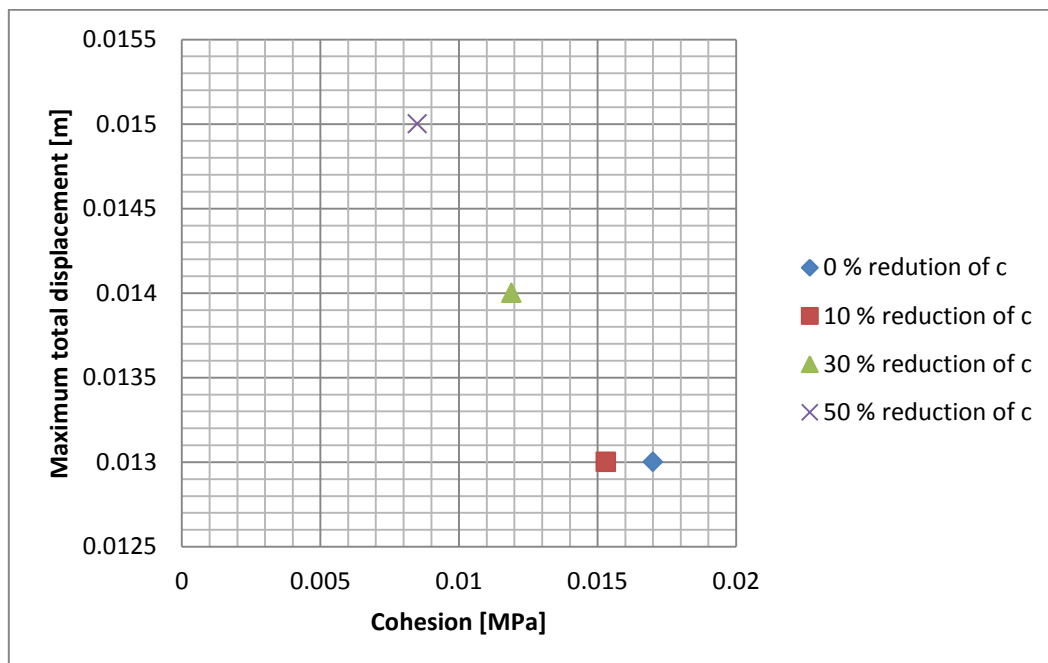


Figure 64: Illustrating the influence of changing the cohesion of the moraine by different percentages.





## 11 Discussion

The stability of an underground construction mainly depends on rock mass quality, field stresses, ground water condition, geometry of the construction and performance and support of the excavation (Nilsen and Palmstrøm, 2000).

### 11.1 Stability and support design of Joberget soil tunnel

2D finite element analysis with Phase<sup>2</sup> are performed to investigate the stability of Joberget tunnel based on the support and excavation method proposed by the NPRA, Sweco and iC-Consulenter (2013). The stability is evaluated based on displacement interpretations and the critical strain limit of approximately 2 % proposed by Sakurai (1983).

#### 11.1.1 Cross section

Unrealistic severe total displacements that are observed for the unsupported cross section indicate the importance of proper support of tunnel face and span. Concerning the analyses of the unsupported model and of some of the models with primary support of pipe umbrella only, the simulation does not converge which indicates unstable problems. Due to the non-convergence of the model, calculated displacements in the model should not be taken as final values.

The numerical model with the initially planned pipe umbrella support method simulated by an improved layer of 130° in the tunnel crown show an unstable problem, especially following excavation of the bench. By increasing the pipe umbrella improved layer to an angle of 145°, a stable situation is established. Hence, installation of additional pipes in the tunnel abutments may increase the tunnel stability. Installation of additional pipes should therefore be evaluated during construction of the first meters of the Joberget tunnel, when more moraine material is present in the tunnel cross section. The increased stability gained by including the improved pipe umbrella layer in the model corresponds to the good experiences with the use of pipe umbrella support method in soil tunneling.

Interpretations of the total displacements analyses for both pipe umbrella layers show lower displacements when only top heading is excavated. This is reasonable, as stability problems generally increase with increasing size of excavations. Therefore, division of face excavation in a top heading and a bench, where the top heading is additionally supported before bench is excavated, is found beneficial. This is a common procedure when excavating in weak rock masses to ensure stable conditions during construction.

The permanent support is simulated by a standard lining of reinforced concrete in Phase<sup>2</sup>. When this lining is applied to the initially planned cross section model, very little displacement is observed. Almost the same total displacement is observed for the cross section with the increased pipe umbrella layer with permanent support. This indicates a stable structure. In comparison to the cross section models without support or with primary support only, permanent support is clearly necessary and very effective. The maximum total displacement observed is 1.3 mm and is low with regard to the critical strain of 2 % allowing 8 - 9 mm deformation for Joberget tunnel. This also indicates the very good permanent

support. It should be emphasized that the permanent support is simulated by a standard lining in Phase<sup>2</sup> and will therefore not fully represent the proposed permanent support.

### 11.1.2 Longitudinal section

The analyses with the longitudinal model indicate possible stability problems at tunnel face, especially in the top heading where the moraine material is located. It is documented by Yoo (2002) that face reinforcement with face bolts will significantly reduce face deformation, thus improve face stability. The numerical model does not include the face bolts and shotcrete included in the design of Joberget soil tunnel which will contribute to stabilize the tunnel.

The reinforcement by the pipe umbrella in tunnel heading increase longitudinal load transfer to unexcavated area and consequently decreases deformation and increase stability (Wang and Jia, 2009). This is true for the longitudinal model and is showed in Figure 57 where displacements below the pipe umbrella advance of tunnel face are less than those above. The deformation values obtained in the numerical model depends on the restricted deformation, chosen from the fully supported cross section to avoid the “beam effect”. Thus, the displacement values should not be taken as real values, but to indicate locations of instability.

As expected, displacements are mainly concentrated in the tunnel roof where the moraine material is present. Since the phyllite layer is stable in all analyses, it is assumed to be a good tunnel base. The design of Joberget tunnel primary and inner lining carried out by iC-Consulnten (2013) indicating that no structural invert is required, is seen in the numerical model.

Generally, numerical analyses from both the cross section and the longitudinal section indicate the importance of support measures, to reduce tunnel displacements. The effective support strength provided by the pipe umbrella method and the chosen permanent support is also clearly observed in both sections. Thus, the support design of Joberget soil tunnel seems to be appropriate for the tunnel. However, keeping in mind that the 2D numerical modeling is a crude approximation of the reality, it is important to be critical to the results obtained and a proper follow-up during tunneling is therefore crucial.

## 11.2 The uncertainties of input parameters

A parameter study is performed in order to understand the reliability of the numerical analysis. The sensitivity of a design by changing input parameters is often more important in judging the acceptability of the design than any single displacement value. The higher the parameter sensitivity and uncertainty is, the more critical it will be for the quality of the model output (Hoek and Diederichs, 2006).

### 11.2.1 Field stress

The in situ rock mass stress is difficult to characterize for soil materials. A common assumption of isotropic stress condition in weak rock masses such as soil is investigated by varying the coefficient of earth pressure at rest,  $K_0$ . Generally, the displacement decreases with increasing  $K_0$  and is seen in the field stress analysis. It is proposed by Queiroz et al. (2006) that the higher the  $K_0$  value is, the more over-consolidated the material is. Measured  $K_0$ -values for clays and granular soils are ranging from 0.3 - 0.7 (Mesri and Hayat, 1993).

Since the soil at Joberget is estimated as an over-consolidated moraine material, a higher  $K_0$ -value is assumed. Identical displacements are obtained for  $K_0$ -value of 0.8 and 1. Hence, an assumption of isotropic condition in this study is reasonable.

### 11.2.2 Soil properties

The soil properties measured in the laboratory may not represent the values on a larger scale, and the parameters estimated from empirical characterization techniques may not be representable for the material at Joberget. Therefore, a parameter study on strength and stiffness of the soil is carried out, assuming these parameters will have the greatest impact on the stability, defining the material deformation and failure criterion

The stiffness of the soil is defined by Young's modulus which is known to be the most difficult parameter to estimate (Nilsen and Broch, 2011). The displacement decreases with increasing stiffness. The value of the displacement indicates a stable situation due to the high support effect provided by the permanent support. However, before the permanent support is installed, low E-values may result in difficulties during construction. The numerical analysis is very sensitive to the Young's modulus and great care in selecting the parameter should be performed. Generally, a higher E value for the moraine material is experienced than what is assumed in the model. Hence, some confidence can be applied to the model.

Concerning the strength properties of the soil, the influence of the cohesion and friction angle is investigated. It is observed that displacements decrease only slightly with increasing cohesion. This may be due to the cohesion being very low resulting in no significant difference to the model when decreasing with some percentages. The same is observed for the friction angle at reasonably lower friction angles. When the friction angle is decreased with 50 %, a sudden increase in the displacement is observed. The reason for this is uncertain and has not been investigated further. However, such a low friction angle is unrealistic for the over-consolidated moraine material.

Rock mass is discontinuous, anisotropic, inhomogeneous and plastic. It is influenced by complex in situ conditions of stresses, temperature and fluid pressure. Additionally, consequences of engineering such as blasting disturbance and construction processes will strongly affect the rock mass. These factors make rock masses difficult to represent in numerical modelling and several assumptions regarding rock mass properties are necessary. Therefore, numerical modelling in rock engineering requires empirical judgements supported by experiences and common sense (Jing, 2003). Also, it is of great importance to calibrate the model with observations and measurements obtained during construction to get more accurate estimation of the input parameters, resulting in more reliable numerical results

### 11.2.3 Improved material layer

There is no available literature on how to weigh and estimate the different parameters of the components in either the improved pipe umbrella layer, or the improved permanent support layer. Both layers show a supporting effect, indicating that improved material layer can be performed to simulate support measures.

The details concerning pipe dimension, spacing and length is impossible to estimate with the improved material layer simulating the pipe umbrella. It is also difficult to know if the grout is perfectly applied, sealing the pipes and the surroundings. Thus, changing the parameters of the improved material layer will provide unreliable information about the pipe umbrella system. The weighting of different components and the estimated size of the improved material layer bring further uncertainties to the model. Therefore, comprehensive studies such as 3D numerical modelling are necessary to understand the details of the pipe umbrella support system.

### **11.3 Ground water influence on tunnel excavation**

Commonly, it is difficult to predict the locations and quantities of potential water leakage in a tunnel excavation.

The strength reduction effect due to water influence is very well demonstrated in the shear box test and the triaxial test. Therefore, the influence of ground water in Joberget soil tunnel is investigated in the 2D numerical model. Assuming normal conditions, where the ground water table is located some 10 m below the surface, no effect on the stability is observed. This is reasonable since the assumed ground water table will be located in the less permeable phyllite and in the lower part of the tunnel where no stability problems are noted. When the ground water table is moved closer to the surface, stability problems arise due to the water being located in the more permeable moraine layer, decreasing material strength. Keeping in mind that the ground water level will change seasonally, drainage and pre-grouting ahead of excavations is crucial to avoid stability problems and in worst case collapses during and after construction.

## 12 Conclusion and recommendation

Instability of face, unsupported span and water leakage are typical problems in soil tunneling. It is recommended from rock mass classification systems, that special evaluation in finding the required support for Joberget soil tunnel is necessary. The importance of sufficient support of tunnel face and span to reduce displacements in Joberget soil tunnel is implied by the 2D numerical analysis performed with Phase<sup>2</sup>. Displacements are mainly distributed in the tunnel heading and face where the weaker moraine material is present.

The pipe umbrella method selected as primary support in Joberget soil tunnel, will be carried out to ensure stability during construction. The method is simulated in the numerical model by a zone of improved material layer. This simulation is found useful in this study, providing reasonable results when showing a significant decrease in displacement in compare to the unsupported model. Division of the tunnel face in top heading and bench is assumed to be a good excavation procedure since less displacement is observed after top heading is excavated. With partial face excavations, short round lengths and immediate installation of permanent support after excavations together with the pipe umbrella support method, Joberget soil tunnel is assumed stable in the numerical analysis.

A parameter study is performed to investigate the uncertainty of the moraine material input parameters and the chosen field stress in the numerical model. The sensitivity of the field stress is investigated and show increasing stability with increasing  $K_0$ . Minor changes in the displacements are observed when decreasing the strength parameters, friction angle and cohesion. The most sensitive parameter investigated, is the Young's modulus,  $E$  showing increasing displacements with decreasing  $E$ .

The evaluation of the Young's Modulus for the moraine material at Joberget is supplemented by triaxial testing. The value obtained is depending on the scale effect, the difficulty in preparing the sample similar to the in situ condition and most importantly, the water content. It is observed that a minor change in water content leads to a major change in the moraine material strength properties.

The reduction of strength due to water is also observed in the numerical analysis. When the water table is located in the moraine layer, closer to the surface, stability problems arise due the permeable moraine material. When normal ground water condition is assumed and the ground water table is located below the moraine layer in the less permeable phyllite, the tunnel is found to be stable. However, due to the elevation of the ground water table varying with seasons and sudden rain falls, a well prepared drainage plan should be implemented in Joberget soil tunnel.

Numerical modelling includes several simplifications and is limited by the reliability of the input parameters. Still, numerical modelling is found useful in the investigation of stability and required support of Joberget soil tunnel.

*Numerical modelling should not be used as a substitute for thinking, but as an aid to thought (Eberhardt, 2003)*

### 12.1 Further investigations and follow-up

A detailed study of Joberget soil tunnel has been carried out by Langåker (2013) and in this thesis. Still, there are important topics concerning soil tunneling at Joberget that require further investigations:

- Additional parameter studies to investigate the influence of changing other material parameters in the 2D numerical model. Also, investigation of the influence of changing excavation procedure in the 2D numerical model, by looking at full face excavation or pocket excavation with further division of face.
- 3D numerical modelling to investigate details of the pipe umbrella method, such as the effect of increasing spacing between the pipes and including face support measures.
- Further evaluation of spiling as an alternative method by using numerical analysis.
- More laboratory tests to achieve more confidence in the test results.
- Stability analysis including frost action and ice formation.
- Most importantly, monitoring of displacement and water pressure during excavation during tunneling to prevent collapse of the tunnel face.

The observational design method in Eurocode 7 is based on monitoring during excavation. This method is commonly performed to check results and prediction in the planned geotechnical design.

Displacement measurements or core logging during construction can be used to calibrate numerical models. The input parameters may be adjusted based on this observation to better represent the in situ condition at Joberget. This may lead to more reliable results of the tunnel stability and support requirements.

During construction of Joberget tunnel, displacement should be monitored and support measures should be adjusted to fit the encounter geological condition, respectively to the monitored displacement (iC-Consulenter, 2013). Such back analyses will provide important information regarding required tunnel support.

### 13 References

- Ardiaca, D. H., 2009, *Mohr-Coulomb parameters for modelling of concrete structures*. Plaxis Bulletin, Spring issue 2009.
- ASTM, 2006, *C136 - 06 Standard Test Method for Sieve Analysis of Fine and Coarse Aggregates*. The American Society for Testing and Materials.
- , 2011a, *D3080/D3080M - 11 Standard Test Method for Direct Shear Test of Soils Under Consolidated Drained Conditions*. The American Society for Testing and Materials.
- , 2011b, *D7181 - 11 Standard Test Method for Consolidated Drained Triaxial Compression Test for Soils*. The American Society for Testing and Materials.
- Barton, N., Lien, R., and Lunde, J., 1974, *Engineering Classification of Rock Masses for the Design of Tunnel Support*, Rock Mechanics, Springer-Verlag, p. 189-236.
- Brattli, B., 2014, *Personal communication about water content in moraine material*. NTNU, Trondheim.
- Cai, M., Kaiser, P. K., Tasaka, Y., and Minami, M., 2007, *Determination of residual strength parameters of jointed rock masses using the GSI system*. International Journal of Rock Mechanics and Mining Sciences, v. 44, no. 2, p. 247-265.
- Deere, D. U., 1968, *Chapter 1: geological considerations*, Rock mechanics in engineering practice: London.
- Drageset, L. N., 2013, *Railway tunnel Holm-Nykirke - "the pipe umbrella method". - Tunnel section with little and no overlying rock cover*. Fjellsprengningsdagen 2013.
- Eberhardt, E., 2003, *Rock Slope Stability Analysis - Utilization of Advanced Numerical Techniques*.
- Freeze, R. A., and Cherry, J. A., 1979, *Groundwater*, Englewood Cliffs, NJ: Prentice-Hall, Inc.
- Gaut, S., 2014, *Personal communication about water content in moraine material*. Sweco Trondheim.
- Gercek, H., 2007, *Poisson's ratio values for rocks*. International Journal of Rock Mechanics and Mining Sciences, v. 44, no. 1, p. 1-13.
- Hoek, E., 1999, *Support for very weak rock associated with faults and shear zones*.
- , 2001, *Big tunnels in bad rock*. Geotechnical and Geoenvironmental Engineering.
- , 2007a, *Rock-Support Interaction analysis for tunnels in weak rock masses*, Rock Mechanics Design, RocScience Inc.
- , 2007b, *Rock mass classification*, Rock Mechanics Design, Rocscience Inc.

- , 2007c, *Rock mass properties*, Practical Rock Engineering, RocScience Inc.
- Hoek, E., and Brown, E. T., 1997, *Practical estimates of rock mass strength*. International Journal of Rock Mechanics and Mining Sciences, v. 34, no. 8, p. 1165-1186.
- Hoek, E., Carranza-Torres, C., and Corkum, B., 2002, *Hoek-Brown failure criterion - 2002 edition*. Proceedings of NARMS-Tac (2002), p. 267-273.
- Hoek, E., and Diederichs, M. S., 2006, *Empirical estimation of rock mass modulus*. International Journal of Rock Mechanics and Mining Sciences, v. 43, no. 2, p. 203-215.
- Hoff, I., 2014, *Personal Communication about triaxial testing*. NTNU, Trondheim.
- iC-Consulenter, 2013, *Technical Report - Soil tunneling section, Joberget tunnel*.
- Jing, L., 2003, *A review of techniques, advances and outstanding issues in numerical modelling for rock mechanics and rock engineering*. International Journal of Rock Mechanics and Mining Sciences, v. 40, no. 3, p. 283-353.
- Langåker, M. Ø., 2013, *Joberget tunnel – Engineering geological aspects of soil tunneling based on Pipe Umbrella method*. NTNU, Trondheim.
- Lebourg, T., Riss, J., and Pirard, E., 2004, *Influence of morphological characteristics of heterogeneous moraine formations on their mechanical behaviour using image and statistical analysis*. Engineering Geology, v. 73, no. 1–2, p. 37-50.
- Mesri, G., and Hayat, T. M., 1993, *The coefficient of earth pressure at rest*. Can. Geotech. J., v. 30, p. 647-666.
- Myrvang, A., 2001, *Bergmekanikk*. Institutt for geologi og bergteknikk, NTNU, Trondheim.
- NFF, 2008, *Håndbok nr.5 - Tung sikring i undergrunnsanlegg*. Norsk forening for fjellsprengningsteknikk.
- NGI, 2013, *Using the Q-system, Rock mass classification and support design*.: Oslo, Norway.
- Nilsen, B., and Broch, E., 2011, *Ingeniørgeologi-berg grunnkurskompendium*, Institutt for geologi og bergteknikk, NTNU.
- Nilsen, B., Lindstrøm, M., Mathiesen, T. K., Holmøy, K. K., Olsson, R., and Palmstrøm, A., 2011, *Veileder for bruk av Eurokode 7 til bergteknisk prosjektering - versjon 1*, Norsk Bergmekanikkgruppe.
- Nilsen, B., and Palmstrøm, A., 2000, *Handbook No 2, Engineering geology and rock engineering*, Norwegian Group for Rock Mechanics (NBG) in cooperation with Norwegian tunneling society (NFF). Oslo, Norway.
- Nordal, S., 2013, *TBA4116 Geotechnical Engineering Advanced course - Lecture notes and background material*, NTNU, Trondheim, akademika forlag.



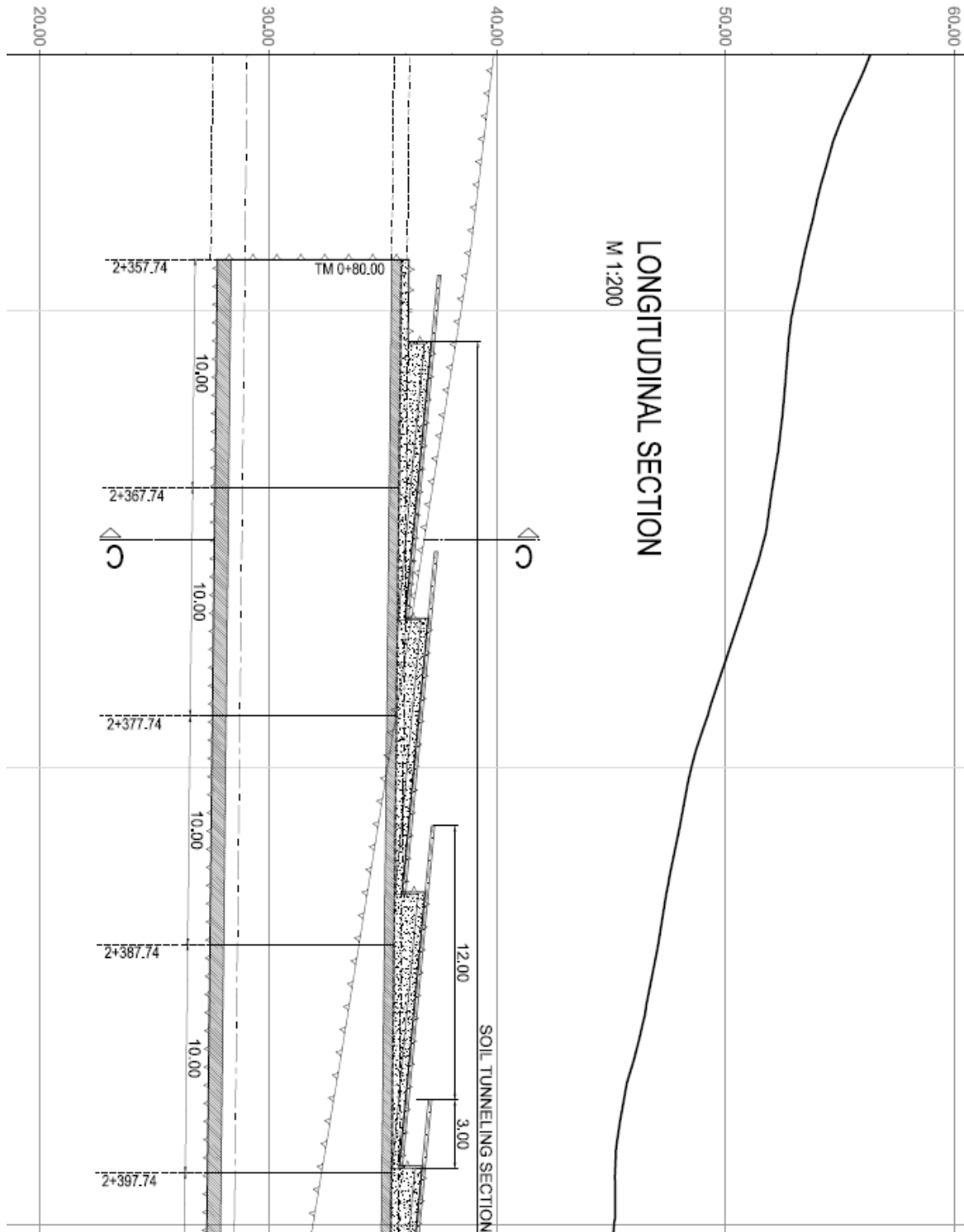
- Norgebilder, 2013, *Norge i bilder* - Norwegian map service. Skog og landskap, Statens vegvesen og Statens kartverk.
- NPRA, 2010, *Statens Vegvesen Håndbok 021-Vegtunneler*. Norway.
- , 2013a, *Geologi Rv 13, hp 13, Jobergtunnelen, Granvin, Hordaland - konkurransegrunnlag, 460, 36040*. Statens Vegvesen Region Vest, Ressursavdelingen, Vegteknisk seksjon.
- , 2013b, *Geoteknikk Rv 13 Jobergettunnelen 36040-470*, Geoteknisk rapport for reg.plan. Statens Vegvesen Region Vest, Ressursavdelingen, Vegteknisk seksjon.
- NS-EN, 1998, *933-1 Prøvningsmetoder for geometriske egenskaper for tilslag Del 1: Bestemmelse av kornstørrelsefordeling Siktemetoden*.
- Oke, J., Viachopoulos, N., and Marinos, V., 2013, *Umbrella Arch Nomenclature and Selection Methodology for Temporary Support Systems for the Design and Construction of Tunnels*. Geotechnical & Geological Engineering.
- Pelizza, S., and Peila, D., 1993, *Soil and Rock Reinforcements in Tunneling*. Tunneling and Underground Space Technology, v. 8, no. 3, p. 357-372.
- Polimac, V., 2007, *A Designers' Simple Guide to BS EN 1997*. Department for Communities and Local Government, London.
- Queiroz, P. I. B., Roure, R. N., and Negro, A., 2006, *Bayesian updating of tunnel performance for K0 estimate of santiago gravel*, Geotechnical Aspects of Underground Construction in Soft Ground. Taylor & Francis Group, London.
- Rahardjo, H., Heng, O. B., and Eng Choon, L., 2004, *Shear strength of a compacted residual soil from consolidated drained and constant water content triaxial tests*. Can. Geotech. J. , v. 41, p. 421-436.
- Rees, S., n.d., *Part one: Introduction to triaxial testing*. Hampshire, UK, Volume 2014, GDS Instruments.
- Rocscience, 2009, *RocSupport interaction and deformation analysis for tunnels in weak rock, Tutorial Manual*. , Rocscience Inc., p. 77.
- , 2014a, *Phase2 Finite Element Analysis for Excavations and Slopes, version 8.0*. Toronto, Ontario, Volume 2014, Rocscience Inc.
- , 2014b, *RocLab Rock Mass Strength Analysis Using the Generalized Hoek-Brown Failure Criterion, version 1.0*. Toronto, Ontario, Volume 2014, Rocscience Inc.
- Rocscience, 2014, *Phase2 v.8.0*.
- Sakurai, S., 1983, *Displacement measurements associated with the design of underground openings*. Proc. Int. symp. field measurements in geomechanics.
- Solli, A., and Nordgulen, Ø., 2007, *Geological map of Norway - M1:250 000*. NGU.

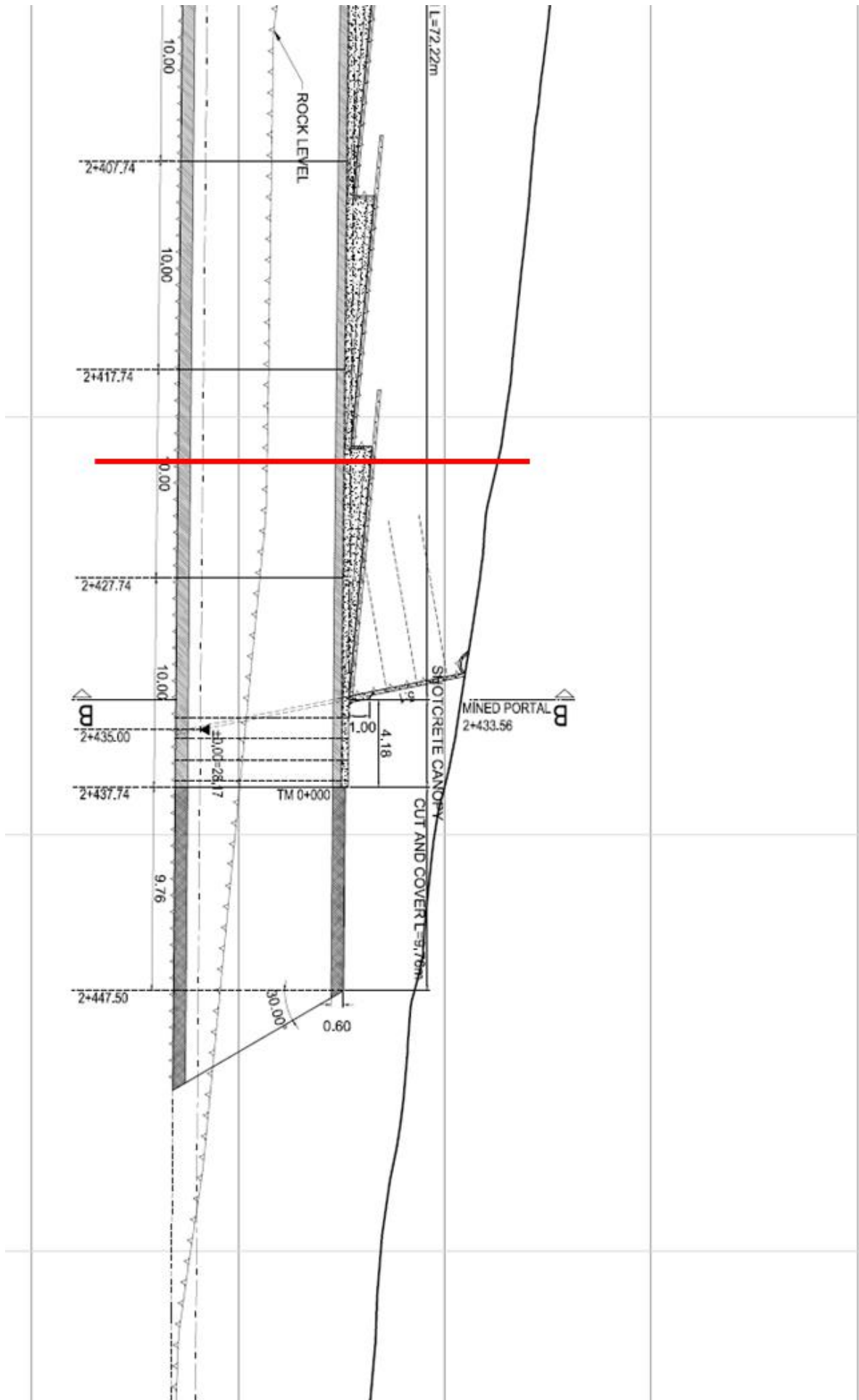
- Sweco, 2013a, *Evaluation of quaternary deposits in the area. Memo 01 of conceptual design report no. 584472*. Trondheim.
- , 2013b, *Permeabilitetsvurderinger - Memo 04 of conceptual design report no. 584472*. Trondheim.
- Sweco, and iC-Consulenter, 2013, *Tunneling in soil, Rv. 13 Granvin, conceptual design, Report no.584472*. Trondheim.
- Thoresen, M. K., 2009, *Kvartærgeologisk kart over Norge, Tema: Jordarter, Quaternary map of Norway*. NGU.
- Thoresen, M. K., Lien, R., Sønstegaard, E., and Aa, A. R., 1995, *HORDALAND fylke, kvartærgeologisk kart M1:250 000*. NGU.
- Trinh, Q. N., 2014, *Personal communication about Phase2*. NTNU, Trondheim.
- Trinh, Q. N., and Broch, E., 2008, *Tunnel Cave-in - Convergence Confinement and 2D Analyses*. SHIRMS 2008 - Y. Potvin, J. Carter, A. Dyskin, R. Jeffrey (eds). Australian Centre for Geomechanics, Perth, ISBN 978-0-9804185-5-2.
- Trinh, Q. N., Broch, E., and Lu, M., 2010, *2D versus 3D modelling for tunneling at a weakness zone*. Rock Engineering in Difficult Ground Condition - Soft Rock and Karst - Vrkljan (ed). Taylor & Francis Group, London, ISBN 978-0-415-80481-3.
- Volkman, G. M., and Schubert, W., 2008, *Tender document specification for pipe umbrella installation methods*.
- Volkman, G. M., and Schubert, W., 2009, *Effects of Pipe Umbrella Systems on the Stability of the Working Area in Weak Ground Tunneling*.
- Wang, H., and Jia, J., 2009, *Face Stability Analysis of Tunnel with Pipe Roof Reinforcement Based on Limit Analysis*. EJGE, v. 14.
- Yoo, C., 2002, *Finite-element analysis of tunnel face reinforced by longitudinal pipes*. Computers and Geotechnics, v. 29, no. 1, p. 73-94.
- Zhao, J., 2014, *Properties of rock materials*, Rock Mechanics for Civil Engineers: School of Architecture, Civil and Environmental Engineering, Swiss Federal Institute of Technology, Lausanne, Switzerland.
- Zhu, T., 2012, *Some Useful Numbers on the Engineering Properties of Materials*: Geology 615 at Stanford University, Department of Geophysics.

## Appendices

### A1 Longitudinal section of Joberget soil tunneling section (iC-Consulteren, 2013)

The red line indicates the location of the cross section used in the numerical analysis.





## A2 Calculations of the Mohr Coulomb circles

These calculations are based on the triaxial data presented in table 5.

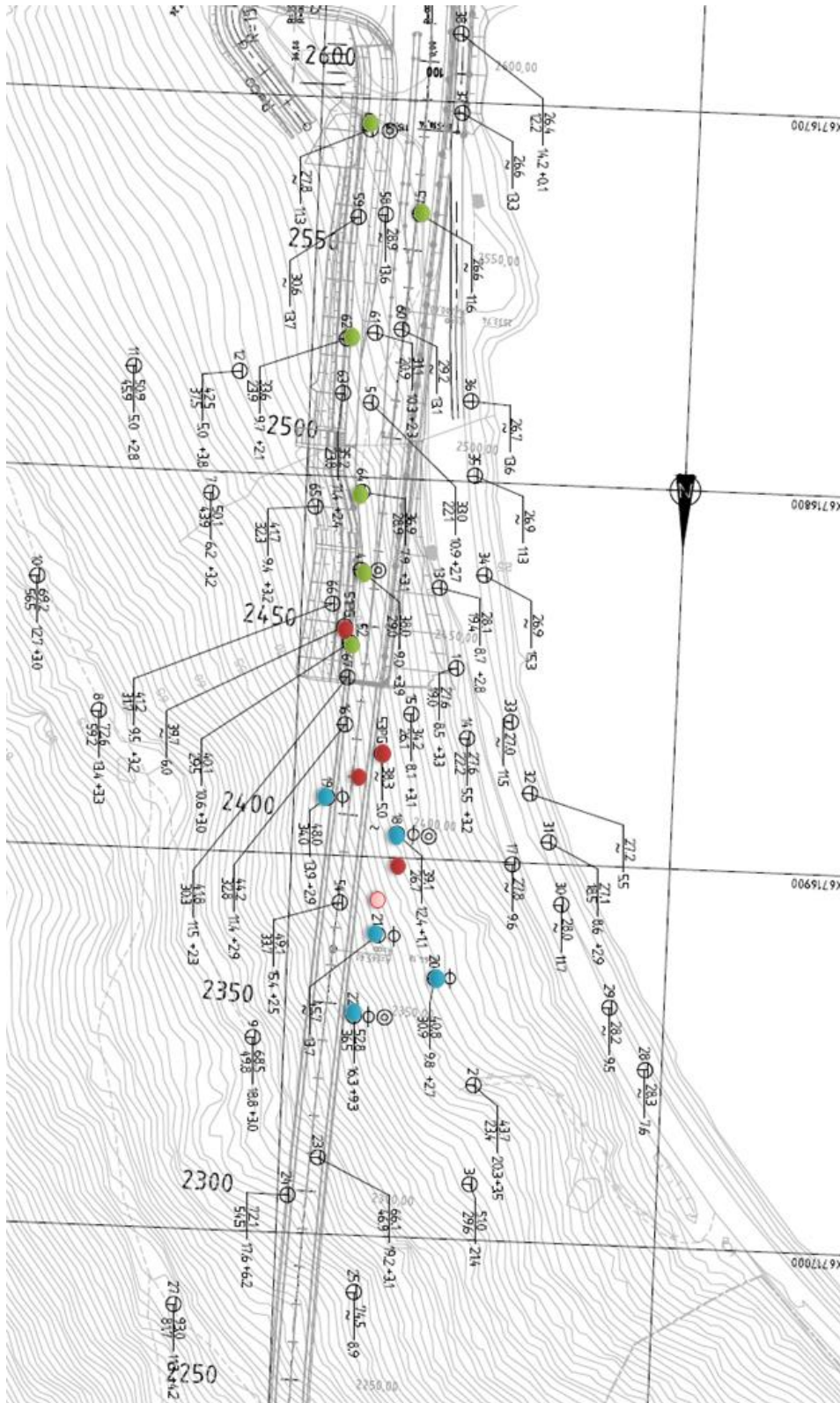
Degree [°]	$\sigma_3 = 50 \text{ kPa}$		$\sigma_3 = 100 \text{ kPa}$		$\sigma_3 = 150 \text{ kPa}$	
	x	y	x	y	x	y
0	270.34	0.00	343.05	0.00	447.38	0.00
10	268.67	19.13	341.21	21.10	445.12	25.82
20	263.70	37.68	335.72	41.56	438.41	50.85
30	255.58	55.09	326.77	60.76	427.46	74.34
40	244.57	70.82	314.62	78.12	412.59	95.58
50	230.99	84.40	299.64	93.09	394.26	113.90
60	215.26	95.41	282.29	105.24	373.03	128.77
70	197.85	103.53	263.09	114.20	349.54	139.72
80	179.30	108.50	242.63	119.68	324.51	146.43
90	160.17	110.17	221.53	121.53	298.69	148.69
100	141.04	108.50	200.42	119.68	272.87	146.43
110	122.49	103.53	179.96	114.20	247.83	139.72
120	105.09	95.41	160.76	105.24	224.34	128.77
130	89.35	84.40	143.41	93.09	203.11	113.90
140	75.77	70.82	128.43	78.12	184.79	95.58
150	64.76	55.09	116.28	60.76	169.92	74.34
160	56.64	37.68	107.33	41.56	158.97	50.85
170	51.67	19.13	101.85	21.10	152.26	25.82
180	50.00	0.00	100.00	0.00	150.00	0.00

$x = \text{circle centrum on x-axis} + \text{radius} * \cos(\text{degree} * \text{PI} / 180)$

$y = 0 + \text{radius} * \sin(\text{degree} * \text{PI} / 180)$

### A3 Plan view of investigations carried out at Joberget

The map is showing location of drillings, sieve analysis (green), permeability tests (blue) test pits (red) by the NPRA (2013b) and the test pit used for sampling to laboratory testing at NTNU/SINTEF (pink) by Langåker (2013).



## A4 Calculations of $S_0$ and $M_d$ for material classification

Calculation of  $S_0$  and  $M_d$  based on grain size distribution curves provided by the NPRA (2013b) and the grain size distribution curve from sieve analysis performed at the NTNU/SINTEF by Langåker (2013) Included is also a figure showing how the calculations are carried out (Sweco, 2013b).

ID:	Set no.	Hole no	Cylinder / bag no.	Test depth (m)	Approx. depth (m.a.s.l)	Commentar y	Q(25) = (mm)	Q(50) = (mm)	Q(75) = (mm)	$S_0 =$	$M_d =$	Q(60) = (mm)	Q(10) = (mm)	
1	3	52		1	0,0 - 0,7		0,122	0,659	5,636	1,7	0,7	1,500	0,055	
2				2	0,7 - 1,0		0,011	0,591	2,727	2,4	0,6	1,000	0,057	
3				3	1,0 - 1,5		0,108	0,886	6,909	1,8	0,9	1,818	0,017	
4				4	2,0 - 2,5		0,122	1,273	7,636	1,8	1,3	2,727	0,012	
5	3	52		5	3,0 - 3,7		0,083	1,21	3,053	1,6	1,2	2,211	0,008	
6				6	4,5 - 5,0		0,164	1,842	4,421	1,4	1,8	3,474	0,012	
7				7	6,0 - 6,7		0,25	1	3,789	1,2	1,0	1,684	0,056	
8				8	8,0 - 8,7		0,096	1,684	9,263	2,0	1,7	3,474	0,009	
9	5	62		1	1,0 - 1,5		0,039	0,3	1,75	1,7	0,3	0,625	0,009	
10				2	2,0 - 2,5		0,1	0,975	5,6	1,7	1,0	1,900	0,015	
11	4	57		1	1,0 - 1,5		0,042	0,169	1,2	1,5	0,2	0,400	0,011	
12				2	2,0 - 2,5		0,0036	0,0092	0,025	0,8	0,009	0,014	-	
13	1	1		1	3,0 - 4,0	Test pit	0,264	1,334	5,778	1,3	1,3	2,444	0,060	
14				2	6,0 - 6,0	Test pit	0,051	0,361	2,223	1,6	0,4	0,806	0,004	
15	2	2		1	2,0 - 2,0	Test pit	0,187	1,056	4,444	1,4	1,1	1,889	0,034	
16				2	5,0 - 5,0	Test pit	0,389	1,833	6,667	1,2	1,8	2,889	0,084	
17		22		1	4,6 - 5,1		0,44	1,182	4,714	1,0	1,2	1,909	0,143	
18				2	8,0 - 8,5		0,486	1,682	5,714	1,1	1,7	3,029	0,100	
19				3	12,0 - 12,5		0,056	0,725	3,619	1,8	0,7	1,500	0,005	
20				4	14,2 - 14,7		0,02	0,486	2,857	2,2	0,5	1,000	0,003	
21		18		1	3,0 - 3,5		0,428	1,454	4,857	1,1	1,5	2,200	0,100	
22				2	6,0 - 8,5		0,5	4,571	12,571	1,4	4,6	7,500	0,047	
23				3	10,0 - 10,5		0,2	1,818	5,429	1,4	1,8	3,143	0,014	
24		4		1	6,0 - 6,5		0,024	0,467	4,909	2,3	0,5	1,227	0,003	
25		6		1	1,5 - 2,0		0,489	7,5	20	1,6	7,5	12,470	0,020	
26				2	2,5 - 3,0		0,0056	0,017	0,733	2,1	0,02	0,031	0,0015	
27			Margrete		2,5 - 3,0	25,5 - 25,0	Test pit	0,434	5,846	51,538	2,1	5,85	9,030	-

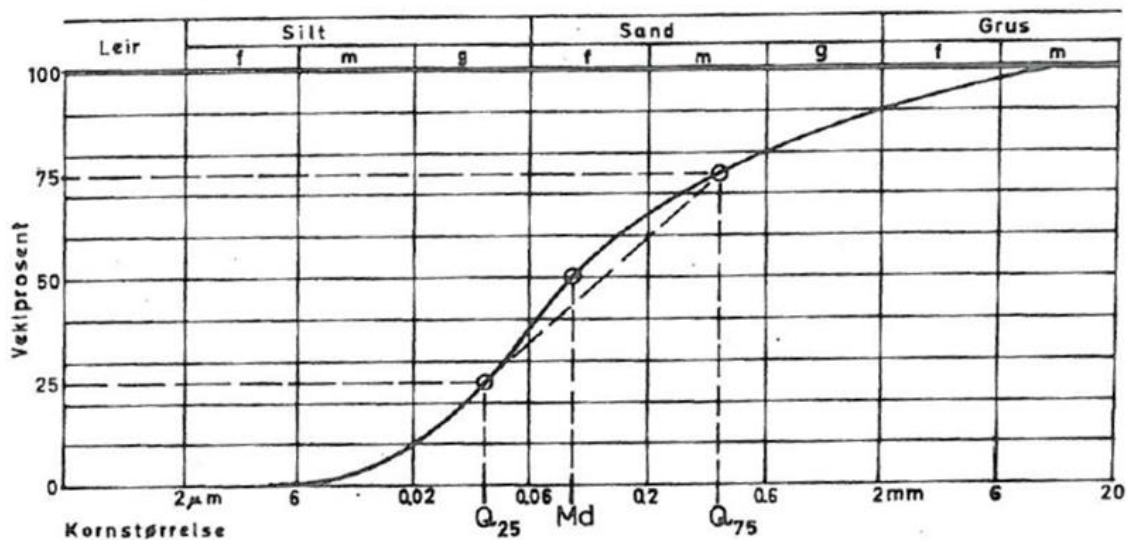


Fig. 5. Sorteringstall og midlere kornstørrelse.

$$\text{Sorteringen} = S_0 = \log Q_{75} - \log Q_{25}$$

$$\text{Midlere kornstørrelse} = M_d = Q_{50}$$

## A5 Calculations from sieve and density analysis (Langåker, 2013)

Sieve analysis:

	Sieve opening [mm]	Dry sample weight retained [g]	Total mass when tested [g]	Percent of mass retained on each sieve [%]	Cumulative percent of total mass retained [%]	Percent passing [%]	Grain size [mm]
Total mass =		22441,7 g					
Hand sieving	63	3412,7	22441,7	15,21	15,21	100	125
	31,5	1853,5	22441,7	8,26	23,47	84,79	63
	19	1397,3	22441,7	6,23	29,69	76,53	31,5
	< 19	15778,2	22441,7	70,31		70,31	19
		22441,7		100,00			
Portion of total mass =		1731,5 g					
Wet sieving	< 0,063	403,3	1731,5	23,29			
Machine sieving	16	49,3	1731,5	2,85	2,00	68,31	16
	8	183,7	1731,5	10,61	7,46	60,85	8
	4	219,4	1731,5	12,67	8,91	51,94	4
	2	195,8	1731,5	11,31	7,95	43,99	2
	1	182,9	1731,5	10,56	7,43	36,56	1
	0,5	134,8	1731,5	7,79	5,47	31,09	0,5
	0,25	123,9	1731,5	7,16	5,03	26,06	0,25
	0,125	120,3	1731,5	6,95	4,88	21,17	0,125
	0,063	94,4	1731,5	5,45	3,83	17,34	0,063
	< 0,063	10,4	1731,5	23,89	16,80	0,54	
			99,2	69,8			

Density analysis:

$$\gamma = \frac{mg}{V \cdot 1000} = \frac{27,678 \cdot 9,81}{0,012529 \cdot 1000} = 21,7$$

$\gamma$  = Unit weight [kN/m<sup>3</sup>]

$m$  = Mass of soil specimen [kg]

$g$  = 9,81 m/s<sup>2</sup>, acceleration of gravity

$V$  = Volume [m<sup>3</sup>]

$$\theta_d = \frac{m_w}{m_s} = \frac{27,4 - 25,1}{25,1} = 9,2$$

$\theta_d$  = Gravimetric water content [%]

$m_w$  = mass of water saturated soil – mass of oven-dried soil [kg]

$m_s$  = mass of oven-dried soil [kg]

Shear box testing:

	Vertical load [kPa]	Max shear stress [kPa]	Linear approx. $y = ax + b$	Friction angle [°] = (DEGREE(ARCTAN(a)))
Joberg1	50	55	$a = 0,9243$	42,7
	100	103		
	200	194		
Joberg2	50	64	$a = 0,9171$	42,5
	100	102		
	200	200		
JobergW1	50	60	$a = 0,8229$	39,5
	100	104		
	200	184		
JobergW2	50	57	$a = 0,8075$	38,9
	100	93		
	200	177		



# A5 The Q-system (NGI, 2013)

1	RQD (Rock Quality Designation)	RQD
A	Very poor (< 27 joints per m <sup>3</sup> )	0-25
B	Poor (20-27 joints per m <sup>3</sup> )	25-50
C	Fair (13-19 joints per m <sup>3</sup> )	50-75
D	Good (8-12 joints per m <sup>3</sup> )	75-90
E	Excellent (0-7 joints per m <sup>3</sup> )	90-100

Note: 1) Where RQD is reported or measured as ≤ 10 (including 0) the value 10 is used to exclude the Q-value

2) RQD-intervals of 5, i.e. 100, 95, 90, etc., are sufficiently accurate

2	Joint set number	J <sub>n</sub>
A	Massive, no or few joints	0.5-1.0
B	One joint set	2
C	One joint set plus random joints	3
D	Two joint sets	4
E	Two joint sets plus random joints	6
F	Three joint sets	9
G	Three joint sets plus random joints	12
H	Four or more joint sets, random heavily jointed "sugar cube", etc.	15
J	Cubed rock, earth like	20

Note: 1) For tunnel intersections, use 3x J<sub>n</sub>

2) For portals, use 2 x J<sub>n</sub>

3	Joint Roughness Number	J <sub>r</sub>
<b>a) Rock-wall contact and b) Rock-wall contact before 10 cm of shear movement</b>		
A	Discontinuous joints	4
B	Rough or irregular undulating	3
C	Smooth, undulating	2
D	Slickensided, undulating	1.5
E	Rough, irregular planar	1.5
F	Smooth, planar	1
G	Slickensided, planar	0.5
<b>c) No rock-wall contact when sheared</b>		
H	Zone containing clay minerals thick enough to prevent rock-wall contact when sheared	1

Note: 1) Add 1 if the mean spacing of the relevant joint set is greater than 3 m (dependent on the size of the underground opening)

2) J<sub>r</sub> = 0.5 can be used for planar slickensided joints having irregularities, provided the irregularities are oriented in the estimated sliding direction

4	Joint Alteration Number	Q <sub>0</sub> approx.	J <sub>a</sub>
<b>a) Rock-wall contact (no mineral fillings, only coatings)</b>			
A	Tightly healed, hard, non-softening, impermeable filling i.e. quartz or epidote		0.75
B	Unhealed joint walls, surface staining only		25-35*
C	Slightly altered joint walls, non-softening mineral coatings, sandy particles, clay-free disintegrated rock, etc.		25-30*
D	Silty or sandy clay coatings, small clay fraction (non-softening)		20-25*
E	Softening or low friction clay/mineral coatings i.e. kaolinite or mica. Also chlorite, talc, gypsum, graphite, etc., and small quantities of swelling clays.		8-16*
<b>b) Rock-wall contact before 10 cm shear (thin mineral fillings)</b>			
F	Sandy particles, clay-free disintegrated rock, etc.		25-30*
G	Strongly over-consolidated, non-softening, clay mineral fillings (continuous, but < 5mm thickness)		16-24*
H	Medium or low over-consolidation, softening, clay mineral fillings (continuous, but < 5mm thickness)		12-16*
J	Swelling clay fillings, i.e. montmorillonite (continuous, but < 5mm thickness). Value of J <sub>a</sub> depends on percent of swelling clay-size particles.		6-12*
<b>c) No rock-wall contact when sheared (thick mineral fillings)</b>			
K	Zones or bands of disintegrated or crushed rock, strongly over-consolidated.		16-24*
L	Zones or bands of clay, disintegrated or crushed rock, medium or low over-consolidation or softening fillings.		12-16*
M	Zones or bands of clay, disintegrated or crushed rock, clay-size particles.		6-12*
N	Thick continuous zones or bands of clay, strongly over-consolidated.		16-24*
O	Thick, continuous zones or bands of clay, medium to low over-consolidation.		12-16*
P	Thin, continuous zones or bands with clay, swelling clay, J <sub>a</sub> depends on percent of swelling clay-size particles.		6-12*

5	Joint Water Reduction Factor	J <sub>w</sub>
A	Dry excavations or minor inflow (5 mm/d or a few drops)	1.0
B	Medium inflow, occasional outwash of joint fillings (many drops/cm <sup>2</sup> /h)	0.66
C	Jet inflow or high pressure in competent rock with unlined joints	0.5
D	Large inflow or high pressure, considerable outwash of joint fillings	0.33
E	Exceptionally high inflow or water pressure decaying with time. Causes outwash of material and perhaps cave in	0.2-0.1
F	Exceptionally high inflow or water pressure continuing without noticeable decay. Causes outwash of material and perhaps cave in	0.1-0.05

Note: 1) Factors C, D, E are crude estimates. Increase J<sub>w</sub> if the rock is drained or grouting is carried out

2) Special problems caused by ice formation are not considered

6	Stress Reduction Factor	S <sub>RF</sub>		
<b>a) Weak zones intersecting the underground opening, which may cause loosening of rock mass</b>				
A	Multiple occurrences of weak zones within a short section containing clay or chemical cemented, very loose surrounding rock (any depth). For squeezing, see 61 and 61H	10		
B	Multiple shear zones within a short section in competent clay-free rock with loose surrounding rock (any depth)	7.5		
C	Single weak zones with or without clay or chemical disintegrated rock (depth ≤ 50m)	5		
D	Loose, open joints, heavily jointed or "sugar cube", etc. (any depth)	5		
E	Single weak zones with or without clay or chemical disintegrated rock (depth > 50m)	2.5		
<b>b) Competent, mainly massive rock, stress problems</b>				
F	Low stress, near surface, open joints	>200	<0.01	2.5
G	Medium stress, favourable stress condition	200-10	0.01-0.3	1
H	High stress, very tight structure. Usually favourable to stability. May also be unfavourable to stability dependent on the orientation of stresses compared to jointing/weakness planes*	10-5	0.3-0.4	0.5-2
J	Moderate spalling and/or slabbing after > 1 hour in massive rock	5-3	0.5-0.65	5-50
K	Spalling or rock burst after a few minutes in massive rock	3-2	0.65-1	50-200
L	Heavy rock burst and immediate dynamic deformation in massive rock	<2	>1	200-400

Note: 1) Reduce these values of S<sub>RF</sub> by 25-50% if the weak zones only influence but do not intersect the underground opening

c) Squeezing rock, plastic deformation in incompetent rock under the influence of high pressure	σ <sub>v</sub> /σ <sub>h</sub>	σ <sub>v</sub> /σ <sub>e</sub>	S <sub>RF</sub>
M	Mild squeezing rock pressure	1-5	5-10
N	Heavy squeezing rock pressure	>5	10-20

Note: 1) Determination of squeezing rock conditions must be made according to relevant literature (i.e. Singh et al., 1992 and Brian and Srinivas, 1996)

d) Swelling rock, chemical swelling activity depending on the presence of water	S <sub>RF</sub>	
O	Mild swelling rock pressure	5-10
P	Heavy swelling rock pressure	10-15

Note: The values for J<sub>r</sub> and J<sub>w</sub> should be chosen based on the orientation and shear strength, τ, (where τ = σ<sub>v</sub> tan φ + c) of the joint or discontinuity that gives the most unfavourable stability for the rock mass, and along which failure most likely will occur.

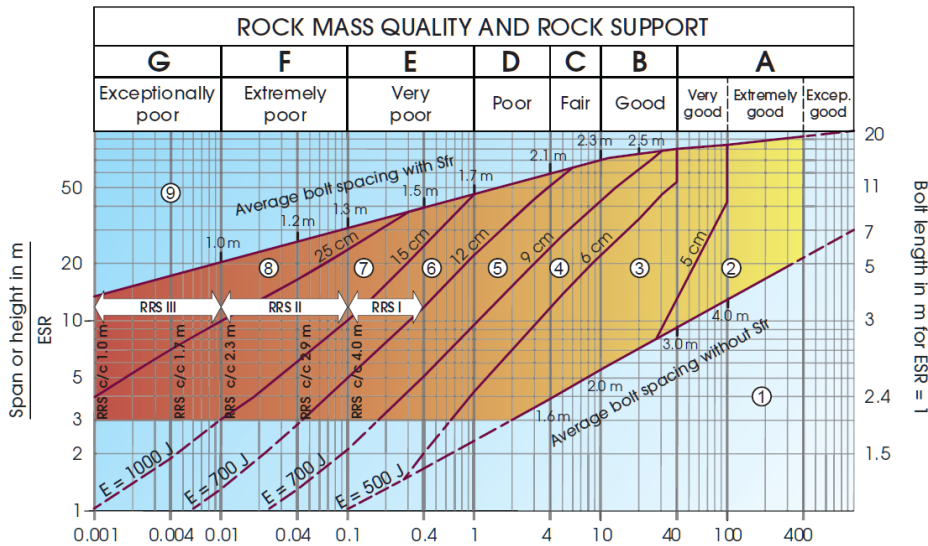
Table 8 Conversion from actual Q-values to adjusted Q-values for design of wall support		
In rock masses of good quality	Q > 10	The actual Q-value is multiplied by 5
For rock masses of intermediate quality	0.1 < Q < 10	The actual Q-value is multiplied by 2.5 (in cases of high stresses the actual Q-value is used)
For rock masses of poor quality	Q < 0.1	The actual Q-value is used

$$Q = \frac{RQD}{J_n} \times \frac{J_r}{J_a} \times \frac{J_w}{SRF}$$

Table 7 ESR - values	
Type of Excavation	ESR
A Temporary mine openings, etc.	ca. 3.5
B Vertical shafts: 1) circular sections 2) rectangular/square section * Dependent of purpose. May be lower than given values.	ca. 2.5 ca. 2.0
C Permanent mine openings, water tunnels for hydro power (exclude high pressure penstocks), water supply tunnels, pilot tunnels, drifts and headings for large openings.	1.6
D Minor road and railway tunnels, surge chambers, access tunnels, sewage tunnels, etc.	1.3
E Power houses, storage rooms, water treatment plants, major road and railway tunnels, civil defence chambers, ports, intersections, etc.	1.0
F Underground nuclear power stations, railways stations, sports and public facilities, factories, etc.	0.8
G Very important caverns and tunnels with a long lifetime, = 100 years, or without access for maintenance.	0.5

For the types of excavation B, C and D, it is recommended to use ESR = 1.0 when Q < 0.1. The reason for that is that the stability problems may be severe with such low Q-values, perhaps with risk for cave-in. ESR together with the span (or wall height) gives the Equivalent dimension in the following way:

$$\frac{\text{Span or height in m}}{\text{ESR}} = \text{Equivalent dimension}$$



$$\text{Rock mass quality } Q = \frac{RQD}{J_n} \times \frac{J_r}{J_a} \times \frac{J_w}{SRF}$$

### Support categories

- ① Unsupported or spot bolting
- ② Spot bolting, **SB**
- ③ Systematic bolting, fibre reinforced sprayed concrete, 5-6 cm, **B+Sfr**
- ④ Fibre reinforced sprayed concrete and bolting, 6-9 cm, **Sfr (E500)+B**
- ⑤ Fibre reinforced sprayed concrete and bolting, 9-12 cm, **Sfr (E700)+B**
- ⑥ Fibre reinforced sprayed concrete and bolting, 12-15 cm + reinforced ribs of sprayed concrete and bolting, **Sfr (E700)+RRS I+B**
- ⑦ Fibre reinforced sprayed concrete >15 cm + reinforced ribs of sprayed concrete and bolting, **Sfr (E1000)+RRS II+B**
- ⑧ Cast concrete lining, **CCA** or **Sfr (E1000)+RRS III+B**
- ⑨ Special evaluation

Bolts spacing is mainly based on Ø20 mm

E = Energy absorption in fibre reinforced sprayed concrete

ESR = Excavation Support Ratio

Areas with dashed lines have no empirical data

### RRS - spacing related to Q-value

**Si30/6 Ø16 - Ø20 (span 10m)**

**D40/6+2 Ø16-20 (span 20m)**

**Si35/6 Ø16-20 (span 5m)**

**D45/6+2 Ø16-20 (span 10m)**

**D55/6+4 Ø20 (span 20m)**

**D40/6+4 Ø16-20 (span 5m)**

**D55/6+4 Ø20 (span 10 m)**

**D70/6+6 Ø20 (span 20 m)**

Si30/6 = Single layer of 6 rebars, 30 cm thickness of sprayed concrete

D = Double layer of rebars

Ø16 = Rebar diameter is 16 mm

c/c = RSS spacing, centre - centre

## A6 The RMR-system (Hoek, 2007b)

A. CLASSIFICATION PARAMETERS AND THEIR RATINGS									
Parameter			Range of values						
1	Strength of intact rock material	Point-load strength index	>10 MPa	4 - 10 MPa	2 - 4 MPa	1 - 2 MPa	For this low range - uniaxial compressive test is preferred		
		Uniaxial comp. strength	>250 MPa	100 - 250 MPa	50 - 100 MPa	25 - 50 MPa	5 - 25 MPa	1 - 5 MPa	< 1 MPa
Rating			15	12	7	4	2	1	0
2	Drill core Quality RQD		90% - 100%	75% - 90%	50% - 75%	25% - 50%	< 25%		
	Rating		20	17	13	8	3		
3	Spacing of discontinuities		> 2 m	0.6 - 2. m	200 - 600 mm	60 - 200 mm	< 60 mm		
	Rating		20	15	10	8	5		
4	Condition of discontinuities (See E)		Very rough surfaces Not continuous No separation Unweathered wall rock	Slightly rough surfaces Separation < 1 mm Slightly weathered walls	Slightly rough surfaces Separation < 1 mm Highly weathered walls	Slickensided surfaces or Gouge < 5 mm thick or Separation 1-5 mm Continuous	Soft gouge >5 mm thick or Separation > 5 mm Continuous		
	Rating		30	25	20	10	0		
5	Groundwater	Inflow per 10 m tunnel length (l/m)	None	< 10	10 - 25	25 - 125	> 125		
		(Joint water press)/ (Major principal $\sigma$ )	0	< 0.1	0.1, - 0.2	0.2 - 0.5	> 0.5		
	General conditions		Completely dry	Damp	Wet	Dripping	Flowing		
	Rating		15	10	7	4	0		
B. RATING ADJUSTMENT FOR DISCONTINUITY ORIENTATIONS (See F)									
Strike and dip orientations			Very favourable	Favourable	Fair	Unfavourable	Very Unfavourable		
Ratings	Tunnels & mines		0	-2	-5	-10	-12		
	Foundations		0	-2	-7	-15	-25		
	Slopes		0	-5	-25	-50			
C. ROCK MASS CLASSES DETERMINED FROM TOTAL RATINGS									
Rating		100 ← 81	80 ← 61	60 ← 41	40 ← 21	< 21			
Class number		I	II	III	IV	V			
Description		Very good rock	Good rock	Fair rock	Poor rock	Very poor rock			
D. MEANING OF ROCK CLASSES									
Class number		I	II	III	IV	V			
Average stand-up time		20 yrs for 15 m span	1 year for 10 m span	1 week for 5 m span	10 hrs for 2.5 m span	30 min for 1 m span			
Cohesion of rock mass (kPa)		> 400	300 - 400	200 - 300	100 - 200	< 100			
Friction angle of rock mass (deg)		> 45	35 - 45	25 - 35	15 - 25	< 15			
E. GUIDELINES FOR CLASSIFICATION OF DISCONTINUITY conditions									
Discontinuity length (persistence)		< 1 m	1 - 3 m	3 - 10 m	10 - 20 m	> 20 m			
Rating		6	4	2	1	0			
Separation (aperture)		None	< 0.1 mm	0.1 - 1.0 mm	1 - 5 mm	> 5 mm			
Rating		6	5	4	1	0			
Roughness		Very rough	Rough	Slightly rough	Smooth	Slickensided			
Rating		6	5	3	1	0			
Infilling (gouge)		None	Hard filling < 5 mm	Hard filling > 5 mm	Soft filling < 5 mm	Soft filling > 5 mm			
Rating		6	4	2	2	0			
Weathering		Unweathered	Slightly weathered	Moderately weathered	Highly weathered	Decomposed			
Ratings		6	5	3	1	0			
F. EFFECT OF DISCONTINUITY STRIKE AND DIP ORIENTATION IN TUNNELLING**									
Strike perpendicular to tunnel axis					Strike parallel to tunnel axis				
Drive with dip - Dip 45 - 90°			Drive with dip - Dip 20 - 45°		Dip 45 - 90°		Dip 20 - 45°		
Very favourable			Favourable		Very unfavourable		Fair		
Drive against dip - Dip 45-90°			Drive against dip - Dip 20-45°		Dip 0-20 - Irrespective of strike°				
Fair			Unfavourable		Fair				

\* Some conditions are mutually exclusive . For example, if infilling is present, the roughness of the surface will be overshadowed by the influence of the gouge. In such cases use A.4 directly.

\*\* Modified after Wickham et al (1972).

Guidelines for excavation and support of 10 m span rock tunnels in accordance with the RMR system (Hoek, 2007b).

Rock mass class	Excavation	Rock bolts (20 mm diameter, fully grouted)	Shotcrete	Steel sets
I - Very good rock <i>RMR: 81-100</i>	Full face, 3 m advance.	Generally no support required except spot bolting.		
II - Good rock <i>RMR: 61-80</i>	Full face , 1-1.5 m advance. Complete support 20 m from face.	Locally, bolts in crown 3 m long, spaced 2.5 m with occasional wire mesh.	50 mm in crown where required.	None.
III - Fair rock <i>RMR: 41-60</i>	Top heading and bench 1.5-3 m advance in top heading. Commence support after each blast. Complete support 10 m from face.	Systematic bolts 4 m long, spaced 1.5 - 2 m in crown and walls with wire mesh in crown.	50-100 mm in crown and 30 mm in sides.	None.
IV - Poor rock <i>RMR: 21-40</i>	Top heading and bench 1.0-1.5 m advance in top heading. Install support concurrently with excavation, 10 m from face.	Systematic bolts 4-5 m long, spaced 1-1.5 m in crown and walls with wire mesh.	100-150 mm in crown and 100 mm in sides.	Light to medium ribs spaced 1.5 m where required.
V – Very poor rock <i>RMR: &lt; 20</i>	Multiple drifts 0.5-1.5 m advance in top heading. Install support concurrently with excavation. Shotcrete as soon as possible after blasting.	Systematic bolts 5-6 m long, spaced 1-1.5 m in crown and walls with wire mesh. Bolt invert.	150-200 mm in crown, 150 mm in sides, and 50 mm on face.	Medium to heavy ribs spaced 0.75 m with steel lagging and forepoling if required. Close invert.

## A7 Analysis of Rock Strength using RocLab

